

Sorption of a branched nonylphenol isomer and perfluorooctanoic acid on geosorbents and carbon nanotubes

Chengliang Li

Forschungszentrum Jülich GmbH
Institute of Bio- and Geosciences (IBG)
Agrosphere (IGB-3)

Sorption of a branched nonylphenol isomer and perfluorooctanoic acid on geosorbents and carbon nanotubes

Chengliang Li

Schriften des Forschungszentrums Jülich
Reihe Energie & Umwelt / Energy & Environment

Band / Volume 110

ISSN 1866-1793

ISBN 978-3-89336-716-0

Bibliographic information published by the Deutsche Nationalbibliothek.
The Deutsche Nationalbibliothek lists this publication in the Deutsche
Nationalbibliografie; detailed bibliographic data are available in the
Internet at <http://dnb.d-nb.de>.

Publisher and
Distributor: Forschungszentrum Jülich GmbH
Zentralbibliothek
52425 Jülich
Phone +49 (0) 24 61 61-53 68 · Fax +49 (0) 24 61 61-61 03
e-mail: zb-publikation@fz-juelich.de
Internet: <http://www.fz-juelich.de/zb>

Cover Design: Grafische Medien, Forschungszentrum Jülich GmbH

Printer: Grafische Medien, Forschungszentrum Jülich GmbH

Copyright: Forschungszentrum Jülich 2011

Schriften des Forschungszentrums Jülich
Reihe Energie & Umwelt / Energy & Environment Band / Volume 110

D 82 (Diss., RWTH Aachen University, 2011)

ISSN 1866-1793

ISBN 978-3-89336-716-0

The complete volume is freely available on the Internet on the Jülicher Open Access Server (JUWEL) at
<http://www.fz-juelich.de/zb/juwel>

Neither this book nor any part of it may be reproduced or transmitted in any form or by any
means, electronic or mechanical, including photocopying, microfilming, and recording, or by any
information storage and retrieval system, without permission in writing from the publisher.

ABSTRACT

Abstract

As metabolites of organic surfactants, both nonylphenol (NP) and perfluorooctanoic acid (PFOA) are toxic and ubiquitous in the environment. Their sorption on soils and sediments is of importance for their fate and transport in the environment. Especially in China, there is still a lack of consolidated knowledge on the sorption behavior of NP and PFOA on geosorbents such as Yangtze River sediments. Thus, the present thesis investigates the sorption of a branched NP isomer [4-(1-ethyl-1, 3-dimethylpentyl) phenol] (NP111) and PFOA on Yangtze River sediments and their model components, *i.e.* a clay mineral (illite), metal oxides (goethite and δ -Al₂O₃) and organic matter (isolated from Yangtze River sediments and commercial organic matter) by both batch and dialysis techniques. NP111 is the most environmentally relevant NP isomer and its fate in the environment is unknown. Because PFOA is weakly adsorbed on geosorbents, multi-walled carbon nanotubes (MWCNTs) were studied as promising adsorbents. One of the MWCNTs studied contained traces of metal catalyst on the outer surface.

Sorption isotherms of NP111 and PFOA on the sediments and their model components were fitted well by the Freundlich model. Sorption of NP111 on the sediments depended largely on their organic carbon content, resulting in organic carbon-normalized sorption coefficient (K_{OC}) values between 6.3×10^3 and 1.1×10^4 L kg⁻¹. The sorption of NP111 on δ -Al₂O₃ and illite was comparable to that on sediments, but significantly lower than that on goethite. In contrast, the sorption of PFOA on the sediments was significantly lower. The affinity of PFOA to goethite and δ -Al₂O₃ was slightly higher than to the sediments, but it was negligible to natural organic matter and illite. The results suggest that the organic carbon content of the sediments plays a dominant role in the sorption of NP111, whereas goethite acts as a potential sink for both NP111 and PFOA in sediments.

SORPTION OF A NONYLPHENOL ISOMER AND PERFLUOROOCTANOIC ACID ON
GEOSORBENTS AND CARBON NANOTUBES

Adsorption isotherms of NP111 on HAs were well described by a linear model. The K_{OC} values ranged from 2.3×10^3 to $1.5 \times 10^4 \text{ L kg}^{-1}$. There was no significant influence of pH on the adsorption of NP111 on organic matter under acidic and neutral conditions. Conversely, adsorption decreased with increasing pH under alkaline conditions. Interestingly, for HAs of comparable origins, a clear correlation between the K_{OC} value and the alkyl C content was observed, indicating that the aliphaticity of HAs significantly dominates the sorption of NP111. These results indicate that the fate of nonylphenols in soil/sediment depends not only on the content of HA but also on its composition.

The sorption isotherms of PFOA on MWCNTs were well described by both Freundlich and Langmuir models. MWCNTs with traces of metal catalyst on the outer surface had higher adsorption affinity and capacity for PFOA than MWCNTs without such traces. Ad/desorption of PFOA on MWCNTs was completely reversible. The thermodynamic data indicated that the sorption of PFOA on MWCNTs was characterized by physisorption. The sorption mechanism of PFOA on MWCNTs was governed by both hydrophobic and electrostatic interactions. In a general way, the PFOA adsorption decreased significantly with increasing salinity and pH. The divalent cation Ca^{2+} significantly enhanced the adsorption compared with the monovalent cation Na^+ . The removal of the metal catalyst from the outer surface of MWCNTs diminished the adsorption capacity of the MWCNTs due to the absence of electrostatic interaction. Therefore, these results show that a surface modification of MWCNTs leading to positive charges on the outer surface may be a promising way to improve the sorption capacity of MWCNTs for PFOA. The sorption isotherms of NP111 on MWCNTs were described well by a linear model (Henry model). Compared with PFOA, NP111 exhibited sorption capacity on MWCNTs higher by two orders of magnitude. The difference is caused by different adsorption mechanisms, *i.e.* hydrophobic and π - π interactions played an important role in the sorption of NP111 on MWCNTs.

TABLE OF CONTENTS

Table of contents

Abstract	I
Table of contents	III
List of figures	V
List of tables	VII
Abbreviations	VIII
Symbols	X
Chapter 1 Introduction	1
1.1 Surfactant degradation products	1
1.2 Nonylphenols in environmental compartments	2
1.3 Perfluorooctanoic acid in environmental compartments	4
1.4 NP and PFOA contamination in Yangtze River	6
1.5 Organic matter interactions with organic pollutants	7
1.6 Innovative material for water treatment — Carbon nanotubes	8
1.7 Objectives of the thesis	10
Chapter 2 Theoretical background	12
2.1 Sorption of organic compounds from aqueous solution	12
2.2 Desorption hysteresis	14
2.3 Sorption of pollutants on organic matter	15
2.4 Sorption models	16
2.4.1 Linear model	16
2.4.2 Nonlinear models	17
Chapter 3 Materials and methods	19
3.1 Chemicals and adsorbents	19
3.1.1 Chemicals	19

SORPTION OF A NONYLPHENOL ISOMER AND PERFLUOROOCTANOIC ACID ON GEOSORBENTS AND CARBON NANOTUBES

3.1.2 Adsorbents	20
3.2 Adsorption experiments.....	23
3.2.1 Batch technique	23
3.2.2 Dialysis technique	24
3.2.3 Solution factors	24
3.3 Analytical methods	25
Chapter 4 Results and discussion	30
4.1 Sorption of NP111 onto Yangtze River sediments and their model components.....	30
4.1.1 The adsorption of NP111 on Yangtze River sediments.....	30
4.1.2 Adsorption of NP111 on model geosorbents.....	34
4.2 Effect of structural composition of humic substances on the sorption of NP111	38
4.2.1 NMR characterization of humic substances	38
4.2.2 Adsorption of NP111 to humic substances.....	43
4.2.3 Influence of pH on NP111 adsorption to selected humic substances	46
4.2.4 The correlation between K_{OC} values and the composition of humic substances	47
4.3 Adsorption of PFOA on Yangtze River sediments and their components	52
4.4 Adsorption of PFOA and NP111 on multi-walled carbon nanotubes	57
4.4.1 Characterization of multi-walled carbon nanotubes	57
4.4.2 Sorption of PFOA on multi-walled carbon nanotubes.....	64
4.4.3 Adsorption of NP111 on multi-walled carbon nanotubes	75
Chapter 5 Conclusions	78
References	82
Acknowledgements	98
Appendix	100
Curriculum vitae	101

LIST OF FIGURES

List of figures

Fig. 3.1 Sediment sampling locations along the Yangtze River.....	22
Fig. 4.1 Adsorption isotherms of NP111 on Yangtze River sediments.....	34
Fig. 4.2 Adsorption isotherms of NP111 on sediment model components.....	36
Fig. 4.3 a) ^{13}C CP/MAS (grey) and b) ^{13}C -DP/MAS (black) NMR spectra of the humic acids and chemical shift regions: alkyl C (47-0 ppm), O-alkyl C (92-47 ppm), anomeric C (110-92 ppm), aromatic C (165-110 ppm), carboxyl C (195-165 ppm)	41
Fig. 4.4 Sorption isotherms of NP111 on HAs isolated from Yangtze River sediments (CME HA, NJ HA, WH HA and ZG HA) and the reference ones (A HA and SR HA).....	44
Fig. 4.5 The relationship between determined and calculated K_{OC} values of NP111 on Yangtze River sediments.....	46
Fig. 4.6 Influence of pH value on NP111 adsorption to A HA and ES FA.....	48
Fig. 4.7 Correlations between K_{OC} of NP111 and alkyl carbon content (a), aliphaticity (b) and aromaticity (c) of HAs isolated from Yangtze River sediments.....	49
Fig. 4.8 Adsorption isotherms of PFOA on sediments (a) and sediment model components (b)	54
Fig. 4.9 Aggregation behavior of pristine M3 sample over salinity (NaCl and CaCl_2 solutions)	59
Fig. 4.10 Titration of pristine (a) and purified (b) MWCNTs	60
Fig. 4.11 Representative overview of TEM images of CP (a, b), BA (c, d) and M3 (e, f)	61
Fig. 4.12 FT-IR spectra of pristine multi walled carbon nanotubes.....	62
Fig. 4.13 Adsorption isotherms of PFOA onto CP and BA MWCNTs in 10 mM of NaCl solution: a) PFOA on pristine MWCNTs, b) PFOA on purified MWCNTs.....	66
Fig. 4.14 Desorption isotherms of PFOA onto pristine MWCNTs.....	69
Fig. 4.15 Adsorption isotherms of PFOA on pristine M3 at 288 K, 303 K and 318 K.....	70
Fig. 4.16 Influence of pH on the adsorption of PFOA on the pristine CP and BA MWCNTs..	72
Fig. 4.17 Influence of salinity on PFOA adsorption on the pristine CP and BA MWCNTs	73
Fig. 4.18 Influence of cation species on PFOA sorption on pristine M3 MWCNTs.....	75

SOPRTION OF A NONYLPHENOL ISOMER AND PERFLUOROOCTANOIC ACID ON
GEOSORBENTS AND CARBON NANOTUBES

Fig. 4.19 Adsorption isotherms of NP111 on pristine (a and b) and purified MWCNTs (c and
d)76

LIST OF TABLES

List of tables

Table 3.1 Some physicochemical properties of NP111 and PFOA	21
Table 4.1 Properties of the Yangtze River sediments.....	32
Table 4.2 Properties of mineral adsorbents.....	32
Table 4.3 Freundlich parameters of and K_{OC} ($L\ kg^{-1}$) values of NP111 calculated based on the organic carbon content and distribution coefficient (K_d) simulated in NP111 equilibrium concentration range 0–200 $\mu g\ L^{-1}$ by the linear model.....	33
Table 4.4 K_{OC} values of NP111 and percentage of functional groups of humic substances (from solid-state ^{13}C DP/MAS NMR spectra)	42
Table 4.5 Freundlich parameters and K_{OC} ($L\ kg^{-1}$) values of PFOA calculated based on the organic carbon content and distribution coefficient (K_d) simulated in PFOA equilibrium concentration range 0–200 $\mu g\ L^{-1}$ by the linear model.....	55
Table 4.6 Zeta potential of pristine and HCl-treated MWCNTs.....	63
Table 4.7 Metal concentrations of MWCNTs before and after HCl treatment.....	64
Table 4.8 The parameters of Freundlich and Langmuir models obtained from mass based PFOA adsorption data.....	67

SOPRTION OF A NONYLPHENOL ISOMER AND PERFLUOROOCTANOIC ACID ON
GEOSORBENTS AND CARBON NANOTUBES

Abbreviations

AS	Agricultural soil in Halle, Germany
BA	Multi walled carbon nanotubes purchased from Bayer Material Science, Germany
BET	Brunauer-Emmett-Teller
BPA	Bisphenol A
CCC	Critical coagulation concentration
CME	Chongming Island East
CMW	Chongming Island West
CNTs	Carbon nanotubes
CP	Multi walled carbon nanotubes purchased from Nano. Tech. Labs Inc., USA
CP/MAS	Cross polarization/magic angle spinning
CQ	Chongqing
DP/MAS	Direct polarization/magic angle spinning
FA	Fulvic acid
FS	Forest soil in Steinkreuz, Germany
FT-IR	Fourier transform infrared spectroscopy
HA	Humic acid
HPLC	High performance liquid chromatography
ICP-MS	Inductively coupled plasma mass spectrometry
LSC	Liquid scintillation counting
MWCNTs	Multi walled carbon nanotubes
M3	Multi walled carbon nanotubes purchased from Chengdu Organic Chemicals Co. Ltd., China
NJ	Nanjing
NMR	Nuclear magnetic resonance

ABBREVIATION

NOM	Natural organic matter
NP	Nonylphenol
NPhEOs	Nonylphenol polyethoxylates
OC	Organic carbon
OM	Organic matter
PAHs	Polycyclic aromatic hydrocarbons
PFCs	Perfluorinated compounds
PFOA	Perfluorooctanoic acid
PFOS	Perfluorooctanoic sulfate
PZC	Point of zero charge
SDS	Sodium dodecyl sulfate
SR	Suwannee River
SSA	Specific surface area
TEM	Transmission electron microscope
TG	Thermogravimetry
TOC	Total organic carbon
WH	Wuhan
ZG	Zigui
ZP	Zeta potential

SOPRTION OF A NONYLPHENOL ISOMER AND PERFLUOROOCTANOIC ACID ON GEOSORBENTS AND CARBON NANOTUBES

Symbols

$1/n$	Freundlich exponent	-
b	The limited monolayer adsorption capacity	$\mu\text{g g}^{-1}$
C	Solute concentration in the liquid phase	$\mu\text{g L}^{-1}$
C_0	Input concentration	$\mu\text{g L}^{-1}$
C_{initial}	Initial solute concentration in the liquid phase	$\mu\text{g L}^{-1}$
C_s	Total solute concentration remaining in the equilibrium solution	$\mu\text{g L}^{-1}$
C_w	Equilibrium solute concentration	$\mu\text{g L}^{-1}$
f_{OC}	Organic carbon content in soil/sediment	g g^{-1}
K_0	The thermodynamic equilibrium constant	L kg^{-1}
K_d	Solid-water distribution coefficient	L kg^{-1}
K_f	Freundlich equilibrium constant	$\mu\text{g}^{(1-1/n)} \text{L}^{1/n} \text{g}^{-1}$
K_L	Langmuir equilibrium constant	$\text{L } \mu\text{g}^{-1}$
K_{OC}	OC standardized distribution coefficient	L kg^{-1}
P_A	The equilibrium pressure of the gas	Pa
pK_a	Acidity constant	-
U_E	The electrophoretic mobility	$\text{cm}^2 \text{V}^{-1} \text{s}^{-1}$
ε	The dielectric constant	-
η	Viscosity	$\text{cm}^2 \text{s}^{-1}$
θ_o	The monolayer coverage	%
θ_A	The gas coverage	%
ζ	Zeta potential	mV

Note: - non-unit

Chapter 1 Introduction

Organic chemicals will be inevitably released into environmental river compartments with the production and application of numerous anthropogenic organic compounds. The transport and degradation of organic chemicals results in adverse effects for the aqueous system, for example decreasing water quality, reduction in aquatic biodiversity, and even a threat to human health. In order to improve water quality and to decrease water source pollution, a mechanistic study of the environmental fate of organic pollutants is the current focus for water researchers. Indeed, in the case of riverine systems, information about the environmental fate and sorption behavior of organic pollutants in river sediments is an important prerequisite for assessing the risk, remedying the contamination and protecting the river and its surrounding area and simultaneously enabling the further safe reuse of this water resource.

1.1 Surfactant degradation products

Nonylphenol polyethoxylates (NPnEOs) are widely used commercially as nonionic surfactants for example in the pulp, paper, and textile industries, as well as for the production of household and industrial detergents (Shao et al., 2005). The global annual consumption of NPnEOs amounts to more than one Mt (Berryman et al., 2004). With this widespread application, NPnEOs inevitably appear in sewage treatment plants, and even in the environment via wastewater or application to agricultural land of sludge from the wastewater treatment plants (Das and Xia, 2008).

Perfluorinated organic compounds (PFCs) are widely utilized as special surfactants in cosmetics, aerospace, electronics, and medical use, and are also employed in different industrial processes such as in protective coatings, wiring insulation for telecommunications and in fire-fighting foams (Prevedouros et al., 2006). Point sources of PFCs such as manufacturing facilities are one of the largest emission sources (Prevedouros et al., 2006; Davis et al., 2007). Effluents from municipal and industrial

SORPTION OF A NONYLPHENOL ISOMER AND PERFLUOROOCTANOIC ACID ON GEOSORBENTS AND CARBON NANOTUBES

wastewater treatment plants are minor sources of the occurrence of PFCs (Schultz et al., 2005; Sinclair and Kannan, 2006). Furthermore, volatile atmosphere precursors, *e.g.* alcohol fluorotelomers, may also make an important contribution to PFC levels in remote regions (Ellis et al., 2004).

While the fate of NPnEOs has been intensively studied (Lu et al., 2009), less is known about the environmental behavior of the PFCs. Nevertheless, NPnEOs can be biodegraded to nonylphenols (NPs) (Jonkers et al., 2003), which are more toxic than their parent (Giger et al., 1984). PFCs can also be degraded to perfluorooctanoic acid (PFOA) (Hansen et al., 2002; Renner, 2008), which have been extensively studied.

1.2 Nonylphenols in environmental compartments

Nonylphenol (NP) is an industrial chemical with a high production volume exhibiting endocrine-disrupting and toxic potential (Granmo et al., 1989; Ekelund et al., 1990). As a consequence of the discharge and biodegradation processes of its precursors, NP ubiquitously occurs in the environment. The technical mixture of NPs actually contains more than 20 isomers with different branches of the alkyl chain (Thiele et al., 2004). Branched NPs have higher endocrinic activity than linear ones (Preuss et al., 2006). The mixture of NPs, which simultaneously emerges, hinders or complicates the study of sorption behavior in the environmental matrixes.

In Europe, NP concentrations range from 0.15 to 7.32 $\mu\text{g L}^{-1}$ in river water (Parrolocco et al., 2006) and from 3.0×10^{-5} to 0.97 $\mu\text{g g}^{-1}$ in sediments based on dry weight (Heemken et al., 2001; Parrolocco et al., 2006; Navarro et al., 2009). In China, NP concentrations range from 3.4×10^{-3} to 7.80 $\mu\text{g g}^{-1}$ in sediments (Hu et al., 2005; Chen et al., 2006; Jin et al., 2008) and from 0.02 to 6.85 $\mu\text{g L}^{-1}$ in fresh surface water of rivers (Shao et al., 2005; Chen et al., 2006).

Although degradation (Ekelund et al., 1993; Cirja et al., 2006; Li et al., 2007) and

CHAPTER 1 INTRODUCTION

removal of NP from waste or drinking water (Brunner et al., 1988; Cirja et al., 2006) have been intensively studied, the sorption of NP on the environmental matrixes *e.g.* soil and sediment is a crucial process that predominates its fate, transport and transformation. Navarro et al. (2009) reported that sorption isotherms of a linear NP isomer (4-*n*-NP) on Ebro River sediments were fitted well by the Freundlich model. Nagasaki et al. (2004) investigated NP sorption on Na-montmorillonite, α -Al₂O₃, α -SiO₂, and gibbsite and observed that NP was adsorbed on the broken edges of octahedral alumina sheets of Na-montmorillonite. In a sorption study of a NP isomers mixture containing branched isomers in soil samples, it was found that the K_{OC} values of NP depended sensitively on organic matter sources from agricultural soils and forest soils, and linear and branched NP isomers have the distinct sorption isotherms (Düring et al., 2002). Indeed, Krahe et al. (2006) found based on 193 soil samples that the quality of soil organic matter presumably played an important but not quantified role in the sorption of a technical mixture of NP. In a sorption study with 4-*n*-NP, Yamamoto et al. (2003) found that K_{OC} values on Aldrich HA and Suwannee River HA were 6.8×10^4 and 9.1×10^4 L kg⁻¹, respectively.

The sorption of NP directly on pure or isolated organic matter is sparsely documented. Hoellrigl-Rosta et al. (2003) used dialysis technique to investigate the association of 4-*n*-NP directly on dissolved organic matter in soil, and illustrated that the sorption coefficient (K_{OC}) is 8970 L kg⁻¹. The binding of a NP mixture on different forms of organic carbon such as cellulose, chitin, lignin and humic acids was evaluated, and it was found that the organic carbon normalized partitioning coefficients (K_{OC}) varied and markedly depended on the forms of organic carbon (Burgess et al., 2005).

Solution chemical factors such as pH seem to be a factor influencing NP affinity to soil/sediment materials and maybe be dependent on both texture of soil/sediments and the properties of solute. Düring et al. (2002) interpreted the difference of the K_{OC} values of NP in agricultural soils and forest soils by differing proton activity in soil samples *i.e.* the pH range of 3.0–4.3 in forest soils and 5.2–7.8 in agricultural

SORPTION OF A NONYLPHENOL ISOMER AND PERFLUOROOCCTANOIC ACID ON GEOSORBENTS AND CARBON NANOTUBES

soils. Furthermore, the pH value in soil samples negatively related to the sorption affinity of a technical NP mixture on soil samples in the pH range of 3–8 although this range of pH is apparently below the pK_a of NP 10.7 (Burgess et al., 2005). Meanwhile, Hoellrigl-Rosta et al. (2005) pointed out that the adsorbed amount of 4-*n*-NP was almost consistent under acidic and neutral conditions, while the amount decreased at alkaline conditions. In fact, there are only a few investigations about the sorption behavior of branched NP.

1.3 Perfluorooctanoic acid in environmental compartments

PFOA is gradually becoming the subject of much concern due to potential toxicity (Kudo and Kawashima, 2003; Fuentes et al., 2007) and widespread occurrence in terrestrial systems (Shoeib et al., 2006; Wania, 2007). PFOA is not only manufactured and directly applied as a surfactant and intermediate in the industry and domestic products, but it is also introduced by degradation of its precursors, such as the fluorotelomer alcohols and perfluoroalkyl sulfonamides (Armitage et al., 2006; Deon et al., 2006; Armitage et al., 2009). In particular, PFOA is used as an adjuvant in the production process of fluoropolymers such as PTFE, Teflon[®] or similar products, and occurs in these applications as aqueous and gaseous emission (Davis et al., 2007). The distribution of PFOA in various environmental compartments, *e.g.* air (McMurdo et al., 2008), aqueous phase (So et al., 2004; McLachlan et al., 2007), snow (Young et al., 2007), sediments (Higgins et al., 2005; Higgins and Luty, 2007), soils (Ellefson, 2001), biota (Dai et al., 2006) and humans (Ericson et al., 2008), has been frequently documented.

The stability of PFOA in the environmental compartments was well documented. PFOA is resistance to natural degradation and transformation such as biodegradation (Liou et al., 2010) and direct photolysis. Hereby the inertness of PFOA is the reason for the ubiquitous occurrence of PFOA in the natural matrixes, in particular for remote area *e.g.* pole area (Wania, 2007). Furthermore, PFOA was referred as a novel chemical

CHAPTER 1 INTRODUCTION

tracer to investigate the global circulation of ocean water due to its outstanding stability under the marine conditions (Yamashita et al., 2008).

The distribution of PFOA has mostly been documented in surface water at America (Hansen et al., 2002), in aqueous phase at Europe (Loos et al., 2007; McLachlan et al., 2007; Pistocchi and Loos, 2009), in water in Japan (Taniyasu et al., 2003) and in snow at the Arctic area (Shoeib et al., 2006; Ko et al., 2007). In China, PFOA was observed in fresh river water (Antelo et al., 2005; Chen et al., 2007).

To our knowledge, there is less studies on sorption of PFOA on the environmental matrixes. In a study of PFOA on sediments, Higgins and Luthy (2006) observed significant sorption of other PFCs rather than PFOA on sediments. A low sorption of PFOA on Brill sandy loam soil was found (Division, 2002). The K_{OC} value of PFOA calculated on the distributed coefficient of PFOA and organic carbon content in soil and sediments ranged from 14 to 130 L kg⁻¹. For the sake of the removal of PFOA, the investigations of sorption on artificial materials are frequently augmenting. In case of the sorption of PFOA on granular activated carbon, zeolite and sludge, the monolayer sorption capacity (Langmuir model) on granular activated carbon is significantly higher than that on zeolite and sludge, certainly higher than that on soils or sediments (Ochoa-Herrera and Sierra-Alvarez, 2008). The sorption of PFOA on powder activated carbon also displays that the sorption capacity of PFOA on powder activated carbon is higher than that on soils and sediments too (Qu et al., 2009). Very recently, the sorption of PFOA on multi walled carbon nanotubes (MWCNTs) with different oxygen contents was investigated (Li et al., 2010).

PFOA, like many other organic surfactants, contains hydrophobic and hydrophilic domains and is ionized as a function of the pH of the matrix. The different forms of PFOA are expected to adsorb on sediment or soil via electrostatic interaction and hydrophobic attraction (Koopal et al., 2004). Both sorption mechanisms were verified by Higgins and Luthy (2006) in case of the sorption of perfluorinated surfactants on

SORPTION OF A NONYLPHENOL ISOMER AND PERFLUOROOCTANOIC ACID ON GEOSORBENTS AND CARBON NANOTUBES

sediments. Accordingly, we assume that the sorption of PFOA is affected not only by the quantity, composition and structure of sediment/soil colloids (Thiele-Bruhn et al., 2000), but also by the specific properties of PFOA.

Due to few studies on PFOA sorption, the effects of environmental factors such as pH value and ionic strength were less evaluated. Higgins and Luthy (2006) found that the sorption of PFCs on sediments increased with increasing the solution concentration of Ca^{2+} and decreasing the pH of supernatant, suggesting that the electrostatic interaction plays an important role in the sorption of PFCs. Li et al. (2010) also reported that sorption capacity of PFOA on MWCNTs decreased with increasing pH, especially for MWCNTs with low oxygen content.

It should be emphasized that normalizing PFOA concentration to organic carbon might not be appropriate because PFOA does not readily partition into lipid or other forms of organic carbon such that using this approach may overestimate effect of organic carbon on the adsorption of this compound to soils and sediments (Hites, 2006). Generally, the sorption affinity of PFOA on environmental matrixes is relatively low, the environmental concentration of PFOA is thus dependent on the discharge extent (Wania, 2007).

1.4 NP and PFOA contamination in Yangtze River

In China, the occurrence of NP has been documented in both water and sediment (Hu et al., 2005; Chen et al., 2006; Jin et al., 2008). Shao et al. (2005) reported that NP concentration ranged from 0.02 to 6.85 $\mu\text{g L}^{-1}$ in the water column of Yangtze River and Jialing River, which is a branch river for Yangtze River, at Chongqing Valley. Lu et al. (2009) investigated biodegradation of NPnEOs, which are the precursors of nonylphenol, in estuary sediment of Yangtze River and found that the biodegradation of NPnEOs was efficient under either aerobic or anaerobic conditions. This will absolutely increase the distribution of NP in the river system. In 2010, it was reported

CHAPTER 1 INTRODUCTION

that NP as one of the endocrine disruptors was monitored in wild carp (*Cyprinus Carpio*) and catfish (Oriental catfish) taken from Chongqing, Wuhan, Maanshan and Nanjing along the Yangtze River (<http://news.sina.com.cn/z/huanjingjisu/index.shtml>).

It is to note that PFOA concentrations range from 2 to 260 ng L⁻¹ in fresh river water and PFOA is the predominant PFCs in water from the Yangtze River (So et al., 2007). The concentrations of PFCs in water taken along the Yangtze River from Chongqing, Yichang, Nanjing and Shanghai are analyzed, and the highest concentration and most PFCs are observed in the sample from Shanghai (So et al., 2007). The concentration range of PFOA in water from the Yangtze River is higher than that from other places in China, such as Hong Kong (0.73–5.5 ng L⁻¹) and Pearl River Delta (0.24–16 ng L⁻¹) (So et al., 2004). Nevertheless, the concentration of PFOA in sediments taken from Huangpu River, which is a branch river for Yangtze River nearby Shanghai, ranged from 0.20 to 0.64 ng g⁻¹ dw. (Bao et al., 2010).

Furthermore, the total PFCs concentration of tap water from Shanghai, Nanjing and Wuhan are around 130, 15 and 35 ng L⁻¹, respectively, while the concentration of PFOA is 78 ng L⁻¹ in Shanghai sample, indicating that PFOA accounts for the prevailing contribution to PFCs. A similar trend is not observed for the samples from Nanjing and Wuhan (Mak et al., 2009).

Conversely, nowadays, the knowledge of the sorption of NP and PFOA on Yangtze River sediments is still lacking. It is well known that the sorption behavior of NP and PFOA on sediments is essential for assessing their environmental risk and remedying their adverse effects.

1.5 Organic matter interactions with organic pollutants

Organic matter (OM) strongly influences the fate of anthropogenic chemicals (Rees,

SORPTION OF A NONYLPHENOL ISOMER AND PERFLUOROOCTANOIC ACID ON GEOSORBENTS AND CARBON NANOTUBES

1980; Kan and Tomson, 1990; Jin et al., 2008). OM fractions such as humic acid (HA), fulvic acid (FA), and humin have been reported to have various sorption capacities of organic contaminant compounds (Weber et al., 1992; Liu et al., 2010). OM is generally defined on the basis of the elemental content and the composition of functional groups, whose polarity, aromaticity, and aliphaticity are characterized (Chin et al., 1997; Kile et al., 1999; Salloum et al., 2002). The polarity, aromaticity, and aliphaticity of OM were usually estimated from its structural components characterized by nuclear magnetic resonance (NMR) spectroscopy *e.g.* solid-state ^{13}C direct polarization/magic angle spinning (DP/MAS) NMR (Hatcher, 1987; Zech et al., 1997).

In fact, it is a challenge to establish the correlations between the OM characteristics and the sorption affinity of organic contaminants, and this has been a matter of controversy (Chiou et al., 1998; Kang and Xing, 2005). On the one hand, the polarity has some advantages in predicting nonylphenol partitioning when merely considering a very few samples consisting of the cellulose, chitin and lignin (Burgess et al., 2005). Thus, OM with a higher aromatic fraction enhanced the sorption affinity of polycyclic aromatic hydrocarbons (PAHs) (Chiou et al., 1998). On the other hand, a direct correlation between K_{OC} values of phenanthrene and the paraffinic carbon content of OM also exists (Salloum et al., 2002). In the same way, the alkyl C and carbonyl C fraction had a strong positive correlation with the sorption of nitro-aromatic compounds, indicating that aliphatic moieties dominate sorption (Singh et al., 2010). The importance of both aliphatic and aromatic moieties has been suggested for the sorption of polycyclic aromatic compounds (PAHs) (Gunasekara et al., 2003).

1.6 Innovative material for water treatment — Carbon nanotubes

Carbon nanotubes (CNTs) consist of graphene sheets rolled into a cylinder (Iijima, 1991), which are generally regarded as ideal candidates for widespread applications in medical science, material science and solar battery due to their unique physicochemical

CHAPTER 1 INTRODUCTION

properties (Nowack and Bucheli, 2007; Klaine et al., 2008). One of potential environmental applications of CNTs, as superior sorbents, has been intensively investigated in the case of toxic chemicals *e.g.* metallic ions such as lead (Chen et al., 2008a) and zinc (Lu and Chiu, 2006), and organic chemicals such as PAHs (Yang et al., 2006), phenolic compounds (Lin and Xing, 2008), chlorophenol (Chen et al., 2009), and trihalomethanes (Lu et al., 2005). Very recently, the sorption of PFOA on MWCNTs with different oxygen contents was investigated at high concentrations (Li et al., 2010).

Sorption mechanisms on CNTs, which have intensively been reported, are dependent not only on the specific physicochemical properties of CNTs, but also on the substantial characteristics of solute. The sorption of metallic ions on CNTs is generally governed by electrostatic interaction (Wang et al., 2005; Lu and Chiu, 2006). Hydrophobic interaction plays an important role in the sorption of hydrophobic organic compounds (HOCs) such as PAHs (Yang et al., 2006) and NP (Li et al., 2010) by CNTs. The π - π interaction between aromatic chemicals and graphene sheet of CNTs has been reported in a few studies (*e.g.* (Chen et al., 2007)). PFOA sorption on MWCNTs is attributed by the hydrophobic interaction (Li et al., 2010). Indeed, Pan and Xing (2008) recently drew a general conclusion that sorption of organic compounds by CNTs was regulated by multiple mechanisms.

Cai et al. (2003) reported that multi walled carbon nanotubes at least was comparable to C₁₈ silica for the extraction of 4-*n*-NP, and was better than XAD-2 copolymer although the sorption coefficients of 4-*n*-NP are not determined. However, to our knowledge, the sorption of a branched nonylphenol isomer on carbon nanotubes has not investigated yet.

Desorption of organic compounds on carbon nanotubes is widely documented. Based on the study of the adsorption-desorption of monoaromatic compounds on carbon nanotubes, Ji et al. (2010) found no hysteresis. The probable reason is attributed to the

SORPTION OF A NONYLPHENOL ISOMER AND PERFLUOROOCTANOIC ACID ON GEOSORBENTS AND CARBON NANOTUBES

interconnected pore structure and less pore deformation of carbon nanotubes. Conversely, the pronounced hysteresis of bisphenol A (BPA) on carbon nanotubes is observed by Pan et al. (2008b). The possible cause refers to that the bundles or aggregates of CNTs could be rearranged after adsorption BPA in this study, resulting in different pathways between adsorption and desorption.

Commercial carbon nanotubes vary significantly with respect to impurities (*e.g.* amorphous carbon and catalysts) that can further complicate their sorption properties for organic contaminants. Although pristine CNTs are usually directly applied without any purification, in the case of sorption studies, CNTs are frequently purified by different methods in order to avoid the impact of impurities (Lu et al., 2005; Wang et al., 2005; Lu and Chiu, 2006; Yang et al., 2006; Chen et al., 2008b). Purification procedures are usually performed by applying a single acid or a mixture of strong acids such as HCl, HNO₃ and H₂SO₄. By this treatment, functional groups can be introduced at the surface of CNTs after an oxidation in the presence of HNO₃ or/and H₂SO₄, which consequently alter the CNTs sorption behavior for organic compounds (Schierz and Zaenker, 2009; Su et al., 2010). HCl treatment removes only the impurities from the outer surface of MWCNTs without any oxidation (Datsyuk et al., 2008). However, the difference in adsorption behavior with or without purification of MWCNTs by HCl has not been studied so far.

1.7 Objectives of the thesis

1) Sorption of NP111 on Yangtze River sediments and model components

So far, the sorption of NP111 (4-[1-ethyl-1,3-dimethylpentyl] phenol) on natural matrices such as soil and sediment has been little studied although NP111 is of environmental relevance. In this study, we evaluated the sorption behavior of ¹⁴C-labeled NP111, which NP isomer had the highest endocrinic activity among all

CHAPTER 1 INTRODUCTION

isomers (Preuss et al., 2006), on Yangtze River sediments. In addition, the sorption mechanism of NP111 on model geochemical sorbents like illite, δ -Al₂O₃, goethite and a reference Suwannee River natural organic matter was studied.

2) Effect of structural composition of humic acids isolated from Yangtze River sediments on the sorption of NP111

It was assumed that the sorption behavior of NP111 is controlled by the properties of HAs, which are characterized by their structural compositions. To better understand the sorption mechanisms, it is advantageous to study HAs of comparable origins where chemical compositions vary but exhibit some structural homogeneity. This can be proposed with isolated HAs from six sampled sediments along the Yangtze River. For comparison, some reference HAs were also involved in the study.

3) Sorption of PFOA on Yangtze River sediments and their model components

As yet, the sorption of PFOA on geosorbents such as soil and sediment has been little studied although PFOA is a problematic environmental pollutant. In this study, we thus evaluated the sorption behavior of ¹⁴C-labeled PFOA on Yangtze River sediments. In addition, the sorption of PFOA on model geochemical sorbents like illite, δ -Al₂O₃, goethite and a reference river natural organic matter was studied.

4) Sorption of PFOA and NP111 on multi-walled carbon nanotubes

Although the PFOA adsorption on MWCNT in high concentration range was reported in a very recent paper (Li et al., 2010), the sorption investigations at environmental relevant low concentrations are still lacking. According to our knowledge, this is the first time that the sorption of NP111 on MWCNTs is studied. Three commercial MWCNTs synthesized with different metallic catalysts were used, one of them with catalyst traces on the outer surface of MWCNTs. Additionally, the effect of both the MWCNTs' purity and solution chemical parameters, such as pH and salinity, were studied.

Chapter 2 Theoretical background

2.1 Sorption of organic compounds from aqueous solution

A sorption process describes the association or diffusion of solute (adsorbate) on/into solid phase (adsorbent) from aqueous phase. Depending on both the adsorbent or adsorbate (adsorptive) properties and the sorption mechanisms, it may be clearly distinguished into partition (dissolution) and adsorption. The term of “sorption” is inclusive of adsorption (a two-dimensional process) and partition/dissolution (a three-dimensional process).

In terms of partition, the principle is the law of similar mutual solubility due to the comparable characteristic of both sorbate and sorbents. Partition process usually takes place in soft, amorphous and penetrable domains, hence it is regularly thought of as a dissolution process in such domains, such as organic matter originated from soil and sediment. The partition coefficient (K_d) is independent of the solute concentration. Thereby, the partition of solute is properly assessed with a partition coefficient by a linear equation (Chiou et al., 1979).

In contrast to the partition process, the adsorption (a two-dimensional process) describes a process in which the solute accumulates onto the surfaces or into the pores of a solid adsorbent (Chiou, 2002). The active site for the adsorption is assumed to be distributed on the surface of adsorbents. The excess of active site on the surface occurs and hence there is more potential for adsorption when the attractive energy of a substance with a solid surface is greater than the cohesive energy of the substance itself (Manes, 1998). The equilibrium will be reached when the attractive energy on the active site equals to the cohesive energy of a solute. Meanwhile, the maximal sorption capacity will appear.

CHAPTER 2 THEORETICAL BACKGROUND

Depending on the adsorption force, adsorption process can be roughly distinguished into physical adsorption and chemical adsorption, though their boundary is not always sharp and clear (Chiou, 2002). For physical adsorption, both Van der Waal's interaction and electrostatic attraction between solutes and adsorbents play the important roles. The specific surface area and porosity of the adsorbent are usually the principal factors affecting the physical adsorption. On the one hand, the different pore size and volume significantly affect the adsorption of solute due to the various capillary actions, the specific site on the inner surface of pore and the size-sieving effect (Zhang et al., 2010b). On the other hand, the surfaces of solids are heterogeneous and consequently adsorption sites with cohesive energies are variable. The adsorption sites are taken up sequentially, starting from the highest energy adsorption sites to the lowest energy adsorption sites, with increasing solute concentration (Chiou, 2002).

In contrast, chemical sorption is commonly owned to specific interactions *i.e.* hydrogen-bond, ligand and covalent interactions (Goss and Schwarzenbach, 2001). Hydrogen-bond interaction occurs between interaction partners with complementary properties, *i.e.* a hydrogen donor-acceptor system. Indeed, H-bonds are specific interactions, where a hydrogen atom covalently bound to two strongly electronegative atoms (Goss and Schwarzenbach, 2001). Covalent interaction is characterized by the sharing of pairs of electrons between atoms. It is very common for the binding of organic compound with radical atoms (Senesi, 1992; Pichon et al., 1998). Ligand binding of organic compounds on the environmental matrixes can be divided into specific binding and non-specific binding. The former one refers to the defined receptors for solute. However, the latter is merely proportional to the equilibrium concentration. In the adsorption of organic contaminants on oxides, ligand interaction governs the sorption (Stone et al., 1993).

Generally, the affinity and capacity of adsorption depends on the physical and chemical properties of both sorbate and adsorbent. For example, high specific surface

SORPTION OF A NONYLPHENOL ISOMER AND PERFLUOROOCTANOIC ACID ON GEOSORBENTS AND CARBON NANOTUBES

area and porosity of adsorbent and small molecular size, planarity characteristics of sorbate will enhance the adsorption uptake (Wang and Xing, 2007). Therefore, the properties of both solute and adsorbents will be essentially considered when the sorption behavior between them is investigated.

2.2 Desorption hysteresis

Desorption hysteresis is the evident asymmetry of sorption-desorption processes (Pignatello and Xing, 1995). The benefit of this phenomenon is to sequester organic compounds or retard the release of organic compounds from the adsorbents to some extent. So characteristics of desorption hysteresis are essential for both remedying the contamination in water and terrestrial compartments, and protecting the environmental surrounding.

There are several reasons resulting in the observed desorption hysteresis phenomena. These reasons were probably attributed to two types *i.e.* steric hindering of adsorbents and chemisorption. First, the chemisorption with specific interaction, ligand interaction or covalent attraction is prevailing. Second, with respect to the adsorption-desorption of organic compounds on solid matrixes such as soils, sediments and charcoal, desorption hysteresis is attributed to irreversible pore deformation of the adsorbent by the sorbate and the formation of meta-stable states of sorbate in the fixed mesopores (Kan et al., 1994; Huang and Weber, 1997; Braida et al., 2002).

Besides, the desorption hysteresis can be resulted from the artifacts, such as non-equilibrium adsorption, loss of sorbate, “colloid effect” due to solubility enhancement and solution replacement (Huang et al., 1998; Pan et al., 2008b).

2.3 Sorption of pollutants on organic matter

Organic matters are complex because of their content of carboxylic and phenolic moieties that also contains nonpolar regions. Thereby, the structure and property of OM enable binding to organic contaminants via ionic, electron donor-acceptor mechanism as well as Van der Waal's forces and hydrophobic interaction (Hoellrigl-Rosta et al., 2003).

Certainly, the electrostatic interaction usually takes place between adsorbent and solute, especially for polar organic compounds, which are potentially deprotonated and have ionic forms. For instance, the sorption of cations on humic substances is assigned to the weak electrostatic attraction of the counterions because of the negative charged humic substances and the positive charged cations (Tipping, 2002). The sorption of polar organic compounds, such as carboxylic acid and phenolic chemicals, on humic substances is frequently interpreted by the electrostatic attraction too (von Oepen et al., 1991). Additionally, with respect to the sorption of pyridine on dissolved humic acids, the π - π interaction predominates the sorption (Nanny and Maza, 2000)

Organic matter in natural environment was distinguished from "rubbery" and "glassy" type carbons (Xing and Pignatello, 1997; Chiou et al., 1998; Kile et al., 1999). In general, the hydrophobic interaction drives partition process, particularly in rubbery carbons (Salloum et al., 2002). Nevertheless, the capillary filling and the specific sorption that take place in glassy carbon domains aren't usually regarded as the partition (Zhang et al., 2010a). The former one requires less time to reach the equilibrium than the latter one. Generally, the partition process will lead to the linear sorption isotherm.

2.4 Sorption models

When a solute is adsorbed into/onto a solid phase or surface from aqueous phase, the adsorbed amount per unit mass of the solid (C_s , $\mu\text{g kg}^{-1}$) is dependent on both its equilibrium aqueous concentration (C_w , $\mu\text{g L}^{-1}$) and the temperature. When the sorption is studied at a fixed temperature, C_s is only a function of C_w . The relation between C_s and C_w at a given temperature is called sorption isotherm. Graphically, it is designed by plotting C_s against C_w .

A sorption isotherm enables one to assess the sorption linearity/nonlinearity and the sorption properties. In order to quantitatively describe and mechanistically interpret the sorption isotherms, different models have been developed and applied for partition and adsorption processes, respectively.

2.4.1 Linear model

Partition is a linear sorption process, and the adsorbed concentration is proportional to that in the aqueous phase. Such linear relation is frequently referred to as Henry's law (Eq. (1)). The constant ratio is defined as a distribution coefficient (K_d , L kg^{-1}).

$$C_s = K_d C_w \dots\dots\dots(1)$$

The chemical sorption of hydrophobic organic solutes to natural soils and sediments is a linear partition process in the OM matrix. Hence, the partition coefficient is frequently normalized by the organic carbon content of soil or sediment (f_{OC} g g^{-1}) to gain the partition coefficient K_{OC} (L kg^{-1}) between the aqueous phase and the organic carbon (OC) phase (Eq. (2)). The assumption to calculate K_{OC} is that nonionic, nonpolar organic compound is adsorbed on the organic matter in soil/sediment.

$$K_{OC} = \frac{K_d}{f_{OC}} \dots\dots\dots(2)$$

Indeed, the K_{OC} and $\log K_{OC}$ values are widely used for the characterization of hydrophobic organic chemicals sorption.

CHAPTER 2 THEORETICAL BACKGROUND

Some organic sorbates like pesticides and surfactants, which composed of polar functional groups as well as nonpolar groups, display neither the sorption characteristics of nonpolar molecules nor the more robust sorption behavior of the acidic, basic, or ionic organic compounds. Consequently, the former equation (Eq. (2)) is not sufficient for this class of organic compounds (Bride, 1994). It is worthwhile to note that the application of the equation at random will produce unreliable result and consequently lead to the serious mistake in the prediction of organic compounds in the environment.

2.4.2 Nonlinear models

Freundlich model

The empirical Freundlich model is often applied for describing nonlinear sorption to natural soils and sediments by fitting two parameters (McGinley et al., 1993). Freundlich model (Eq. (3)) is followed as

$$C_s = K_f C_w^{1/n} \dots\dots\dots(3)$$

in which, K_f ($\mu\text{g}^{(1-1/n)} \text{L}^{1/n} \text{g}^{-1}$) is the Freundlich coefficient and $1/n$ is the exponent with value <1 standing for a convex nonlinear curve. K_f is a measure of the sorption capacity where the unit depends on the $1/n$ value; $1/n$ is a measure of the heterogeneity of the sorption sites (Weber et al., 2002).

The values of $1/n$ are often found in the range of 0–1. As $1/n$ approaches 0, the surface site heterogeneity increases. It can be noticed that the Freundlich equation is identical to the linear sorption equation with $1/n = 1$, where the K_f equals to the partition coefficient K_d given by the Henry's law.

With two parameters, the Freundlich model and its transformed type were widely applied for fitting nonlinear sorption isotherms of organic compounds from aqueous

SOPRTION OF A NONYLPHENOL ISOMER AND PERFLUOROOCTANOIC ACID ON GEOSORBENTS AND CARBON NANOTUBES

phase onto solid adsorbents with heterogeneous surface properties, generally for heterogeneous solid surfaces. For example, the PAHs sorption to natural soils and sediments was often described well by the Freundlich equations, meanwhile the both partition and adsorption processes occurred (Xing, 1997).

Langmuir model

The Langmuir model originally derives from a monolayer gas adsorption onto a homogeneous dry surface of solid adsorbents that contains a constant number of energetically identical active sites (Langmuir, 1918). The Langmuir model assumes that sorbate molecules form a monolayer on the surface of adsorbents and there is no interaction between the molecules adsorbed on adjacent sites. The same rate of adsorption and desorption on the surface is considered as reaching equilibrium. The equation is followed

$$\theta_A = \frac{\theta_0 K_L P_A}{1 + K_L P_A} \dots\dots\dots(4)$$

where, θ_A and θ_0 is the current gas coverage and the monolayer coverage. P_A (Pa) is the equilibrium pressure of the gas. The Langmuir coefficient K_L is the ratio of adsorption and desorption rate constant, which is related to the heat of adsorption and is considered to be independent of the adsorbed amount (Mathias et al., 1996; Sekar et al., 2004).

Langmuir model is widely applied for the sorption process from aqueous solution. The equation may be written as

$$C_s = \frac{b K_L C_w}{1 + K_L C_w} \dots\dots\dots(5)$$

where, b ($\mu\text{g kg}^{-1}$) is the limited monolayer adsorption capacity. C_s is the adsorbed amount on the solid adsorbent at the equilibrium concentration C_w . The Langmuir coefficient K_L ($\text{L } \mu\text{g}^{-1}$) is the adsorption affinity.

Chapter 3 Materials and methods

3.1 Chemicals and adsorbents

3.1.1 Chemicals

Perfluorooctanoic acid (PFOA)

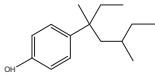
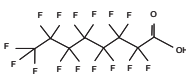
Non-labeled PFOA (96% purity) was purchased from KMF Laborchemie Handels GmbH (Germany) and ^{14}C -labeled PFOA (99% radiochemical purity and 2.04×10^9 Bq mmol $^{-1}$ specific activity) was purchased from Biotrend Chemikalien GmbH (Germany). Non-labeled PFOA stock solution was prepared by suspending one gram of non-labeled PFOA in 1 L Milli-Q water and ultrasonication for 0.5 hour (Sonicator, 50–65 KHz). ^{14}C -radiolabeled PFOA stock solutions were prepared by diluting ^{14}C -PFOA with non-labeled PFOA stock solution. All PFOA solutions were stored at 4°C prior to usage.

4-[1-ethyl-1, 3-dimethylpentyl] phenol (NP111)

Non-labeled NP111 with 99.3% purity was synthesized in large scale by *Friedel-Crafts* alkylation from phenol (Merck, Hohenbrunn, Germany) and 3, 5-dimethyl-3-heptanol (Acocado, Heysham, UK) in presence of boron trifluoride (Merck, Hohenbrunn, Germany) as catalyst (Vinken et al., 2002). ^{14}C -U-ring labeled NP111 (Purity > 97 %) was synthesized from ^{14}C -U-ring labeled phenol (Hartmann Analytic, Braunschweig, Germany) according to the same method (Li et al., 2007). The specific radioactivity of ^{14}C -labeled NP111 was 9.7×10^8 Bq mol $^{-1}$. A stock solution (3.333 g L $^{-1}$) in methanol was prepared by mixing non-labeled and ^{14}C -labeled NP111, and stored in the refrigerator at 4°C prior to usage. Some physicochemical properties of NP are presented in Table 3.1.

SOPRTION OF A NONYLPHENOL ISOMER AND PERFLUOROOCTANOIC ACID ON GEOSORBENTS AND CARBON NANOTUBES

Table 3.1 Some physicochemical properties of NP111 and PFOA

	NP111	PFOA
Structure		
Chemical formula	C ₁₅ H ₂₄ O	C ₈ HF ₁₅ O ₂
Molecular weight	220.35	414.07
Solubility in water (mg L ⁻¹)	4.9±0.4	3400
Log <i>K</i> _{OW}	4.5 ^a	-
p <i>K</i> _a	10.7 ^b	3.8 ^c

Note: ^a (Ahel and Giger, 1993), ^b (Maguire, 1999), ^c (Burns et al., 2008), - not determined

3.1.2 Adsorbents

Sediments and soils

Sediments were taken from Chongqing (CQ), Zigui (ZG), Wuhan (WH), Nanjing (NJ), Chongming West (CMW) and Chongming East (CME) along the Yangtze River, China, in November 2008 (Fig. 3.1). Soil samples were taken from an agricultural soil in Halle (AS) and a forest soil (FS) in Steinkreuz (Germany) (Vinken et al., 2005), respectively. The soil and sediment samples were air-dried, ground and sieved through 2-mm meshes.

Aluminium oxide (δ-Al₂O₃)

Aluminum oxide C (δ-Al₂O₃) (99.6% purity) was purchased from Degussa. It was produced by flame hydrolysis of anhydrous aluminium chloride (AlCl₃). The chlorine impurity, which originated from the production procedure, is residual in the product. In order to eliminate chlorine contamination, δ-Al₂O₃ was heated for 6 h at 1000°C (Tombacz and Szekeres, 2002).

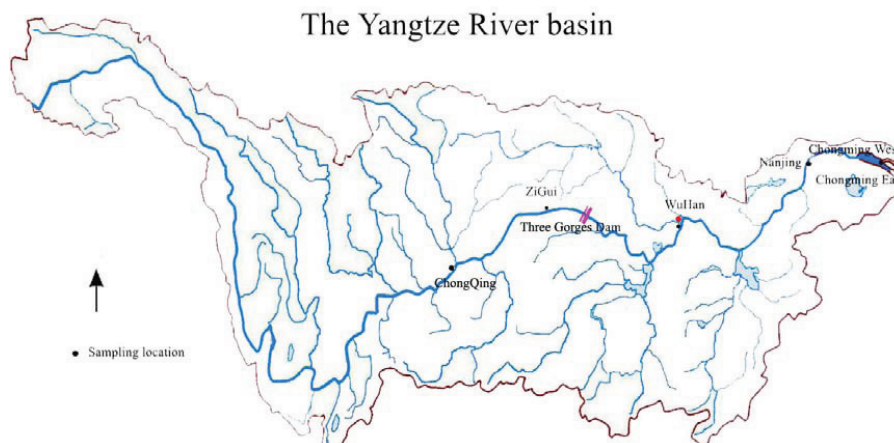


Fig. 3.1 Sediment sampling locations along the Yangtze River

Goethite (α -FeOOH)

For the removal of active cationic species, goethite (Merck, 99% purity) was washed until the conductivity of the leachate was lower than $5 \mu\text{S cm}^{-1}$, and dried at 80°C in the oven.

Illite

Illite (99% purity) was purchased from Cs-Ker Illite Bt (Bekecs, Hungary). To get the homogeneous particles, illite was cleaned by a fractionation method. Briefly, 100 g of illite was suspended with 200 mL Milli-Q water in a 1 L glass bottle and shaken for 6 hours on a horizontal shaker at 150 rpm. Afterwards, 600 mL water was added in and shaken shortly by hand to make it homogeneous. After 6 min sedimentation, the big particles larger than $20 \mu\text{m}$ were deposited on the bottom of the bottle. Illite in the suspension (approx. 700 ml) was collected, frozen-dry, and ground into fine powder for further usage.

Organic matter

Humic acids were isolated from sediments or soils according to an adjusted method recommended by the International Humic Substances Society (IHSS)

SOPRTION OF A NONYLPHENOL ISOMER AND PERFLUOROOCTANOIC ACID ON GEOSORBENTS AND CARBON NANOTUBES

(<http://ihss.gatech.edu/ihss2/>). Briefly, the soil or sediment sample was extracted by 0.1 M NaOH solution at solid-liquid ratio 1:10. The suspension was shaken for 4 hours at 150 rpm on a horizontal shaker. The supernatant after separation was acidified to around pH 1 by 1 M HCl solution. The mixture was left to flocculate overnight, and then centrifuged. The pellet was completely re-dissolved in 0.1 M NaOH solution and then centrifuged again to remove impurities. Afterwards, the supernatant was neutralized with 1 M HCl to pH 6.3–6.5 as raw HA solutions.

Suwannee River (SR) HA and Elliott soil (ES) HA were purchased from the IHSS. Aldrich HA was purchased from Sigma-Aldrich Chemicals (Germany). The raw solutions with commercial organic matters were individually prepared in Milli-Q water. The size fraction of less than 1 kDa was removed from all raw organic solutions by a dialysis technique (1kDa dialysis Membrane from cellulose, VWR International GmbH, Langenfeld, Germany) (Vinken et al., 2002). Afterwards the total organic carbon concentration (TOC) of the organic solutions was determined with a carbon/nitrogen analyzer (Carlo-Erba, NA 1500, Milan, Italy). Finally, one part of solution was freeze-dried to characterize the organic substances by solid-state ^{13}C -direct polarization magic angle spinning (DP/MAS) nuclear magnetic spectroscopy (NMR); the other part of solution was prepared with a TOC of 200 mg L⁻¹ in a water solution containing 200 mg L⁻¹ of NaN₃ solution as a bactericide, and was stored at 4°C in the refrigerator before usage.

Carbon nanotubes

Multi-walled carbon nanotubes (MWCNTs) of a purity greater than 95% were individually purchased from Chengdu Organic Chemicals Co. Ltd., Chinese Academy of Sciences (M3), Nano. Tech. Labs Inc. (Yadkinville, NC, USA, CP00011) (CP), and Bayer Material Science, Germany (Baytubes C 150 P) (BA). According to manufactured report, MWCNTs were synthesized by using chemical vapour deposition (CVD) method, using Ni containing catalyst for M3 MWCNTs, Co/Mn containing catalyst for BA MWCNTs and Fe containing catalyst for CP MWCNTs. In

order to purify the MWCNTs, pristine MWCNTs were mixed in 12.5% of hydrochloric acid (HCl) solution with the ratio of solid to liquid (1: 5000). The mixture was ultrasonicated for 10 minutes (Sonicator, 50–65 KHz), stirred over night, washed by Milli-Q water to neutral pH, filtrated, and then dried at 80°C in an oven.

3.2 Adsorption experiments

3.2.1 Batch technique

Sorption kinetics

To investigate the equilibrium time of adsorption, 0.1 g of goethite, 0.2 g of δ -Al₂O₃, 0.5 g of illite, 1.0 g soil or sediments were weighted into glass tubes for each sample. 10 mL of the ¹⁴C-radiolabeled PFOA or NP111 stock solution was added into each tube. All the samples were shaken at 150 rpm under room temperature in the darkness. At the defined interval time *i.e.* 0.5, 1, 2, 7 hours and 1, 2, 3, 6 and 8 days, samples were taken and centrifuged for 20 min at 10 000 g. 0.2 mL supernatant was taken out and its radioactivity was measured by LSC.

Sorption isotherms

All sorption-desorption experiments were performed in 16 ml volumetric Pyrex glass tube equipped with Teflon-lined screw caps using a batch technique at 293 K. Prior to initiating an adsorption experiment, a certain amount of solid sorbent was weighed into the glass tube and suspended with 10 mL stock solution of NP111 and PFOA. For the sorption on MWCNTs, MWCNTs were prewetted for 24 hours before the sorption started. These tubes were immediately sealed with the caps after spiking aliquots of stock solution of NP111 and PFOA and were mixed for 48 hours at 150 rpm on a horizontal shaker. Previous experiments demonstrated that 48 hours is sufficient for reaching adsorption equilibrium. After the equilibrium, the solid and liquid phases were separated by a centrifugation for 20 minutes at 10 000 g. For the desorption experiment of PFOA on MWCNTs, half of the volume of the supernatant was

SORPTION OF A NONYLPHENOL ISOMER AND PERFLUOROOCTANOIC ACID ON GEOSORBENTS AND CARBON NANOTUBES

immediately replaced by the solute-free electrolyte solution following the completion of sorption experiments. 48 hours was also taken as the equilibrium time for the desorption experiment. The radioactive concentration of chemical in the supernatant was determined by means of LSC. Adsorbent-free control measurements with the same protocol were also performed. The adsorbed amounts of chemical were calculated from the concentration difference between the corresponding control and sorbent data. All experiments were performed in triplicate.

3.2.2 Dialysis technique

Dialysis technique was described in a paper written by Hoelrigl-Rosta et al. (2003). Two dialysis cells were clamped together and simultaneously separated by a 1 kDa cut-off membrane. One of the cells was filled with the stock solution containing humic acids, the other with chemical solutions (NP111 concentrations were 250–5000 $\mu\text{g L}^{-1}$; PFOA concentration ranged from 32 $\mu\text{g L}^{-1}$ to 400 $\mu\text{g L}^{-1}$). The cells were sealed by a Teflon plug and rotated at 10 rpm until equilibrium was achieved at 48 hours. Aliquots of solution from both sides of the membrane were sampled in order to quantify the solute concentration by means of liquid scintillation counting (LSC). The adsorbed amounts of solute on HAs were calculated from the concentration differences of solute between the solutions of the two sides. All experiments were performed in duplicate.

3.2.3 Solution factors

Effect of temperature

The effect of sorption temperature e.g. 15°C, 30°C and 45°C on PFOA sorption to pristine M3 MWCNTs was studied with gaseous thermostatic reciprocal shaker.

Influence of pH

The pH of electrolyte solution and stock solution varied from 2 to 12 by 1 M NaOH and HCl solution based on mass.

CHAPTER 3 MATERIALS AND METHODS

Influence of salinity

Influence of salinity on the sorption of PFOA on MWCNTs was evaluated under that range of 1 to 500 mM NaCl.

Influence of species

To evaluate the effect of cation species, namely Ca^{2+} and Na^+ , on PFOA sorption, subsequent experiments were conducted with pristine M3 sample in 10 mM NaCl and 3.33 mM CaCl_2 under the same ionic strength to limit saline impact, respectively.

3.3 Analytical methods

Liquid scintillation counting (LSC)

Aliquots of the supernatant were mixed with 4 mL of Insta-Gel Plus scintillation cocktail (USA) in 5-ml vials and counted for radioactivity on a Tri-Carb B 2500 liquid scintillation counter (Packard Bioscience GmbH, Germany) for 10 min (< 2% standard deviation).

Oxidizer

The chemical concentration bound onto solid adsorbents (minerals and soil/sediments) was determined by measuring the radioactivity after total combustion of the solid samples with oxidizer (Robox 192, Zinsser Analytik GmbH, Frankfurt, Germany). Briefly, the solid sample containing tested radiolabeled compounds was weighted into the boat. The sample was completely combusted at around 900°C for 3.5 min with pure oxygen supplying in the chamber. Then nitrogen as carrier gas was blown for 1 min to completely remove $^{14}\text{CO}_2$. The emitting gas was flowed throughout 10 ml of Oxsolve C-400 scintillation cocktail (Zinsser Analytics, Germany) in which the $^{14}\text{CO}_2$ was completely trapped. Then the radioactivity of the cocktail was measured by LSC. Both blank and standard samples were run before and after the samples to access background contamination and the recovery of the standard chemical (^{14}C -anilazine) during the measurement process. The combustion process was

SORPTION OF A NONYLPHENOL ISOMER AND PERFLUOROOCTANOIC ACID ON GEOSORBENTS AND CARBON NANOTUBES

accepted when the recovery was > 95%. The total concentration of chemical in the adsorbents was calculated from the mass of the adsorbents, the specific radioactivity of the applied chemical and the measured radioactivity corrected with the corresponding recovery.

Solid-state NMR spectroscopy

A 7.05 T Varian INOVATM Unity spectrometer (Varian Inc., Palo Alto CA, USA), operating at 75.4 MHz for ¹³C, was used to acquire the ¹³C-spectra of the humic acids. The samples were placed in a 6 mm zirconium rotor with custom-made boron nitride bottom and top spacers and Vespel[®] drive tips. The boron nitride spacers were necessary to avoid a background signal from the spacers and to restrict the sample to the homogeneous region of the coil (Berns and Conte, 2010). The samples were spun at 7500 ± 1 Hz at 25°C. The spectra were collected with a sweep width of 25 kHz or 30 kHz and an acquisition time of 30 ms. Proton decoupling was done with a SPINAL sequence. A simple Bloch decay (direct polarization, DP) sequence was used to obtain quantifiable spectra. Spectra of HAs were collected with a scan number of 4k and a relaxation delay of 300 s to ensure a complete relaxation of the sample. Data processing was done with Mestre-C software (Version 4.9.9.9, Mestrelab Research, Santiago de Compostela, Spain). The FIDs were transformed by first applying a zero filling by doubling the data points and then an exponential filter function with a line broadening of 30 Hz. Baseline correction was done using a Bernstein algorithm.

The ¹H{¹³C} cross-polarization spectra were recorded on a Varian INOVATM unity equipped with a 7.05 T magnet. The samples were placed in 6 mm zirconia rotors and spun at 7500 ± 1 Hz. Spectra were collected with a spectral width of 25 kHz, an acquisition time of 30 ms and a recycle delay of 3 s. A total number of scans of 32 *k* was used to collect spectra with a good signal-to-noise (S/N) ratio. A standard contact time of 1 ms was used for cross-polarization. The radio frequency (r.f.) field applied on ¹³C during the spin lock pulse was kept constant at 54.1 kHz, whereas an ascending

CHAPTER 3 MATERIALS AND METHODS

ramp (3.5 kHz) was used on the ^1H r.f. field centered at 65.3 kHz. Decoupling was done using a SPINAL sequence with a ^1H r.f. field strength of 56 kHz, a pulse width of 9 μs and a phase of 5° . VNMRJ 2.2D software (Varian Inc., Palo Alto CA, USA) was used to acquire all the free induction decays (FID) and spectra elaboration was done with MestReC 4.9.9.9 (Mestrelab Research, Santiago de Compostela, Spain). All the FIDs were transformed by applying a zero filling and an exponential filter function with a line broadening (LB) of 50 Hz. The baseline correction was done with a multipoint baseline correction.

TEM measurement

The morphology and impurity of MWCNTs were probed by transmission electron microscopy (TEM) (FEI Technic. G2 F20 field-emission electron microscope at the Ernst Ruska Centre for Microscopy and Spectroscopy with Electrons (ER-C)). The samples were dispersed in ethanol and deposited on a holey carbon film supported on a copper grid. The microscope was operated at an acceleration voltage of 120 kV. High-resolution electron micrographs of the carbon nanotubes were taken under Scherzer-focus conditions.

Thermogravimetry (TG) of MWCNTs

Thermogravimetry of MWCNTs was conducted by means of simultaneous thermal analyzer 429 (Netzsch, Gerätebau GmbH, Germany). Generally, 80–100 mg of dry MWCNTs was weighed on a thermobalance, the heat rate was 2°C per minute and the maximal temperature was 1400°C .

Fourier transform infrared spectroscopy (FT-IR)

0.6 mg of MWCNTs was mixed with 399.4 mg of KBr and ground and pressed to pellets. All samples were used as pure solids. FT-IR spectra were interferometrically recorded with a BRUKER EQUINOX-55 spectrometer equipped with a DLATGS detector (Koglin et al., 2003). Single-beam IR spectra were the result of about 1000 co-added interferograms and ranged from 500 to 4500 cm^{-1} with a spectral resolution of 4.0 cm^{-1} .

SOPRTION OF A NONYLPHENOL ISOMER AND PERFLUOROOCTANOIC ACID ON GEOSORBENTS AND CARBON NANOTUBES

Potentiometric acid-base titration of MWCNTs

Potentiometric acid-base titration of pristine and purified MWCNTs suspension with approx. 2 g L^{-1} concentration under 10 mM of ionic strength (NaCl solution) was conducted as described in ref. (Tombacz and Szekeres, 2006).

Electrophoretic mobility of MWCNTs

Electrophoretic mobility of the MWCNT suspension was determined by Zeta Sizer Nano Series (Malvern) after ultrasonication for 10 minutes (Sonicator, 50–65 KHz) in 10 mM of NaCl solution.

Elemental analysis

Elemental analysis of pristine and purified MWCNTs was performed with inductively coupled plasma (ICP) mass spectrometry (MS) (Elan 6000). Briefly, 30–50 mg of MWCNTs was fused with one gram lithium borate mixture at 1050°C , dissolved in HNO_3 solution and diluted with Milli-Q water to 100 mL. The concentration of elements in the solution was finally determined by ICP-MS.

Measurement of specific surface area

The specific surface area of sediment samples and MWCNTs were measured from N_2 adsorption-desorption at liquid phase temperature (77K) using an Autosorb-6B KR sorptometer (Quantachrome). Prior to the measurement, the moisture of samples was removed at 105°C in an oven over night. The porosity of MWCNTs was determined with CO_2 . The specific surface area and the porosity of samples were calculated on the basis of adsorption-desorption data by means of Brunauer-Emmett-Teller (BET) method and T-method, respectively.

Total organic carbon analysis

Total organic carbon content of the sediments was determined as follows: The carbonate in sediment was removed by hydrochloric acid. Carbonate-free sediment sample was weighed (approximately 1 g) into a tin capsule. The samples were incinerated and subjected to thermal conductivity detection by a carbon/nitrogen

CHAPTER 3 MATERIALS AND METHODS

analyzer (Carlo-Erba, NA 1500, Milan, Italy).

In the solutions, the concentration of organic carbon was quantified by total organic carbon analyzer (TOC-5050A, Shimadzu, Germany).

pH detection

pH of sediment was measured in a 1:2.5 (w/w) mixture of sediment with 10 mM CaCl_2 solution by a pH meter (Mettler Toledo, MP 230).

Fractionation of sediments

The fractionation method of soil/sediment was described in the paper of Stemmer et al. (1998). Briefly, 10 gram sediment based on dry mass was placed into a 150 ml glass beaker and dispersed in 45 ml of distilled water using probe-type ultrasonication. The device was set to $50 \text{ J}\cdot\text{s}^{-1}$ output energy for 120 s, and the tip was plunged 15 mm into the suspension. Coarse sand ($> 200 \mu\text{m}$) and fine sand ($200\text{--}53 \mu\text{m}$) were separated by manual wet sieving using roughly 4 liters of distilled water. Particles left on the $200 \mu\text{m}$ and $53 \mu\text{m}$ sieves were collected, 70°C oven-dried and weighed as sand fraction. The suspension was made homogeneously by a magnetic stirring. Afterwards, 200 ml of the suspension were sampled into four 250 ml centrifuged bottles, and centrifuged at 150 g for 2 min. The supernatant was discarded and the pellet was re-suspended by distilled water, and repeated the centrifugation process until the supernatant was clear. The pellet in the tube as slit fraction were deeply frozen and lyophilized and weighed. The clay content was calculated from the initial mass and sand, slit fractionations. Each sample was performed in duplicate.

Chapter 4 Results and discussion

4.1 Sorption of NP111 onto Yangtze River sediments and their model components

Fate and transport of nonylphenol in riverine system are mainly dependent on its sorption behavior on sediments including organic and inorganic sediment components. The properties of organic matrixes, especially humic acids, are important factors for sediments and consequently predominates the sorption processes of organic compounds. Indeed, the sorption of NP on terrestrial soils (Düring et al., 2002), river sediments (Navarro et al., 2009), reference humic substances such as Aldrich humic acid and Suwannee River humic acid (Yamamoto et al., 2004), and minerals like Na-montmorillonite, gibbsite and α -SiO₂ (Nagasaki et al., 2004) have already been reported. But to our knowledge, the sorption of a branched NP isomer on geosorbents has not been evaluated yet. We therefore investigated the sorption of a branched nonylphenol isomer (NP111) on geosorbents, such as Yangtze River sediments and their model components *i.e.* goethite, δ -Al₂O₃ and illite. In addition, the contribution of humic substances to the sorption was studied with the reference Suwannee River natural organic matter (NOM).

4.1.1 The adsorption of NP111 on Yangtze River sediments

Sediments sampled from the Yangtze River were characterized by several methods and the data are presented in Table 4.1. The total organic carbon (TOC) content in sediment samples ranged from 2.8 to 9.6 mg g⁻¹. The pH range fell into 7.3–7.4. The specific surface area (SSA) ranged from 6.2 to 23.0 m² g⁻¹. For all sediment samples, silt accounted for the dominant proportion. The inorganic model minerals were characterized and are presented in Table 4.2.

CHAPTER 4 RESULTS AND DISCUSSION

Table 4.1 Properties of the Yangtze River sediments

	CQ	ZG	WH	NJ	CMW	CME
TOC (mg g ⁻¹)	6.51	9.44	9.61	6.97	7.50	2.84
SSA (m ² g ⁻¹)	9.82	8.25	12.77	22.99	6.23	13.51
pH value	7.39	7.25	7.33	7.35	7.33	7.38
Sand (%)	26.61	18.40	17.87	4.21	7.24	10.14
Silt (%)	58.54	71.66	84.13	78.25	79.21	84.13
Clay (%)	14.85	9.95	4.09	17.55	13.55	5.73

Table 4.2 Properties of the model minerals

	SSA (m ² g ⁻¹)	pH (in 10 mM NaCl)	Point of zero charge
δ-Al ₂ O ₃	133.6	8.2	8.1 ^a
Goethite	21.4	6.8	9.3 ^b
Illite	13.6	4.0	3.5 ^c

^a (Tombácz and Szekeres, 2001), ^b (Antelo et al., 2005), ^c (Lan et al., 2007)

The sorption kinetics of NP111 on solid adsorbents and organic matter solution demonstrated that the equilibrium reached at around 20 hours. The similar result *i.e.* 22 hours was also found with soils by Duering et al. (2002). In this study, in order to avoid non-equilibrium conditions, 48 hours was applied as the equilibrium time for all sorption of NP111. There was no degradation of NP111 observed by high performance liquid chromatography during the sorption process. Additionally, the recovery of NP111 ranged from 96% to 102%.

Adsorption isotherms of NP111 on Yangtze River sediments are presented in Fig. 4.1a. The adsorption isotherms of NP111 were properly simulated by the Freundlich model ($r^2 > 0.942$) (Table 4.3). A similar result was noted by Navarro et al. for nonlinear

SORPTION OF A NONYLPHENOL ISOMER AND PERFLUOROOCTANOIC ACID ON
GEOSORBENTS AND CARBON NANOTUBES

sorption isotherms of 4-*n*-NP containing a linear side chain on Ebro River sediments (Navarro et al., 2009).

Table 4.3 Freundlich parameters and K_{OC} ($L\ kg^{-1}$) values of NP111 calculated based on the organic carbon content and distribution coefficient (K_d) simulated in NP111 equilibrium concentration range 0–200 $\mu g\ L^{-1}$ by the linear model.

	$K_f (\mu g^{(1-1/n)} L^{1/n} g^{-1})$	$1/n$	r^2	$K_{OC} (L\ kg^{-1})$
CME	0.04 (± 0.01)	0.84 (± 0.03)	0.98	7952
CMW	0.03 (± 0.01)	1.10 (± 0.06)	0.95	8341
NJ	0.09 (± 0.03)	0.91 (± 0.08)	0.94	8385
WH	0.07 (± 0.02)	0.98 (± 0.07)	0.96	7589
ZG	0.16 (± 0.03)	0.88 (± 0.03)	0.98	10565
CQ	0.05 (± 0.01)	0.95 (± 0.03)	0.99	6317
δ -Al ₂ O ₃	5.05×10^{-5} ($\pm 8.92 \times 10^{-5}$)	1.72 (± 0.28)	0.94	-
Goethite	12.87 (± 6.24)	0.80 (± 0.09)	0.86	-
Illite	9.97×10^{-4} ($\pm 4.87 \times 10^{-4}$)	1.36 (± 0.08)	0.98	-

Note: - not determined

The $1/n$ values for CMW, WH and CQ samples range from 0.95 to 1.10, indicating that adsorption isotherms are of linear tendency. Nevertheless, the $1/n$ values for CME, NJ and ZG samples are 0.84, 0.91 and 0.88, respectively, suggesting the typical nonlinear sorption.

The K_{OC} values of NP111 were calculated based on the organic carbon content and K_d values that were simulated in the equilibrium concentration range 0–200 $\mu g\ L^{-1}$ by a linear model (Henry's law). The K_{OC} value of NP ranged from 6.3×10^3 to 1.1×10^4

CHAPTER 4 RESULTS AND DISCUSSION

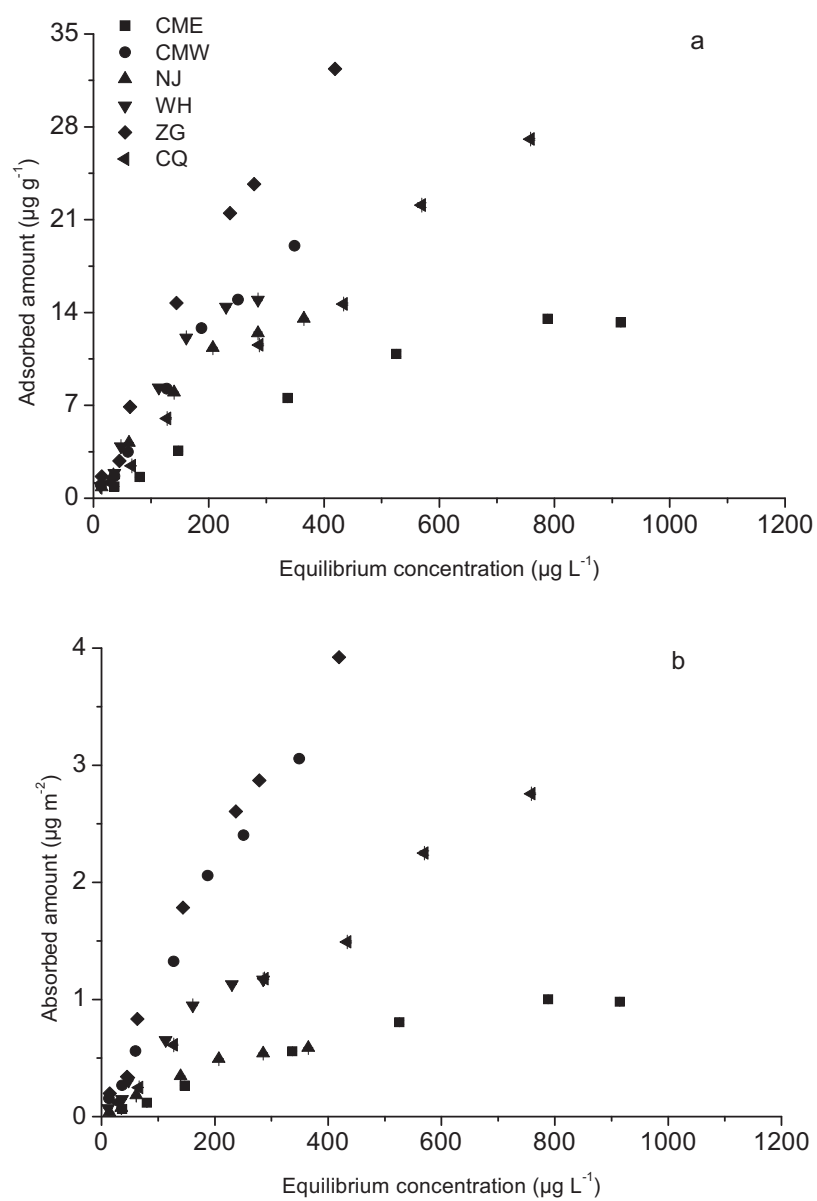


Fig. 4.1 Adsorption isotherms of NP111 on Yangtze River sediments (a and b) (a: the unit of NP111 adsorption is based on mass, b: the unit of NP adsorption is normalized by specific surface area)

L kg^{-1} with an increasing trend $\text{CQ} < \text{WH} < \text{CME} < \text{CMW} < \text{NJ} < \text{ZG}$. The K_{OC} values

SORPTION OF A NONYLPHENOL ISOMER AND PERFLUOROOCTANOIC ACID ON GEOSORBENTS AND CARBON NANOTUBES

for 4-*n*-NP reported for Ebro River sediments ranged from 4.0×10^3 to 4.9×10^4 L kg⁻¹ (Navarro et al., 2009).

The adsorption data of NP on sediments were normalized by means of the specific surface area (Fig. 4.1b) revealing three groups in the order: CMW \approx ZG > WH \approx CQ > CME \approx NJ. The average organic carbon contents were 8.47 mg g⁻¹ for CMW and ZG, 8.06 mg g⁻¹ for WH and CQ, and 4.91 mg g⁻¹ for CME and NJ. It thus appears that the adsorption depends on both the organic matter content and the specific surface area of sediments. Nevertheless, it is not possible to distinguish the roles of organic carbon content and specific surface area for sediments. In addition, the effect of organic matter on the sorption of a compound depends not only on its quantity, but also on its maturity and composition (Kleineidam et al., 1999; Thiele, 2000), the latter known to differ significantly (Hedges et al., 1994).

As shown in Table 4.1, the pH values of the sediment samples ranged from 7.3 to 7.4 in this work. We thus assume that the small variances of pH do not significantly impact on the sorption of NP111 to the Yangtze River sediments.

4.1.2 Adsorption of NP111 on model geosorbents

There was a significant adsorption of NP111 on the reference Suwannee River NOM (Fig. 4.2b). The linear model properly simulated the adsorption isotherms ($r^2 = 0.997$) (Table 3). It is known that NP sorption on organic matter was dominated by hydrophobic interactions (Yamamoto et al., 2003). The partitioning coefficient (K_{OC} value) of NP111 on Suwannee River NOM was 1.8×10^3 L kg⁻¹ (log K_{OC} value: 3.26). This value is lower than the K_{OC} values determined with Yangtze River sediments. A probable reason is that Suwannee River NOM was directly isolated from river water and NOM “molecules” with molecular weight less than 1 kDa were removed by

CHAPTER 4 RESULTS AND DISCUSSION

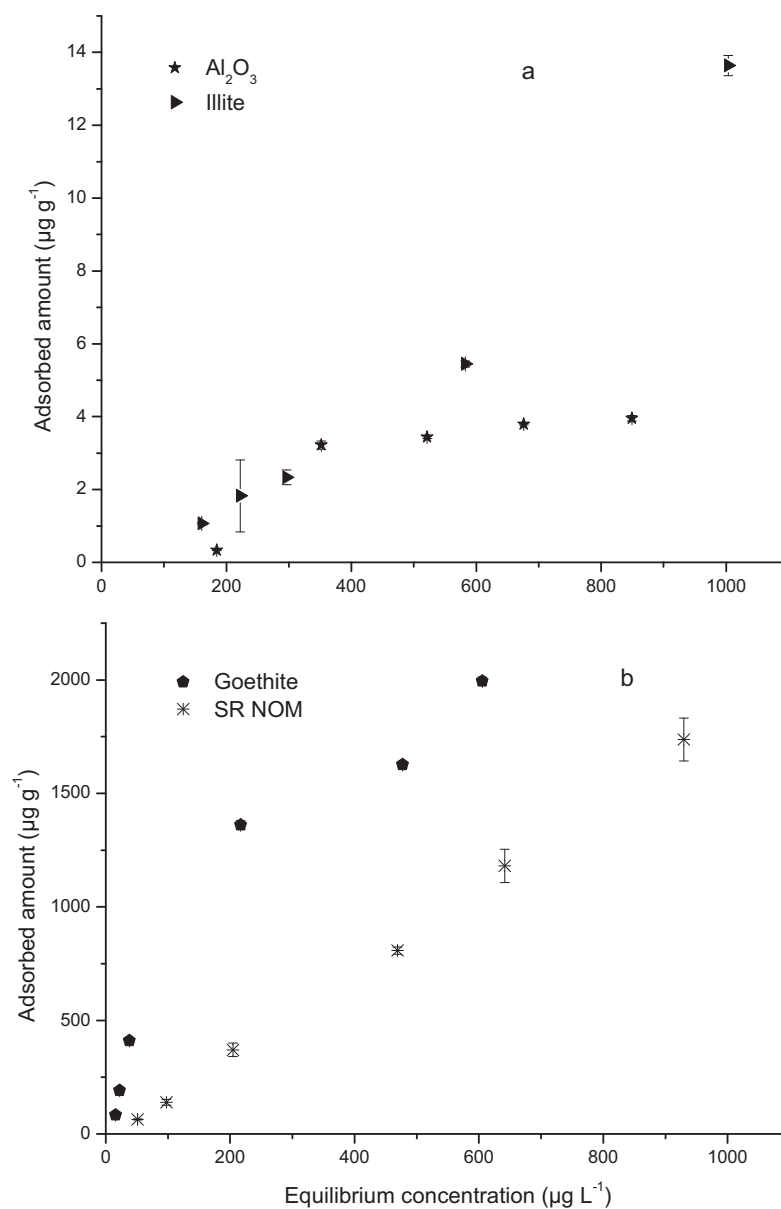


Fig. 4.2 Adsorption isotherms of NP111 on sediment model components

dialysis (Hoellrigl-Rosta et al., 2003). Furthermore, organic matter isolated from river water usually contains less hydrophobic domains than that extracted from soils and

SORPTION OF A NONYLPHENOL ISOMER AND PERFLUOROOCTANOIC ACID ON
GEOSORBENTS AND CARBON NANOTUBES

sediments (Martin-Mousset et al., 1997). In addition, in this work, a branched isomer of NP was used. The K_{OC} values of branched 4-NP and linear 4-*n*-NP reported in soils were about $1.0 \times 10^4 \text{ L kg}^{-1}$ and $7.9 \times 10^4 \text{ L kg}^{-1}$, respectively (Düring et al., 2002).

Adsorption isotherms of NP111 on sediment model components such as $\delta\text{-Al}_2\text{O}_3$, goethite and illite are presented in Fig. 4.2a and b. The adsorption isotherms were fitted well by the Freundlich model ($r^2 > 0.855$) and the parameters are listed in Table 4.3. It should be noted that the linear model was able to fit the adsorption isotherms of NP on Na-montmorillonite well (Nagasaki et al., 2004).

The strong sorption of NP111 on goethite was much higher than on $\delta\text{-Al}_2\text{O}_3$ and illite (Fig. 4.2a and b). When NP111 adsorbed amounts on $\delta\text{-Al}_2\text{O}_3$, goethite and illite were normalized to specific surface area, it was elucidated that sorption isotherms were not significantly dependent on the specific surface area.

Interactions between the positive charge of the model minerals and the dipole of the phenol functional group in NP111 might presumably be responsible for the different sorption of NP111 on investigated adsorbents. The points of zero charge (PZC) are 8.1 for $\delta\text{-Al}_2\text{O}_3$ (Tombácz and Szekeres, 2001) and 9.3 for goethite (Antelo et al., 2005), respectively. Thus, in the observed pH ranges (7.6–7.8 for studies with $\delta\text{-Al}_2\text{O}_3$, 6.9–7.0 for goethite), goethite carries significantly more positive surface charges than $\delta\text{-Al}_2\text{O}_3$. However, the above interaction alone is not adequate to account for the substantial difference of NP111 sorption between goethite and $\delta\text{-Al}_2\text{O}_3$. Thus, it can be assumed as another possible mechanism that on the surface of goethite NP aggregates are formed. A similar interpretation was given by Nagasaki et al. for adsorption of NP on gibbsite (Nagasaki et al., 2004). However, the adsorption of NP111 on goethite requires further investigation to elucidate the mechanisms.

Adsorption of NP111 on illite was obviously higher than that on $\delta\text{-Al}_2\text{O}_3$ (Fig. 4.2a). Nagasaki et al. assumed that NP adsorbs on broken-edge octahedral alumina layers of

CHAPTER 4 RESULTS AND DISCUSSION

Na-montmorillonite (Nagasaki et al., 2004) which might also be the case in illite, but not in $\delta\text{-Al}_2\text{O}_3$.

At the equilibrium concentrations, the adsorbed amount of NP on $\alpha\text{-Al}_2\text{O}_3$ (Nagasaki et al., 2004) is about five times higher than that on $\delta\text{-Al}_2\text{O}_3$ used in our study. This difference is accounted for by the various isomers of NP and the different forms of Al_2O_3 used. Unfortunately in Nagasaki et al. (Nagasaki et al., 2004) paper, NP was not described in detail with respect to the isomer composition.

4.2 Effect of structural composition of humic substances on the sorption of NP111

HAs compose of various structural components that dominate the overall features and consequently impact on its sorption behavior of organic compounds. Indeed, the correlation between HAs characteristics and the sorption affinity of organic compounds was intensively studied (Chiou et al., 1998; Gunasekara et al., 2003; Kang and Xing, 2005). However, so far, the relationship between HAs characteristics and the sorption affinity of NP has not been established. Therefore, in this study, the sorption on NP111 on HAs was investigated. HAs isolated from Yangtze River sediments were used as adsorbents, and some reference HAs were also involved for the comparison. All investigated HAs were characterized by solid state ^{13}C -CP or DP/MAS NMR.

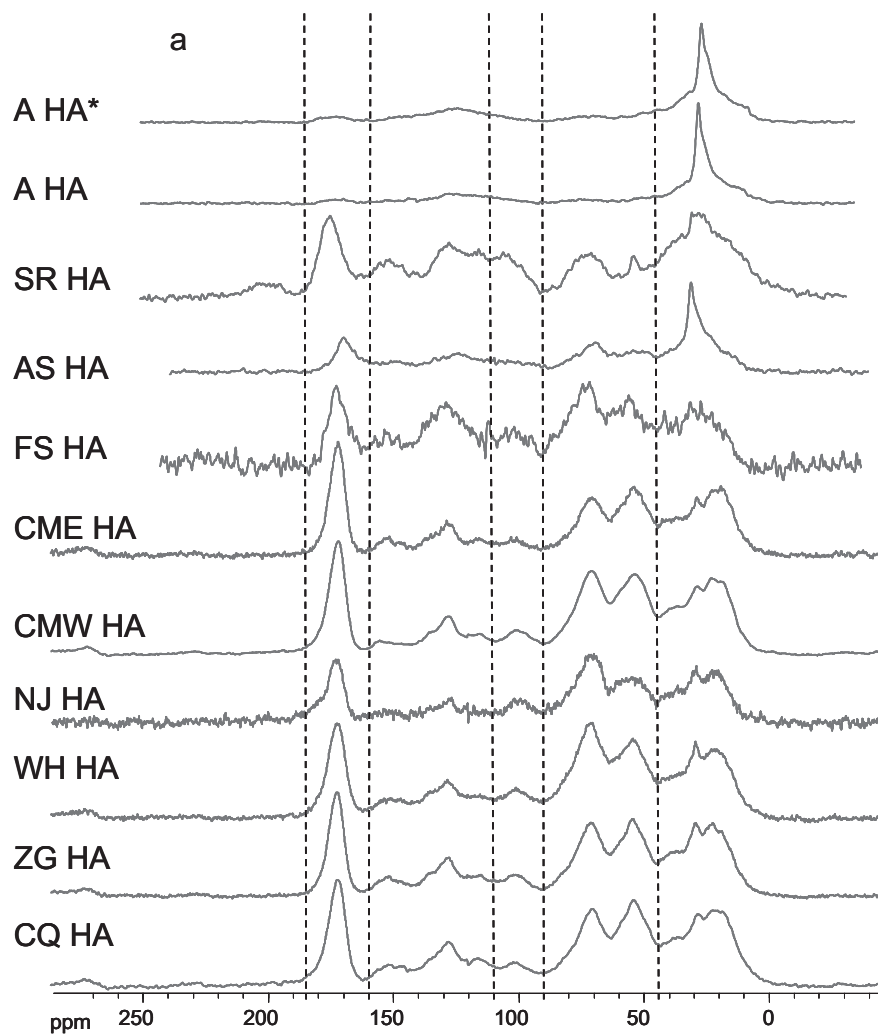
4.2.1 NMR characterization of humic substances

HAs from different origins were characterized by solid state ^{13}C CP/MAS NMR and ^{13}C DP/MAS NMR as shown in Fig. 4.3a and 4.3b, respectively. The spectra were divided into five chemical shifts regions, representing alkyl C (0–45 ppm), O-alkyl C (45–90 ppm), anomeric C (90–110 ppm), aromatic C (110–160 ppm), and carboxyl C (160–185 ppm), respectively (Wilson, 1987). Relative quantities of each type of C in the five regions were determined by integration of the DP/MAS spectra and are expressed as a percentage related to the total organic carbon content. The distributions of C in the five regions of the spectra are presented in Table 4.4.

The spectra generally have three well-resolved peaks and one poorly resolved peak (Fig. 4.3a). The clear resolved peaks with HAs isolated from Yangtze River sediment refer to the region of 10–35 ppm (methyl, methylene groups), 50–90 ppm (methoxyl, C-O and C-N groups), and 160–190 ppm (carboxyl and ester groups). The poor

CHAPTER 4 RESULTS AND DISCUSSION

resolved peak occurs between 110 to 140 ppm (aromatic carbon). The peaks with HAs from Yangtze River sediments are comparable. Particularly, the change of two peaks in the region of 50–90 ppm was dependent on the sediment location. For two HAs



SORPTION OF A NONYLPHENOL ISOMER AND PERFLUOROOCTANOIC ACID ON
GEOSORBENTS AND CARBON NANOTUBES

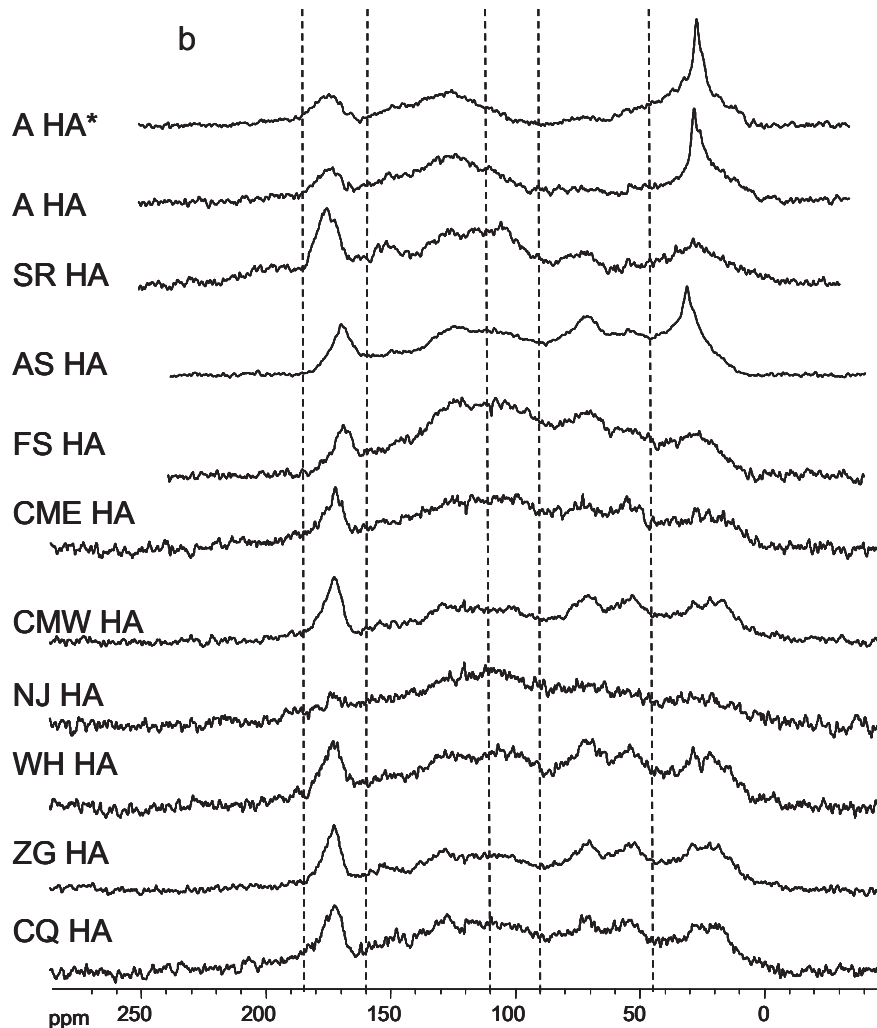


Fig. 4.3 a) ^{13}C CP/MAS (grey) and b) ^{13}C DP/MAS (black) NMR spectra of the humic acids and chemical shift regions of alkyl C (45–0 ppm), O-alkyl C (90–45 ppm), anomeric C (110–90 ppm), aromatic C (160–110 ppm), carboxyl C (185–165 ppm) (* pristine Aldrich HA)

separated from soils, the peak in the region of 160–190 ppm was pronounced but was smaller than that of HAs isolated from Yangtze River sediments. The clear peaks with 50–90 ppm and 110 to 140 ppm occurred in FS HA. However, the more pronounced peak in the region of 30 to 50 ppm appeared in AS HA. With respect to

CHAPTER 4 RESULTS AND DISCUSSION

SR HA, the sharp peak occurred in the region of 160–190 ppm, however, in other regions the peaks appeared but not pronounced. Nevertheless, the sharp peak emerged in the region of 30 to 50 ppm such as A HA relatively concealed the peaks in other regions. Compared with pristine and treated A HA, there was not pronounced difference in the spectra (Fig 4.3a), indicating that the dialysis treatment negligibly affects on humic acids.

Table 4.4 K_{OC} values of NP111 and percentage of functional groups of humic substances (from solid-state ^{13}C DP/MAS NMR spectra)

Organic matter	K_{OC}	Alkyl C	O-alkyl C	Anomeric C	Aromatic C	Carboxyl C	Aliphaticity*	Aromaticity ^o
	L kg ⁻¹							
Aldrich HA	15312	29	12	6	43	11	52	48
FS HA	6330	24	29	10	25	12	72	28
ES HA	3997	12	11	7	54	17	36	64
HA HA	2583	14	21	9	40	17	52	48
SR HA	2340	13	16	21	33	16	60	40
CME HA	6124	18	26	14	31	12	65	35
CMW HA	7363	23	28	11	25	13	71	29
NJ HA	3858	16	26	15	34	9	63	37
WH HA	6931	20	28	12	29	12	67	33
ZG HA	10025	23	28	10	27	12	69	31
CQ HA	6821	20	26	12	30	13	66	34
SR FA	1098	23	14	16	28	19	65	35
ES FA	1138	18	22	9	30	21	62	38
SR NOM	1703	33	10	14	17	25	77	23

In the case of HAs isolated from the Yangtze River sediments, the peak in the spectra at 110–160 ppm, which corresponds to the aromatic C region, was not sharp. Nevertheless, the percentage in this region ranged from 25% to 34% (Table 4.4). This indicates that aromatic carbon constitutes the major structure component for HAs from Yangtze River sediments. Oren and Chefetz (2005) have also pointed out that

SOPRTION OF A NONYLPHENOL ISOMER AND PERFLUOROOCTANOIC ACID ON
GEOSORBENTS AND CARBON NANOTUBES

aromatic carbons predominate in HA extracted from Kishon River sediments. The similar sources for HAs likely resulted into the identical structural components. The percentage of O-alkyl C was similar in all HAs isolated from the Yangtze River sediments (26%–28%). The percentage of alkyl C, anomeric C and carboxyl C ranged from 16% to 23%, from 10% to 15%, and from 9% to 13% (Table 4.4), respectively. These results suggest that the structural components of HAs isolated from the Yangtze River sediments at different locations exhibit a pronounced analogy. In case of HA isolated from agricultural soils in Halle, aromatic C accounted for the major composition. However, the percentage of carboxyl C is higher in comparison with the HAs isolated from the Yangtze River sediments. On the contrary, alkyl C, O-alkyl C and aromatic C constituted the essential compositions of FS HA separated from forest soil. Furthermore, alkyl carbon and anomeric carbon were the second most abundant structures in Aldrich HA and Suwannee River HA, where the major component was aromatic carbon.

The aliphaticity and aromaticity of organic samples was calculated based on the carbon content at different chemical shift range that was determined by ^{13}C -DP/MAS NMR spectroscopy. The aliphaticity and aromaticity of the samples was calculated by Eq. (6) and Eq. (7) (Zech et al., 1997), respectively.

$$\text{Aliphaticity} = C(\delta_{0-110}) / C(\delta_{0-160}) \times 100\% \dots\dots\dots(6)$$

$$\text{Aromaticity} = C(\delta_{110-160}) / C(\delta_{0-160}) \times 100\% \dots\dots\dots(7)$$

where, δ is chemical shift, C is the content of C-containing functional group.

The aliphaticity and aromaticity of the different organic matters are presented in Table 4.4. The aliphaticity of HAs extracted from the Yangtze River sediments ranged from 63% to 71%. They were similar to those of HAs isolated from other sediments of rivers and lakes in China namely 58%–77% (He et al., 2008).

4.2.2 Adsorption of NP111 to humic substances

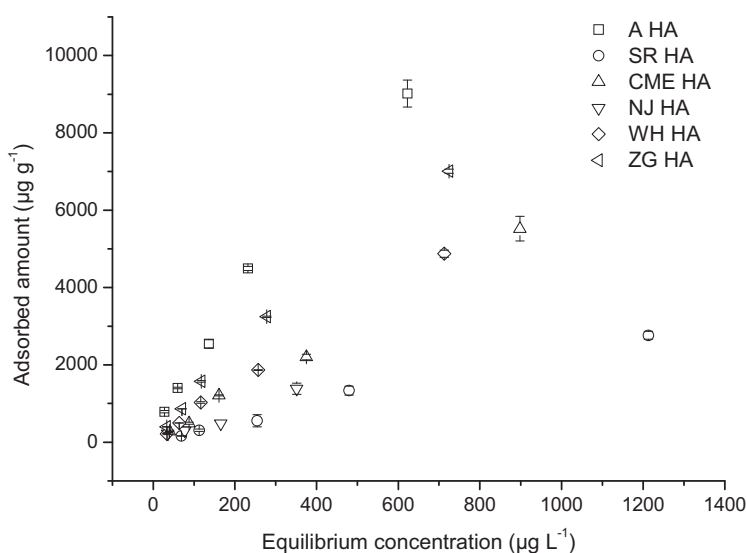


Fig. 4.4 Sorption isotherms of NP111 on HAs isolated from Yangtze River sediments (CME HA, NJ HA, WH HA and ZG HA) and the reference ones (A HA and SR HA)

Representative NP111 sorption isotherms on different HAs are shown as examples in Figure 4.4. The K_{OC} values of NP111 sorption on different HAs are presented in Table 4.4. Sorption isotherms of NP111 were well described by a linear model (Henry's model) ($r^2 > 0.976$, $n = 5$). Linear model was also used to fit the relationship between aqueous- and particulate-phase of nonylphenol mixtures (Burgess et al., 2005). Similar linear isotherms were reported by Chiou et al. (1983) in the case of the sorption of nonionic organic compounds on soil organic matter from water. On the contrary, the sorption of nonpolar compounds like PAHs such as phenanthrene on organic matters, isolated from soil, is fitted by a nonlinear model (Kang and Xing, 2005). It must be remarked that the sorption of nonpolar compounds like PAHs on organic matter in pristine sediments requires a fitting by nonlinear composite models (Zhang et al., 2010a). In that paper, the partition of PAHs into amorphous organic carbon (Henry law) and the adsorption in the porous structure of black carbon can be

SORPTION OF A NONYLPHENOL ISOMER AND PERFLUOROOCTANOIC ACID ON
GEOSORBENTS AND CARBON NANOTUBES

differentiated.

Although HAs were isolated from the Yangtze River sediments at different locations, the K_{OC} values of NP111 were almost consistent (K_{OC} : $3.9\text{--}7.4 \times 10^3 \text{ L kg}^{-1}$) except for ZG HA (K_{OC} : $1.00 \times 10^4 \text{ L kg}^{-1}$) (Table 4.4). In the last case, it must be noted that ZG HA originated from the sediment of the reservoir formed by the Three Gorges Dam on the Yangtze River, *i.e.* under biodegradation and redox conditions close to lake sediments.

The K_{OC} values of NP111 on HAs isolated from Yangtze River sediments are consistent with the data published by Hoellrigl-Rosta et al. (2003). The K_{OC} value of 4-*n*-NP on HA isolated from a loamy silt soil is $9.5 \times 10^3 \text{ L kg}^{-1}$. However, in most cases, K_{OC} values of NP were determined by sorption experiments directly with soils and sediments, respectively. Based on sorption experiments, the K_{OC} values of 4-*n*-NP measured on Ebro River sediments range from 4.0×10^3 to $4.9 \times 10^4 \text{ L kg}^{-1}$ (Navarro et al., 2009). In fact, the natural enrichment of NP in soils, sediments and their fractions results in higher K_{OC} . The K_{OC} value of the mixture of NP isomers on suspended particle matter ranges from 7×10^4 to $4 \times 10^5 \text{ L kg}^{-1}$ (Ferguson et al., 2001). Different isomers of NP behaved differently regarding sorption from their mixture, e.g. the K_{OC} value for 4-*n*-NP and branched 4-NP on soils is $7.9 \times 10^4 \text{ L kg}^{-1}$ and $1.0 \times 10^4 \text{ L kg}^{-1}$, respectively; the K_{OC} value of linear NP is roughly eight times higher than that of branched one (Düring et al., 2002). Branched NP has a reduced sorption coefficient (K_{OC} value) (Düring et al., 2002). These data indicate that both the properties of investigated organic matter and the characteristics of different NP isomers are crucial for the sorption behavior.

The K_{OC} values of NP111 among HAs from various origins ranged from 2.3×10^3 to $1.0 \times 10^4 \text{ L kg}^{-1}$ except for Aldrich HA with $1.5 \times 10^4 \text{ L kg}^{-1}$ in our case. Aldrich HA and Suwannee River HA are commonly used as standard organic substances. In a sorption study with 4-*n*-NP, Yamamoto et al. (2003) found that K_{OC} values on Aldrich

CHAPTER 4 RESULTS AND DISCUSSION

HA and Suwannee River HA were $6.8 \times 10^4 \text{ L kg}^{-1}$ and $9.1 \times 10^4 \text{ L kg}^{-1}$, respectively. The above values are significantly higher than our data. Besides the different NP isomers applied as the abovementioned, the investigated humic acids were pretreated differently. Indeed, the low molecular weight fraction (<1 kDa) of Aldrich HA and Suwannee River HA was removed in this work. In Yamamoto et al. (2003) paper, the higher molecular weight fraction (>10 kDa) of Aldrich HA was removed prior to usage. The removal of weight fractions likely alters the sorption behavior. Furthermore, the fluorescence method used for determination of sorption in that study may overestimate K_{OC} value of NP (Yamamoto et al., 2003).

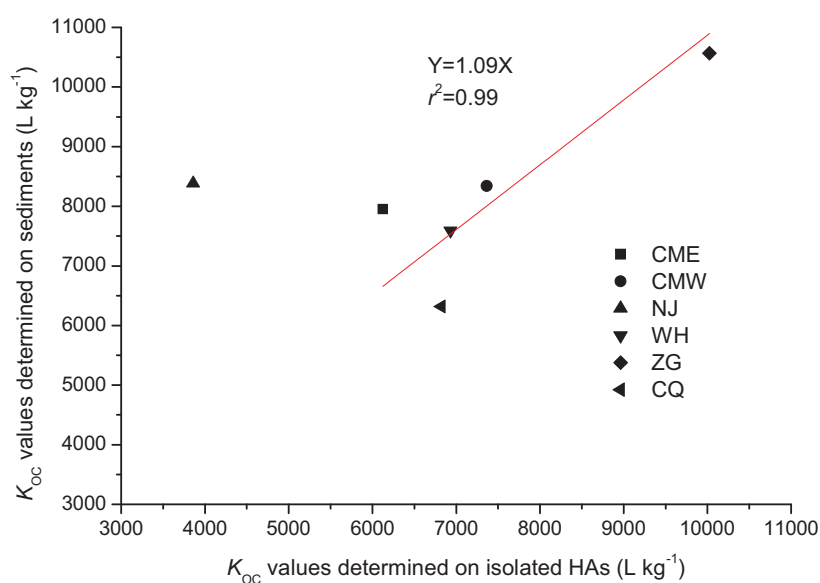


Fig. 4.5 The correlation between K_{OC} determined on isolated HAs and K_{OC} determined on Yangtze River sediments

For the comparison, both K_{OC} values of NP111 determined on isolated HAs from Yangtze River sediments and K_{OC} values of NP111 determined on Yangtze River sediments are presented in Fig. 4.5. A linear trend between K_{OC} values of NP111 determined by different methods was observed for sediments ($r^2 = 0.99$) excluding

SORPTION OF A NONYLPHENOL ISOMER AND PERFLUOROOCTANOIC ACID ON GEOSORBENTS AND CARBON NANOTUBES

NJ sediment. The slope parameter was 1.09, indicating that the K_{OC} values determined on sediments are slightly larger than the ones determined on isolated HAs. The reason may be assigned to that the remained organic carbon fractions on sediment after humic acid isolation such as black carbon and humin were still sufficient for the sorption of NP111.

4.2.3 Influence of pH on NP111 adsorption to selected humic substances

The influence of pH on NP111 sorption onto Aldrich humic acid (A HA) and Elliott soil fulvic acid (ES FA) is shown in Fig. 4.6. Despite the difference between HA and FA, the adsorbed amount of NP111 was not effected by pH in the solution under acidic and neutral conditions, while the adsorbed amount decreased at alkaline situation. A similar result was found by Hoellrigl-Rosta et al. (2005) in the case of the 4-*n*-NP sorption with humic acids vs. pH. Similarly, the change of pH weakly affects K_{OC} value for neutral chemicals like benzo(a)pyrene (De Paolis and Kukkonen, 1997). By contrast, the sorption affinity of pyrene on humic acids decreases with the solution pH increasing (Pan et al., 2008a). The possible reason of pH impact was attributed to that the solution pH perhaps resulted in the molecular structure changes of either organic substances or solutes. On the one hand, the negative charge increases with pH due to deprotonation of functional groups, *e.g.* carboxylic group and phenolic group. On the other hand, NP111 will be deprotonated when the solution pH value is close to pK_a value 10.7 of NP. Consequently, the electrostatic repulsion reduced the sorption affinity.

At the similar pH, the adsorbed amount on A HA was around 10 times higher than on ES HA (Fig. 4.6). In sorption of 4-*n*-NP, HA (K_{OC} : 1479 L kg⁻¹) had around three times higher sorption capacity than FA (K_{OC} : 513 L kg⁻¹) (Hoellrigl-Rosta et al., 2005). Similarly, De Paolis and Kukkonen (1997) also found that HAs had higher sorption capacity of nonionic organic compounds than FAs. The difference of sorption

behaviors on HA and FA was generally assigned to the difference of their chemical composition.

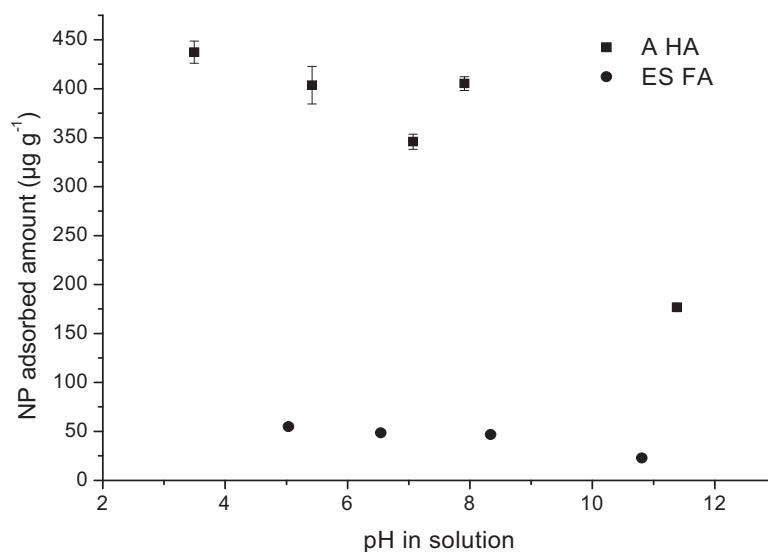
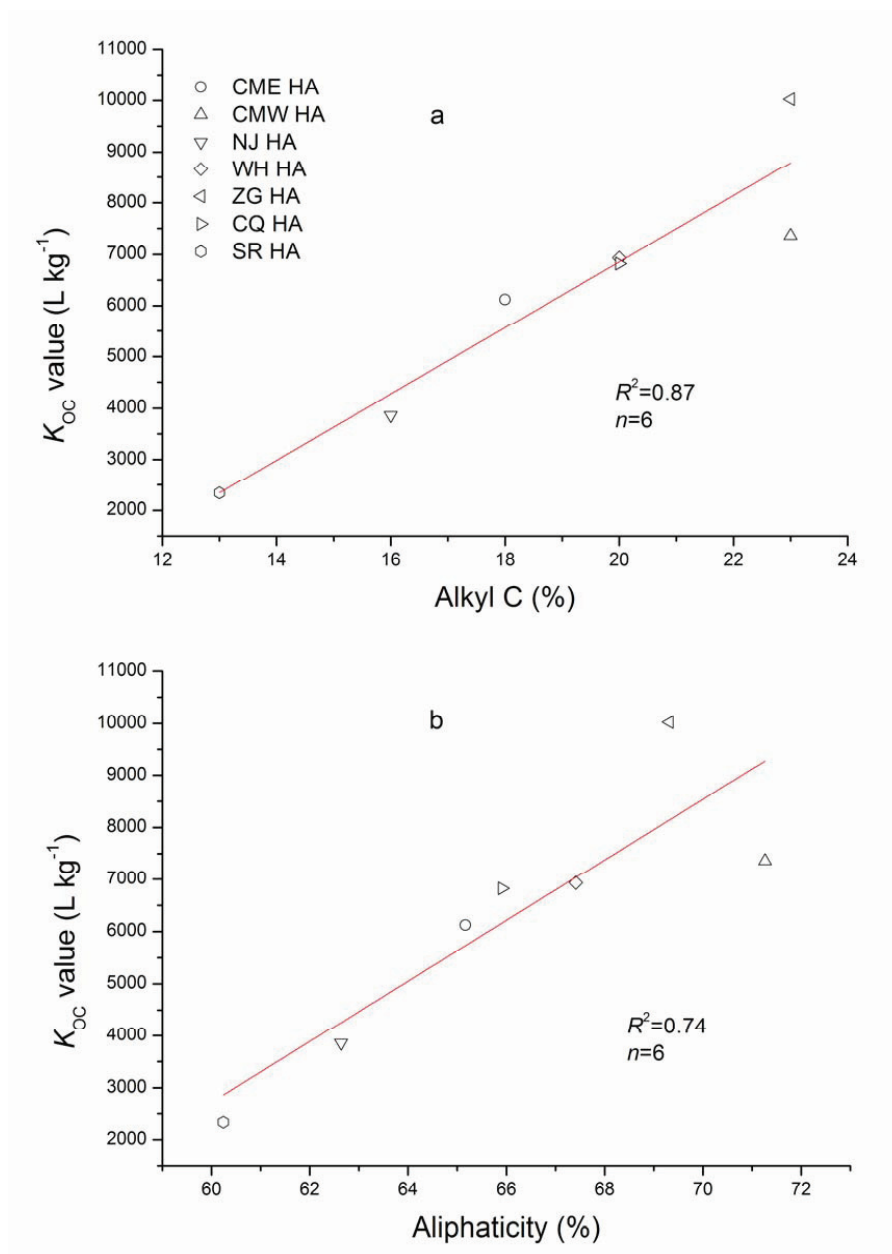


Fig. 4.6 Influence of pH on NP111 adsorption to A HA and ES FA

4.2.4 The correlation between K_{OC} values and the composition of humic substances

It is controversial which structural components dominate the sorption of hydrophobic organic compounds (Chiou et al., 1998; Kang and Xing, 2005). In order to obtain some insight into the role of chemistry of various humic acids, possible correlations between K_{OC} values of NP111 and structural components quantified from solid-state ^{13}C DP/MAS NMR spectra were analyzed.

SOPRTION OF A NONYLPHENOL ISOMER AND PERFLUOROOCTANOIC ACID ON
GEOSORBENTS AND CARBON NANOTUBES



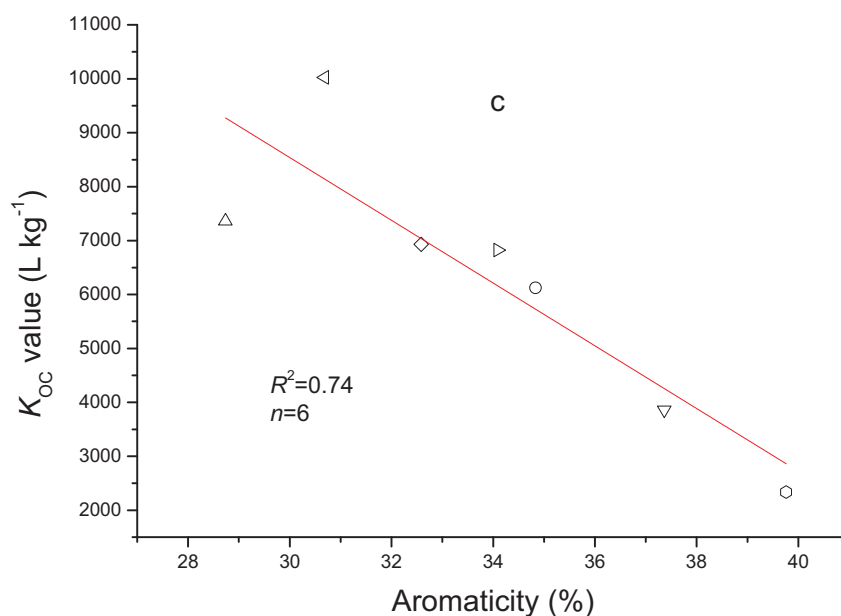


Fig. 4.7 Correlations between K_{OC} of NP111 and alkyl carbon content (a), aliphaticity (b) and aromaticity (c) of HAs isolated from Yangtze River sediments ((○) CME HA, (△) CMW HA, (▽) NJ HA, (◇) WH HA, (◁) ZG HA and (▷) CQ HA) and of the reference Suwannee River HA ((◻) SR HA)

A distinct relationship between K_{OC} value and the percentage of alkyl carbons ($r^2 = 0.87$) was observed for HAs isolated from Yangtze River sediments and for the reference SR HA (Fig. 4.7a). In the same way, the K_{OC} values were significantly correlated with the aliphaticity of the HAs ($p < 0.05$) (Fig. 4.7b). Consequently, a negative relationship between K_{OC} value and aromaticity of humic acids was also observed (Fig. 4.7c).

Conversely, Burgess et al (2005) pointed out that K_{OC} values of NP mixture positively related to the polarity of lignin, chitin and cellulose. It must be noted that this result should be carefully considered because of the low number of samples.

SORPTION OF A NONYLPHENOL ISOMER AND PERFLUOROOCTANOIC ACID ON GEOSORBENTS AND CARBON NANOTUBES

Actually, our results confirm the solubilization of hydrophobic organic contaminants (HOCs) such as branched NP in organic matter from sediment. A probable cause is that the hydrophobic interaction drives the partition of branched NP in structured microdomains of HAs where alkyl C groups dominate (Traina et al., 1996; Koopal et al., 2004). These observations are consistent with the hypothesis suggested by Hu et al. (1999) that the sorption of nonionic organic compounds took place primarily at a polymethylene structure in humic substance, which composes of alkyl moieties. Thus, Salloum et al (2002), in the case of hydrophobic compounds sorption like PAHs to organic matters, has established a direct correlation between K_{OC} values of phenanthrene and the paraffinic carbon content. A similar trend between the sorption coefficient of phenanthrene and the aliphaticity of HAs is observed (Chefetz et al., 2000; Kang and Xing, 2005). These data and the inherent trend imply that sorption to aliphatic domains is similar to sorption to “rubbery” rather than “glassy” type carbon (Xing and Pignatello, 1997). It is suggested that the binding of bulky NP111 in organic matter was related to the higher molecular flexibility of aliphatic microdomains (Engelbreton and von Wandruszka, 1999; Bassmann-Schnitzler and Sequaris, 2005).

However, a negative relationship between K_{OC} value of NP111 and aromaticity of HAs was observed. A similar result was observed by Chefetz et al. (2000) and Kang and Xing (2005) that a negative relationship between K_{OC} value of PAHs, such as pyrene and phenanthrene, and the aromaticity of organic matters was established. Indeed, hydrophobic interaction and π - π interaction may drive NP sorption to the adsorbents with aromatic domains. The positive relationship between NP and the content of aliphatic moieties does not completely deny the correlation between NP and the content of aromatic domains, perhaps hinders or relatively reduces this action. Salloum et al (2001) already pointed out that the sorption to organic matter may be regulated by the physical accessibility to specific structures rather than the structures themselves.

The satisfactory linear relationship between K_{OC} values of NP111 and the percentage

CHAPTER 4 RESULTS AND DISCUSSION

of alkyl C allows the K_{OC} to be calculated in the case of microstructure exclusively formed by alkyl groups (100%). A log K_{OC} value of 4.7 can be thus calculated, which is comparable to the reported log K_{OW} value of 4.5 (Ahel and Giger, 1993). This confirms the hydrophobic efficiency of alkyl microdomains for the adsorption NP111 by analogy to the partition of the NP111 in the organic octanol phase.

4.3 Adsorption of PFOA on Yangtze River sediments and their components

The distribution of PFOA in fresh water (So et al., 2007) and sediments (Bao et al., 2010) of Yangtze River has been documented. The stability of PFOA in the environmental compartments was well documented. PFOA is resistance to natural degradation such as biodegradation (Liou et al., 2010) and direct photolysis, and consequently environmentally persistent. Thus, consolidated knowledge of the sorption of PFOA on sediment not only plays an important role in its fate and transport in the aquatic system, but also is a prerequisite for assessing the environmental risk of PFOA and remedying its adverse effects. Although the sorption of PFOA on sediments has been investigated (Higgins and Luthy, 2006), the pronounced sorption isotherm was not observed perhaps due to the limited determination. We thus investigated the sorption of PFOA on Yangtze River sediments, including inorganic sediment components like goethite, $\delta\text{-Al}_2\text{O}_3$ and illite, and the organic component humic acid with the radioactive trace method.

The sorption kinetics of PFOA on solid adsorbents and HA solution demonstrated that the equilibrium was reached at around 20 hours. In order to avoid non-equilibrium conditions, 48 hours as the equilibrium time was applied for all sorption isotherms of PFOA. The recovery of PFOA in the sorption investigations ranged from 101% to 104%.

Adsorption isotherms of PFOA on the Yangtze River sediments are presented in Fig. 4.8a. The isotherms were found to be slightly nonlinear and were properly simulated by the Freundlich model ($r^2 > 0.923$, Table 4.5).

CHAPTER 4 RESULTS AND DISCUSSION

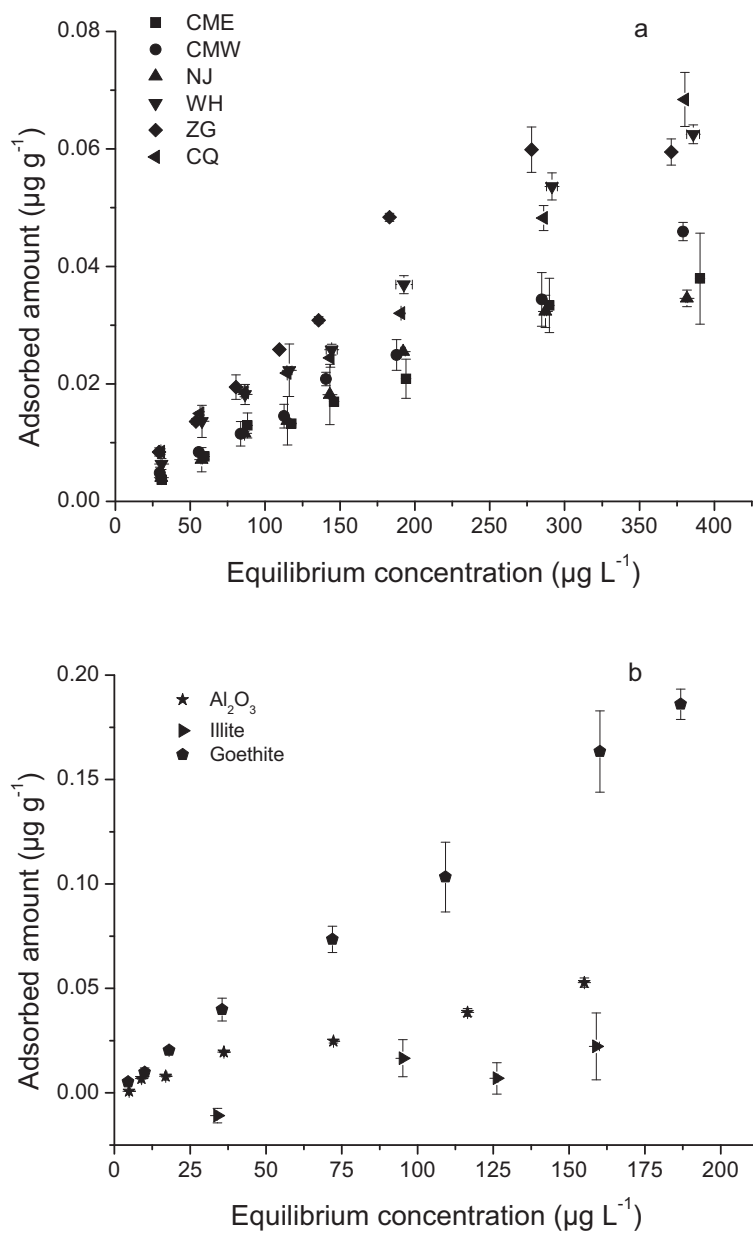


Fig. 4.8 Adsorption isotherms of PFOA on sediments (a) and sediment model components (b)

The K_{OC} (L kg^{-1}) values of PFOA were calculated based on the organic carbon content

SORPTION OF A NONYLPHENOL ISOMER AND PERFLUOROOCTANOIC ACID ON
GEOSORBENTS AND CARBON NANOTUBES

and the distribution coefficient (K_d) simulated in 0–200 $\mu\text{g L}^{-1}$ equilibrium concentration range by the linear model. The K_{OC} values for PFOA on sediments ranged from 18.32 L kg^{-1} to 40.53 L kg^{-1} . A higher K_{OC} value of 129 L kg^{-1} on freshwater sediment was reported by Higgins and Luthy (2006) which can be explained by the bridging effect of Ca^{2+} . The bivalent cation like Ca^{2+} used in that study can act as a bridge between the anionic sorbate and the negatively charged surface leading to an enhanced adsorption. In our study, experiments with PFOA on Suwannee River NOM did not show any sorption in the presence of Na^+ . Under neutral and alkaline conditions, natural organic matter is negatively charged and the anionic form of PFOA is prevailing. In general, there is no significant PFOA adsorption on sediments because of the electrostatic repulsion.

Table 4.5 Freundlich parameters and K_{OC} (L kg^{-1}) values of PFOA calculated based on the organic carbon content and distribution coefficient (K_d) simulated in PFOA equilibrium concentration range 0–200 $\mu\text{g L}^{-1}$ by the linear model

	$K_f (\mu\text{g}^{(1-1/n)} \text{L}^{1/n} \text{g}^{-1})$	$1/n$	r^2	$K_{OC} (\text{L kg}^{-1})$
CME	1.38×10^{-4} ($\pm 1.89 \times 10^{-5}$)	0.96 (± 0.03)	0.99	40.53
CMW	2.38×10^{-4} ($\pm 1.52 \times 10^{-5}$)	0.89 (± 0.01)	0.99	18.32
NJ	2.01×10^{-4} ($\pm 1.23 \times 10^{-5}$)	0.89 (± 0.07)	0.97	18.49
WH	3.39×10^{-4} ($\pm 6.78 \times 10^{-5}$)	0.88 (± 0.04)	0.99	19.98
ZG	4.49×10^{-4} ($\pm 2.10 \times 10^{-4}$)	0.87 (± 0.10)	0.92	26.30
CQ	8.44×10^{-4} ($\pm 1.40 \times 10^{-4}$)	0.69 (± 0.03)	0.99	27.88
$\delta\text{-Al}_2\text{O}_3$	6.38×10^{-4} ($\pm 3.29 \times 10^{-4}$)	0.93 (± 0.14)	0.91	-
Goethite	1.22×10^{-3} ($\pm 2.55 \times 10^{-5}$)	0.96 (± 0.01)	0.99	-

Note: - not determined

Sorption isotherms of PFOA on goethite and $\delta\text{-Al}_2\text{O}_3$ were well described by

CHAPTER 4 RESULTS AND DISCUSSION

Frendlich model ($r^2 > 0.930$) and the relative parameters are presented in Table 4.5.

PFOA adsorbed more strongly on goethite than on δ -Al₂O₃, but not at all on illite (Fig. 4.8b). This difference likely resulted from the electrostatic interactions. The pH values in supernatants with δ -Al₂O₃ ranged from 7.63 to 7.76, from 6.92 to 6.99 for goethite and from 6.75 to 6.97 for illite. The points of zero charge (PZC) are 8.1 for δ -Al₂O₃ (Tombácz and Szekeres, 2001), 9.3 for goethite (Antelo et al., 2005) and 3.5 for illite (Lan et al., 2007), respectively. Thus, under such conditions, goethite carries more positive charges than δ -Al₂O₃ due to their different PZC. In contrast, illite is negatively charged on the surface under the experimental conditions. In this pH range, also PFOA was predominantly negatively charged due to the pK_a value of 3.8 (Goss, 2008). Therefore, it can be concluded that electrostatic interaction causes various sorption affinities among goethite, δ -Al₂O₃ and illite. The results indicate that goethite (iron oxide) could be generally responsible for the sorption of PFOA in sediments.

No significant sorption of PFOA on humic acids was observed although the K_{OC} value of PFOA on humic substances in sediment was calculated on basis of the organic fraction and the distributed coefficients. This result is mainly assigned to the electrostatic repulsion. Similarly, no significant binding was observed between the anionic surfactant (SDS: sodium dodecyl sulfate) and purified Aldrich humic acid (Koopal et al., 2004). However, the significant sorption of cationic surfactants such as dodecyl- and cetylpyridinium chloride on purified Aldrich humic acid is observed (Koopal et al., 2004). The strong adsorption of cationic surfactants is due to both electrostatic interaction and hydrophobic attraction (Koopal et al., 2004). For the sparse sorption of anionic surfactants and PFOA, the cause is that the electrostatic repulsion is stronger than the hydrophobic attraction.

Hence, it must be emphasized that normalizing PFOA sorption coefficient to organic carbon is not appropriate because PFOA does not readily partition into lipid or other forms of organic carbon. A similar finding was elaborated by Hites (2006). Thus, the

SOPRTION OF A NONYLPHENOL ISOMER AND PERFLUOROOCTANOIC ACID ON
GEOSORBENTS AND CARBON NANOTUBES

calculated K_{OC} value of organic compounds overestimates the effect of organic carbon on the adsorption of this compound to soils and sediments, and the calculation of the K_{OC} value of organic compounds on the sediments investigated is “contradictory” although it was applied in the sorption of PFCs on sediments (Higgins and Luthy, 2006).

4.4 Adsorption of PFOA and NP111 on multi-walled carbon nanotubes

There are a lot of papers published about the sorption of inorganic and organic contaminants on CNTs (Lu and Chiu, 2006; Yang et al., 2006; Lin and Xing, 2008). The sorption isotherms of linear NP and PFOA, respectively, on multi walled carbon nanotubes (MWCNTs) have already been reported (Li et al., 2010), but the concentrations of NP and PFOA were extremely higher than those in the environment. Hereby, we investigated the sorption of a branched NP isomer and PFOA on multi walled carbon nanotubes in the environmentally relevant concentration range.

4.4.1 Characterization of multi-walled carbon nanotubes

Aggregation behavior of MWCNTs as a function of salt concentration

The critical coagulation concentration (CCC) of pristine M3 MWCNTs was studied in NaCl and CaCl₂ solutions by a turbidity method (Sano et al., 2001). The results are presented in Fig. 4.9. The salt concentration was taken as the CCC value when the normalized dispersive amount was 0.5. The CCC value of NaCl and CaCl₂ were 51.4 mM and 0.28 mM, respectively. Salsh et al. (2008b) reported the CCC value of MWCNTs was 25 mM NaCl measured by dynamic light scattering. Sano et al (2001) studied the aggregation of single-walled CNTs and the CCC value observed was 37 mM NaCl by turbidity. The previous value is close to the value observed in this study.

SOPRTION OF A NONYLPHENOL ISOMER AND PERFLUOROOCTANOIC ACID ON GEOSORBENTS AND CARBON NANOTUBES

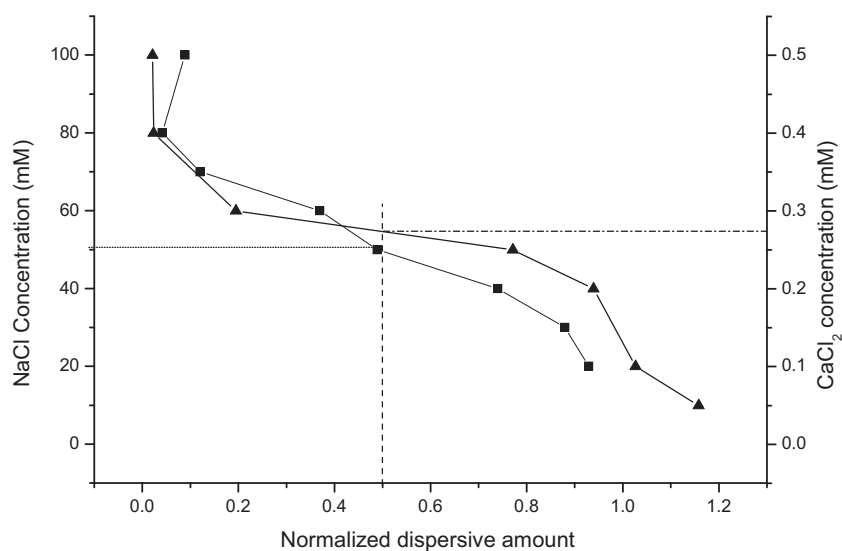


Fig. 4.9 Aggregation behavior of pristine M3 sample over salinity (■ NaCl and ▲ CaCl₂ solutions)

The net proton surface excess density of MWCNTs

The net proton surface excess density on multi walled carbon nanotubes with or without HCl treatment was determined by potentiometric acid-base titration. As evidenced in Fig. 4.10a and b, the net proton surface excess decreased from positive to negative values with increasing pH. At the given pH, the order of the net proton surface excess density of pristine MWCNTs is BA>CP>M3. However, there was no significant net proton surface excess density of purified MWCNTs observed (Fig 4.10b). The purification process significantly decreased the net proton surface excess density for BA. In contrast, it was not efficient for CP and M3.

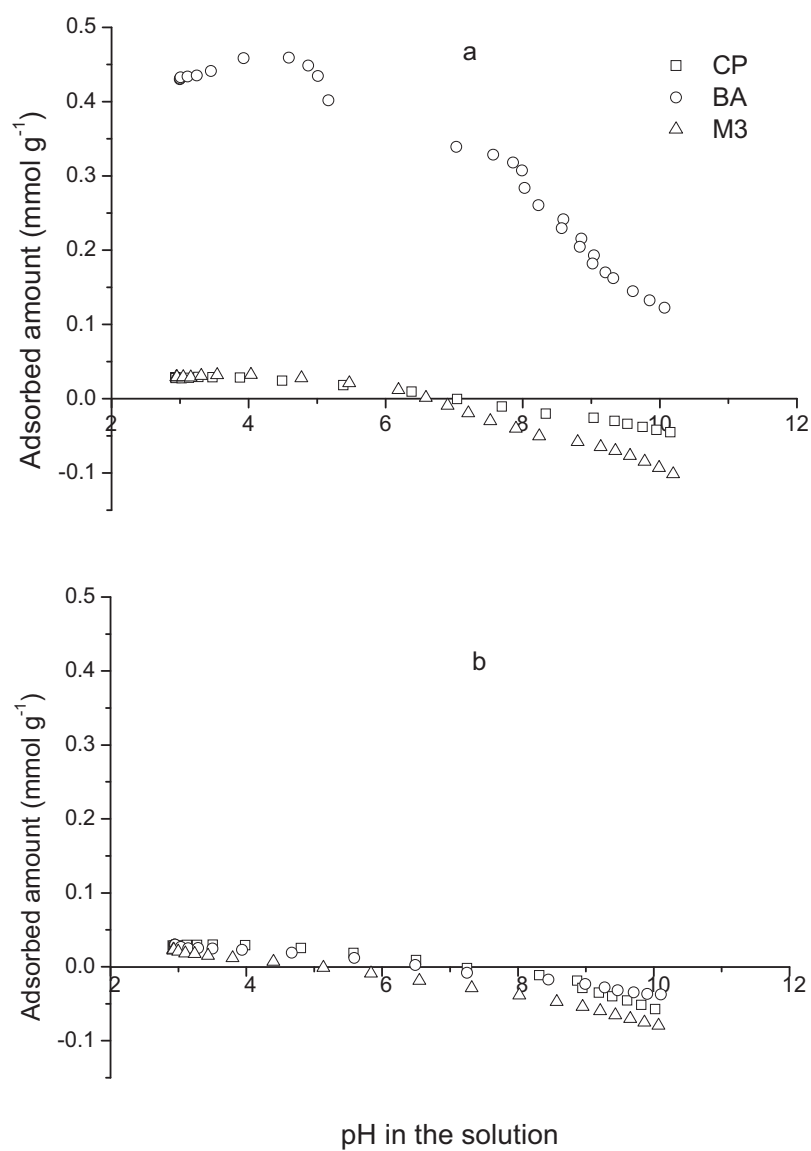


Fig. 4.10 Titration of pristine (a) and purified (b) MWCNTs

TEM images of MWCNTs

Representative TEM images of samples are presented in Fig. 4.11. As shown

SORPTION OF A NONYLPHENOL ISOMER AND PERFLUOROOCTANOIC ACID ON GEOSORBENTS AND CARBON NANOTUBES

in Fig. 4.11, internal and external diameters were in the similar appearance to that reported by manufacturers. Free amorphous carbon coating was apparently observed on the outer surfaces of all pristine MWCNTs at high resolution images (Fig. 4.11b, 4.11d and 4.11f). As seen in Fig. 4.11a, 4.11c and 4.11e, CP sample displayed more black spots in the central of tubes, which were representative for metal catalyst particles, than BA and M3 samples. These results were identical with the purity of MWCNTs verified by thermogravimetry (TG) (see below) and the metal concentration determined by elemental analysis.

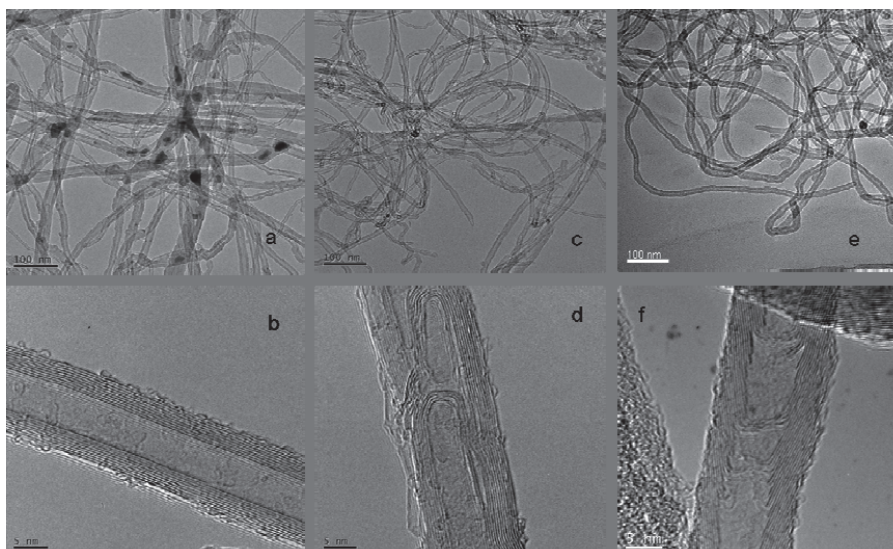


Fig. 4.11 Representative overview of TEM images of CP (a, b), BA (c, d) and (e, f)

Multi walled carbon nanotubes were sinuous and always entangled. The typical carbon nanotubes were with cylindrical layers parallel to the tube axis (Fig. 4.11b). The carbon nanotubes with stacked aromatic layer not parallel to the tube axis were illustrated and several layers of graphenes were perpendicular to the tube axis (Fig. 4.11d). In most case, a cap was observed at the end of tubes (Fig 4.11f).

Thermogravimetry (TG) of MWCNTs

The impurities of MWCNTs were determined by simultaneous thermal analyzer (TG). The TG spectra are presented in Figure A1. As shown in Fig. A1, a mass decrease of CP, BA and M3 samples was not observed before 350°C, indicating that the amorphous carbon on the sample is not significant. Saleh et al (2008a) pointed out that MWCNTs had a small peak (0.7% of the total integrated area under the peaks) near 300°C, indicative of amorphous carbon. The residual mass of CP, BA and M3 samples was 5.17%, 2.37% and 1.31% to initial total mass after burning at 1400°C and was considered to be residual metal catalyst (Fig. A1).

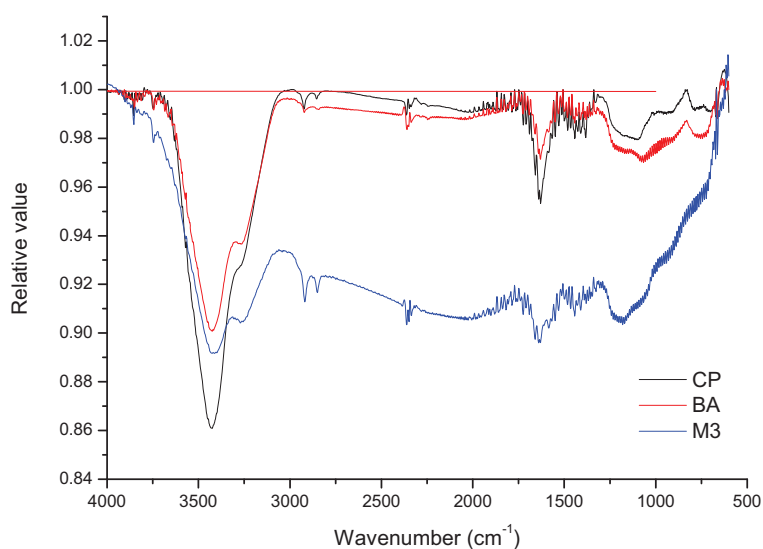
Fourier transform infrared spectroscopy (FT-IR) of pristine MWCNTs

Fig. 4.12 FT-IR spectra of pristine multi walled carbon nanotubes

Structural composition of MWCNTs was usually probed by Fourier transform infrared spectroscopy (FT-IR) (Hamwi et al., 1997; Chen et al., 1998). The FT-IR spectra of pristine MWCNTs are presented in Fig. 4.12. As shown, the

SORPTION OF A NONYLPHENOL ISOMER AND PERFLUOROOCTANOIC ACID ON
GEOSORBENTS AND CARBON NANOTUBES

strong and broad peaks of 3200–3600 cm⁻¹ were attributed to the –OH functional group on the surface of pristine MWCNTs. The peaks within 2800–2900 cm⁻¹ were representative for –CH₂– or –CH₃ structural component. The peaks within 1450–1600 cm⁻¹ were assigned to the *sp*²-hybridized carbon in the graphitic structure of MWCNTs. The peaks with 2300–2400 cm⁻¹ referred to CO₂ from the air.

Zeta potential (ZP) of multi walled carbon nanotubes

Table 4.6 Zeta potential of pristine and HCl-treated MWCNTs

MWCNTs	CP		BA		M3	
	pH	ζ, mV	pH	ζ, mV	pH	ζ, mV
Pristine	5.91	-23 ± 3	6.29	11 ± 4	6.46	-33.8 ± 3
HCl-treated	5.83	-24 ± 3	6.48	-20 ± 5	6.37	-35.3 ± 2

Zeta potential of MWCNTs is an important parameter for ionic organic compounds sorption. The zeta potential of MWCNTs was calculated by the electrophoretic mobility with the Henry's function (Ohshima, 1994). The Henry equation is

$$U_E = \frac{2\varepsilon\zeta f(K_a)}{3\eta} \dots\dots\dots(8)$$

where, U_E (cm² V⁻¹ s⁻¹) is the electrophoretic mobility, ζ (V) is the zeta potential, ε is the dielectric constant, η (cm² s⁻¹) is viscosity of medium, $f(K_a)$ in this case is 1.5, and is referred to as the Smoluchowski approximation. Hence, ZP of pristine and purified MWCNTs used in our study is presented in Table 4.6. For pristine CNTs, ZP of BA was positive. Nevertheless, zeta potentials of M3 and CP were apparently negative. MWCNTs usually have negative zeta potential under neutral solution conditions (Tessonier et al., 2009). Interestingly, the zeta potential of BA became negative after purification. HCl treatment did not obviously influence on the ZP of M3 and CP.

Metal concentration of MWCNTs

Carbon nanotubes are usually synthesized in the presence of specific metal catalysts. Consequently, the products still contained some metal catalysts even after the purification by manufacturer. The presence of traces of metal catalysts will inevitably complicate the fate and sorption behavior of organic compounds. In order to assess the effect of metal catalysts distributed on the outer surface of MWCNTs on the sorption, HCl treatment was applied in this work. The metal concentration of MWCNTs before and after the HCl treatment was analyzed and the data are presented in Table 4.7.

Table 4.7 Metal concentrations of MWCNTs before and after HCl treatment

Sources	Metal	Catalyst concentration (mg kg ⁻¹)	
		Pristine MWCNTs	Treated MWCNTs
CP	Fe	28291±872	24506 ±107
	Al	308±18	< 5.7
BA	Co	2994±163	1418±33
	Fe	<266	<376
	Al	2500±119	986±113
	Mg	2155±190	61±1
	Mn	2931±193	285±11
M3	Ni	5585±321	3344±62
	Fe	2151±62	< 120
	Al	426±21	< 5.7

In comparison with pristine MWCNTs, HCl treatment efficiently removed Al from CP. But it was less efficient for Fe. HCl treatment was more successful for BA because catalyst traces are also distributed on the outer surface of MWCNTs (http://www.baytubes.com/product_production/baytubes_data.html). To

SORPTION OF A NONYLPHENOL ISOMER AND PERFLUOROOCTANOIC ACID ON GEOSORBENTS AND CARBON NANOTUBES

some extent, the removal of catalyst traces for M3 was also observed.

The percentage of metal catalysts is 2.88%, 1.14% and 0.87% for CP, BA and M3, respectively. These values are proportional to TG results although catalyst concentrations measured by TG are generally higher. The probable cause is that the residue of MWCNTs after combustion is not completely dissolved in the extraction solvent for the measurement of metal concentration.

4.4.2 Sorption of PFOA on multi-walled carbon nanotubes

Adsorption isotherms of PFOA

Adsorption isotherms of PFOA normalized to the surface area on both pristine and HCl-treated MWCNTs are shown in Figure 4.13a and b. In addition, the insert in Fig. 4.13a shows the adsorption isotherm of PFOA on BA up to 50 000 $\mu\text{g L}^{-1}$. The log-log presentation of the isotherm clearly indicated two-step sorption of PFOA to MWCNTs in the large concentration range. In this study, the focus was on the low PFOA concentration range (on the first-step in the sorption isotherms), which is of environmental interest.

The surface area of pristine CP and BA samples were 111 and 206 $\text{m}^2 \text{g}^{-1}$, respectively. Adsorption data normalized to the mass of the MWCNTs were used for the nonlinear Freundlich and Langmuir models (Table 4.8). According to the coefficients of determination (r^2), both Freundlich and Langmuir models described the sorption isotherms well. A similar result was found when PFOA was adsorbed at high concentrations on MWCNTs with different oxygen contents (Li et al., 2010).

In the investigated concentration range (Fig. 4.13a), the adsorption of PFOA on pristine BA was significantly higher than that on CP. The plot in Fig. 4.13

CHAPTER 4 RESULTS AND DISCUSSION

suggests that a surface area dependent mechanism does not play the only role in the sorption of PFOA on MWCNTs. BA containing traces of Co/Mn/Mg/Al catalysts on the surface adsorbed roughly three times as much PFOA than CP. The pH of the supernatant of pristine CP and BA during the sorption experiments varied in the ranges of 5.8–5.9 and 6.2–6.6, respectively. The difference in PFOA sorption affinities likely results from the influence of pH and the surface functional groups as well as specific catalyst traces-dependent physicochemical characteristics of the MWCNTs. It must be noted that the metal catalyst in the tubes is generally not available to the solutes from aqueous solutions. Therefore, the higher catalyst content of CP MWCNTs (see Table 4.7) is of no significance.

As we mentioned above, zeta potential of pristine BA MWCNTs was positive, but it displayed negative after HCl treatment. In contrary, CP consistently exhibited negative with or without HCl treatment. As the anionic form of PFOA predominates under the studied solution conditions according to its pK_a value of 3.8 (Goss, 2008), the electrostatic interaction will play a role in the PFOA uptake. Thus, the differences in surface charge of the MWCNTs can be assumed to be responsible for the different adsorption affinities and capacities. Nevertheless, at high concentrations, the adsorption of PFOA on the pure graphene surface of MWCNTs can be driven by hydrophobic interaction (Li et al., 2010).

SORPTION OF A NONYLPHENOL ISOMER AND PERFLUOROOCCTANOIC ACID ON
GEOSORBENTS AND CARBON NANOTUBES

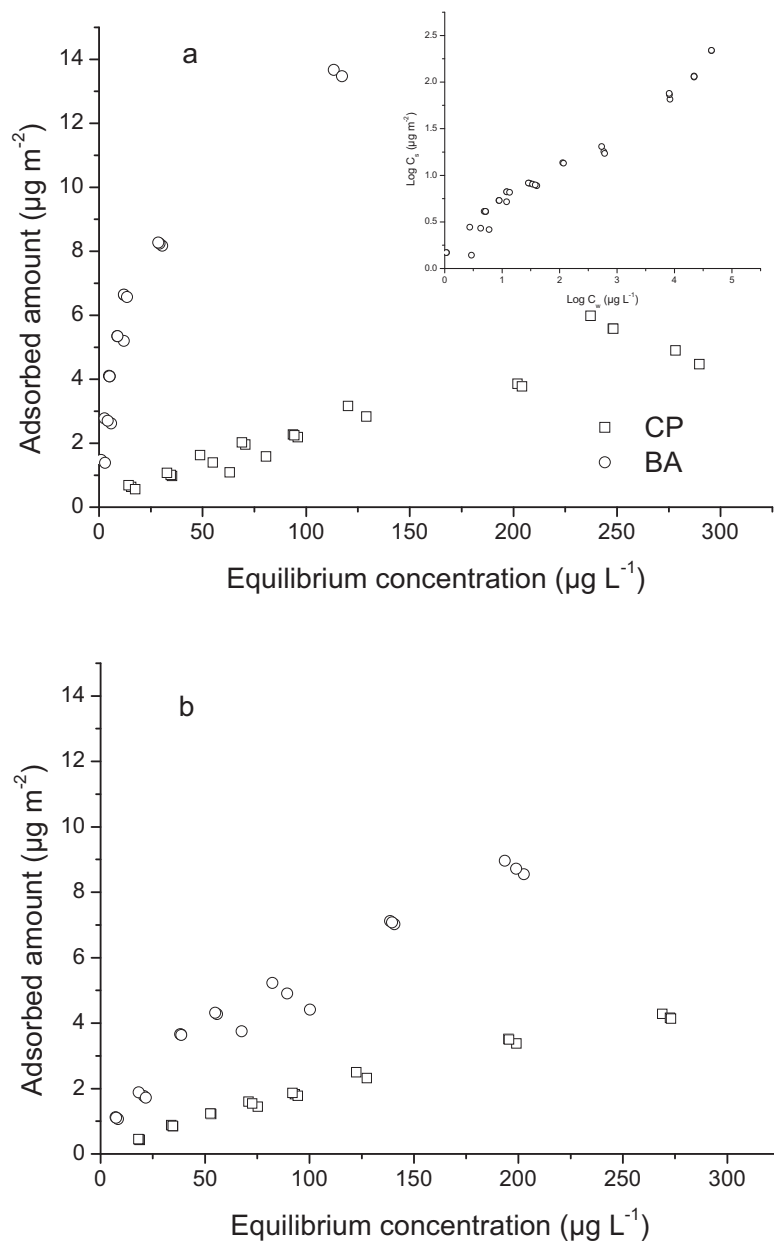


Figure 4.13 Adsorption isotherms of PFOA onto (□) CP and (○) BA MWCNTs in 10 mM of NaCl solution: a) PFOA on pristine MWCNTs, b) PFOA on purified MWCNTs (The adsorbed amount of PFOA was normalized by surface area) (The insert plot shows the sorption isotherms of PFOA on pristine BA up to 50 000 μg L⁻¹)

CHAPTER 4 RESULTS AND DISCUSSION

Table 4.8 The parameters of Freundlich and Langmuir models obtained from mass based PFOA adsorption data

Source of MWCNTs		Pristine		HCl-treated	
		CP	BA	CP	BA
Freundlich model	$K_f [\mu\text{g}^{(1-1/n)} \text{L}^{1/n} \text{g}^{-1}]$	7.1±2.3	410±34	6.8±0.6	74. ±12
	$1/n$	0.79±0.06	0.41±0.02	0.77±0.02	0.62±0.03
	r^2	0.92	0.95	0.99	0.97
Langmuir model	$b (\mu\text{g g}^{-1})$	1071 ± 469	3072 ±160	1371 ± 87	3393 ±365
	$K_L (\text{L } \mu\text{g}^{-1})$	0.0030 ±0.0008	0.0559 ± 0.0070	0.0022 ± 0.0002	0.0068± 0.0013
	r^2	0.92	0.95	0.99	0.95

Fig. 4.13b shows that the sorption affinity of PFOA on HCl-treated BA significantly decreased, while only a slight effect was observed on the CP sample. Indeed, the Langmuir modeling indicates a large K_L decrease by a factor of 10 (Table 4.8) in the case of HCl-treated BA. The HCl treatment strongly reduced the metal content of the BA, while that of CP decreased only slightly (Table 4.7). However, a concurrent rise in the surface area (approx. 10% increase) upon purification occurred for both MWCNTs (CP: 122 m² g⁻¹, BA: 231 m² g⁻¹). The pH of the aqueous phase during the sorption experiments with purified CP and BA was in the range of 5.7–6.0 and 6.2–6.7, respectively. In comparison with the pristine MWCNTs, there was no significant shift in pH. We therefore assume that the depletion of the metal concentration may diminish the adsorption affinity of the nanotubes, particularly in the case of BA. The comparison of the zeta potential of the MWCNTs studied gives some indication of this hypothesis. We assume that the surface charge arises from the surface acidic groups and the oxidized metal catalyst material. The positive zeta potential of BA thus indicates a higher concentration of metal (hydro)oxide related surface sites, which would favor an electrostatic sorption as indicated by the high K_L (affinity parameter) of the Langmuir model in Table 4.8. However, the lack of information about the catalyst composition

SORPTION OF A NONYLPHENOL ISOMER AND PERFLUOROOCTANOIC ACID ON GEOSORBENTS AND CARBON NANOTUBES

and distribution makes the interpretation of these observations difficult.

Desorption of PFOA

Desorption of PFOA from pristine MWCNTs revealed no pronounced hysteresis (see Fig. 4.14), indicating that adsorption completely reversible. In contrast, desorption hysteresis of atrazine with various MWCNTs was observed and appeared to be dependent on their aggregation in the presence of cation species (Chen et al., 2008a). The reversible sorption of PFOA on MWCNTs indicates that physical adsorption rather than chemical sorption prevails. In case of the sorption-desorption of monoaromatic compounds such as phenol on carbon nanotubes, Ji et al. (2010) found the adsorption reversibility for organic compounds, the cause was assigned to the interconnected pore structure and less pore deformation of CNTs.

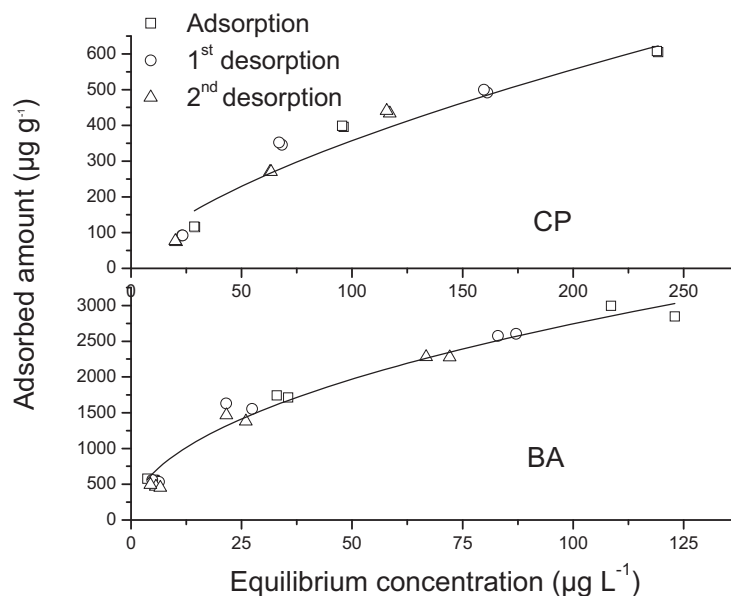


Figure 4.14 Desorption isotherms of PFOA onto pristine MWCNTs (The line was generated with the Freundlich equation on the basis of sorption data) ((□) Sorption, (○) 1st desorption and (△) 2nd desorption)

Thermodynamic parameters

The adsorption isotherms of PFOA on pristine M3 were determined at 288K, 303K and 318K, respectively. The sorption capacity decreased with increasing temperature (Fig. 4.15). Thermodynamic parameters such ΔG , ΔH , and ΔS are calculated by

$$K_d = \frac{C_s}{C_w} \dots\dots\dots (1)$$

$$\Delta G = -RT \ln K_0 \dots\dots\dots (9)$$

$$\ln K_0 = \frac{-\Delta H}{RT} + \frac{\Delta S}{R} \dots\dots\dots (10)$$

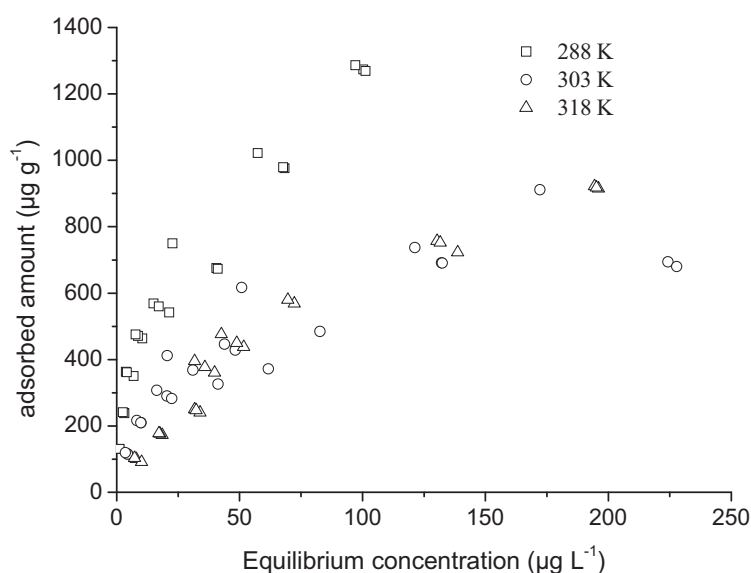


Fig. 4.15 Adsorption isotherms of PFOA on pristine M3 sample at 288K, 303K and 318 K

where K_d is the adsorption coefficient ($L g^{-1}$). The thermodynamic equilibrium constant (K_0) is obtained by plotting $\ln(K_d)$ versus C_s , extrapolating C_s to zero. The intercept of straight line obtained by the least square fit equals to $\ln K_0$. R is the universal gas constant and T is the temperature (K). Eq. (10) predicts the adsorption enthalpy (ΔH) and entropy (ΔS). Both terms are obtained by

SORPTION OF A NONYLPHENOL ISOMER AND PERFLUOROOCTANOIC ACID ON GEOSORBENTS AND CARBON NANOTUBES

plotting $\ln K_0$ versus $1/T$. The slope of Eq. (9) is $-\Delta H / R$, and the intercept is $\Delta S / R$ (Shen et al., 2009).

The ΔG values calculated were -12.35 , -9.09 and -6.67 kJ mol^{-1} at 288 K, 303 K and 318 K, respectively. The negative value of ΔG confirmed that the sorption of PFOA on pristine M3 was spontaneous and thermodynamically favourable. The ΔH value of -67.05 kJ mol^{-1} indicated an exothermic sorption. The sorption of PFOA on this MWCNT is a physisorption process because the absolute value of ΔH in the case of chemisorption is larger than -80 kJ mol^{-1} (Dörfler, 2002). The assumed physisorption was also confirmed by the reversible ad/desorption curves. A ΔS value of -0.19 kJ (mol K)^{-1} indicated a decrease randomness at the solid-liquid interface during the sorption.

Influence of pH

Figure 4.16 shows the effect of pH on PFOA adsorption to the pristine CP and BA, respectively. A decreasing adsorption of PFOA with increasing pH value was observed on both MWCNTs in the pH range 2–12. As is reported, increasing the pH value decreases the sorption of perfluorinated chemicals on sediments or MWCNTs due to electrostatic repulsion (Higgins and Luthy, 2006; Li et al., 2010).

Carboxyl and phenolic hydroxyl functional groups have been identified on the surface of CNTs (Hu et al., 2001; Schierz and Zaenker, 2009). Thus, with increasing pH the negative surface charge does increase. Moreover, the partial surface charge of the carbon chain (C8) part of PFOA is also negative due to the high electronegativity of the attached fluorine atoms. In parallel, the concentration of anionic species of PFOA increases with increasing pH up to about pH 6 due to the pK_a value of 3.8 (Goss, 2008) resulting in a repulsion between the anionic carboxylate surface groups and deprotonated PFOA and thus reduced the adsorption. The further reduction of the adsorption capacity,

especially for BA above pH 6–7 may result from metallic catalyst compounds. Indeed, the negative surface charge of the catalyst also increases along the pH.

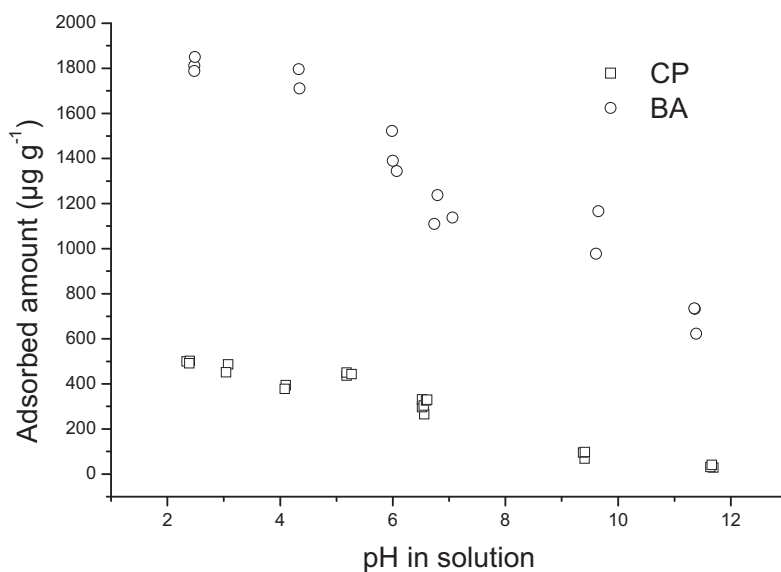


Figure 4.16 Influence of pH on the adsorption of PFOA on the pristine (□) CP and (○) BA MWCNTs

Influence of salinity (ionic strength)

The influence of salinity on PFOA adsorption on pristine MWCNTs is shown in Fig. 4.17. In the concentration range of 0.001–0.03 M NaCl the adsorption capacity decreased with increasing salt concentration; above 0.03 M NaCl, the adsorbed amount was almost constant. However, Chen et al. reported that the

SORPTION OF A NONYLPHENOL ISOMER AND PERFLUOROOCTANOIC ACID ON
GEOSORBENTS AND CARBON NANOTUBES

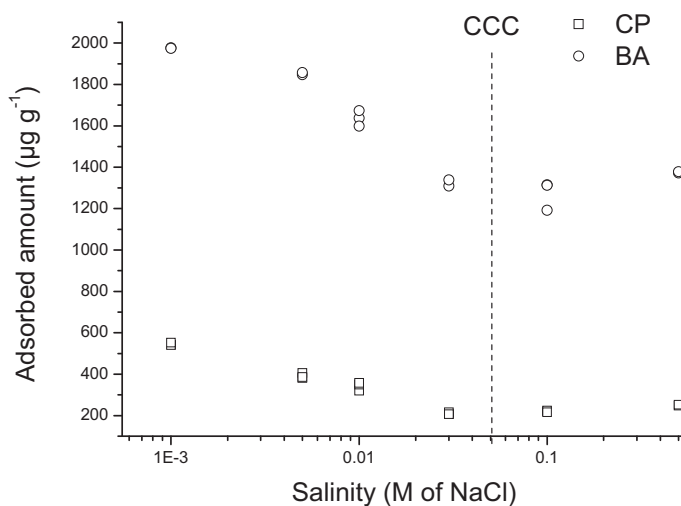


Figure 4.17 Influence of salinity on PFOA adsorption on the pristine (\square) CP and (\circ) BA MWCNTs

impact of salinity on the sorption of neutral compounds to single-walled CNTs was not observed in 0.02 M to 0.1 M NaNO_3 (Chen et al., 2008b). This finding is identical with our data in the same concentration range of NaCl . However, this result contrasts with an increased uptake of polar compounds by activated carbon fiber because of screening the effect of the surface charge produced by the addition of salt (Fontecha-Cámara et al., 2007). It may thus be assumed that the decrease of PFOA adsorption was attributed to the increasing aggregation by the addition of salt. Indeed, the aggregation of suspended MWCNTs depends on the salt concentration (Saleh et al., 2008a). In this work, the critical coagulation concentration (CCC) for carbon nanotubes observed was around 0.051 M NaCl . The effect of salt concentration on PFOA sorption may be attributed to a reduced availability of the surface area of the MWCNTs (Zhang et al., 2009). The surface area of MWCNTs decreased with salinity due the facilitation of aggregation behavior before that critical coagulation

CHAPTER 4 RESULTS AND DISCUSSION

concentration was reached, and the surface area became constant over the critical coagulation concentration. The internal region of the aggregate is hardly available for PFOA molecules. Under these conditions the slow PFOA diffusion into the aggregate increases the equilibration time. It must be noted that the surface coverage of PFOA on MWCNTs is about 1% in 10 mM NaCl solution as calculated from the molecular size of PFOA (108 \AA^2 estimated by the MOLDEN software (Schaftenaar and Noordik, 2000)) and the surface area of MWCNTs. A direct effect of PFOA on the MWCNTs aggregation is thus improbable.

Solutes with the same kind of charge in electrolyte solution would compete with each other, and then reduced the target sorption affinity (Pettersson et al., 2008; George et al., 2009). The presence of Cl^- in the electrolyte will screen the positive impact of metal catalysts compounds in the adsorption of PFOA because metal catalysts compounds show positive charge in aqueous phase. Hence the reduction of PFOA adsorbed amount could be accounted for the Cl^- concentration.

Influence of the cationic species

Ca^{2+} and Na^+ commonly coexist as the majority of cation species in terrestrial system. The adsorption in the presence of Ca^{2+} was pronouncedly higher than that with Na^+ (Fig. 4.18). The difference of adsorbed amount proportionally increased with equilibrium concentration increasing. Higgins and Luthy reported that Ca^{2+} could significantly enhance adsorbed amount compared with Na^+ , especially in large concentration (Higgins and Luthy, 2006). It was concluded that the “bridging” effect of Ca^{2+} led to the increased adsorbed amount of PFOA in this study. Bivalent ions like Ca^{2+} used in the study can act as a bridge between the anionic adsorptive and the negatively charged surface of MWCNTs, resulting in an enhanced adsorption.

SORPTION OF A NONYLPHENOL ISOMER AND PERFLUOROOCTANOIC ACID ON
GEOSORBENTS AND CARBON NANOTUBES

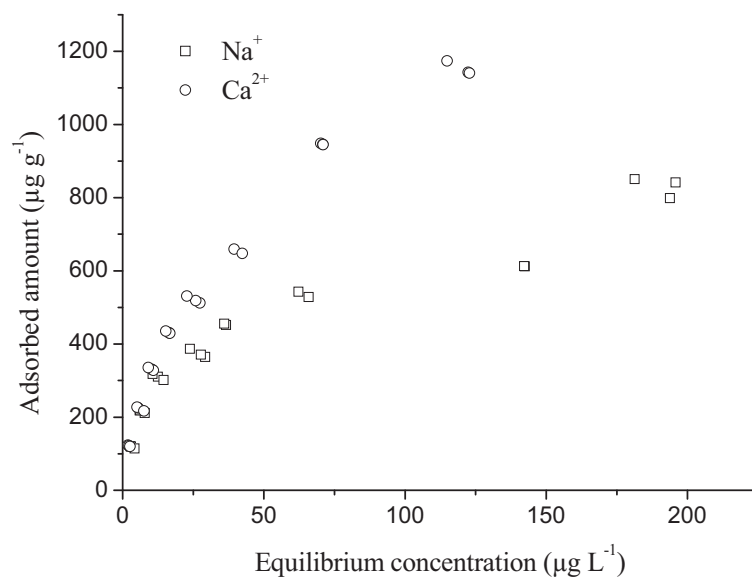


Fig. 4.18 Influence of cation species on PFOA sorption on pristine M3 MWCNTs (10 mM of NaCl and 3.33 mM of CaCl₂)

4.4.3 Adsorption of NP111 on multi-walled carbon nanotubes

The adsorption isotherms of NP111 on pristine and purified MWCNTs are presented in Fig. 4.19. Based on the coefficients of determination ($r^2 > 0.95$), Sorption isotherms of NP111 on MWCNTs normalized to mass were well described by a linear model (Henry model).

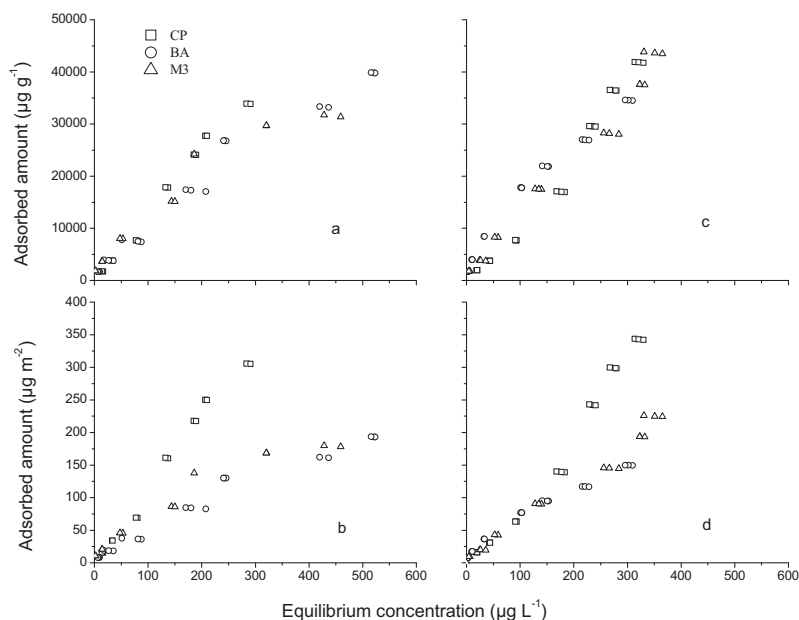


Fig. 4.19 Adsorption isotherms of NP111 on pristine (a and b) and purified MWCNTs (c and d). (a and c: NP111 sorption based on mass; b and d: sorption normalized by specific surface area)

As seen in Fig. 4.19a and c, there was not significant difference of the sorption isotherms of NP111 among pristine or purified MWCNTs based on mass in the low equilibrium concentration range. However, in the high equilibrium concentration range, purified MWCNTs exhibited higher sorption capacity of NP111 than pristine ones. It was probably caused by the specific surface area

SORPTION OF A NONYLPHENOL ISOMER AND PERFLUOROOCTANOIC ACID ON
GEOSORBENTS AND CARBON NANOTUBES

increase due to the purification process. Chen et al. (2007) pointed out that the stronger adsorption of non-polar aromatics was attributed to the π - π interaction between the flat surfaces of both aromatic molecules and carbon nanotubes. Because NP111 is a non-polar aromatic compound under environmental conditions, the sorption mechanism of NP111 on MWCNTs was therefore interpreted by the π - π interaction. Besides, the alkyl chain of NP111 exhibits the hydrophobic properties, the hydrophobic interaction also promotes the sorption of NP111 on MWCNTs.

Indeed, Cai et al. (2003) reported that multi walled carbon nanotubes as solid phase extraction materials at least was quite efficient for the extraction of 4-*n*-NP from the aqueous phase comparable to C18 silica, but is better than XAD-2 copolymer. Therefore, the sorption capacity of MWCNTs for NP111 suggests that MWCNTs is the ideal and potential materials to effectively remove NP111 from the aquatic system.

The sorption coefficients (K_d) of NP111 on pristine CP, BA and M3 were 1.24×10^5 , 8.20×10^4 and 8.56×10^4 L kg⁻¹, respectively. Interestingly, the K_d values of NP111 on purified CP, BA and M3 were 1.24×10^5 , 1.25×10^5 and 1.18×10^5 L kg⁻¹, respectively. The HCl treatment significantly enhanced the sorption coefficients for BA and M3 samples. It can be concluded that the enhancement of K_d was not completely assigned to the slight increase of the surface area due to the purification process. It was thus assumed that the removal of impurities on the surface of MWCNTs was responsible for the increasing of the sorption sites that was originally covered by the impurity.

However, CP MWCNTs had higher NP111 sorption normalized to the surface area than BA and M3 MWCNTs, while the latter two MWCNTs had the similar sorption affinity (Fig.4.19b and d). The same trends were observed for both

CHAPTER 4 RESULTS AND DISCUSSION

pristine and purified MWCNTs. The consistent sorption isotherms of NP111 on BA and M3 MWCNTs indicated that the sorption was also dependent on the specific surface area.

The impact of pH value on the sorption of NP111 on pristine MWCNTs (in appendix Table A1) was negligible because the pK_a value is 10.7 of NP111 and the hydrophobic interaction is prevailing in the sorption.

In comparison with the sorption affinity of PFOA on MWCNTs, NP111 sorption affinity was 5–20 times higher than PFOA on the same MWCNTs. Briefly, the coverage of PFOA is around 1%. However, the coverage of NP111, which is calculated by the size of NP111 molecule and the specific surface area of MWCNTs, ranged from 40% to 70% depending on which side of the cubic structure of NP111 estimated by the MOLDEN software (Schaftenaar and Noordik, 2000) was considered. It is indicative that the specific surface area dependent mechanism is predominant for the sorption of NP111 on MWCNTs.

Chapter 5 Conclusions

The sorption behavior of NP111 and PFOA on geosorbents such as Yangtze River sediments and their inorganic and organic components, including metal oxides (δ - Al_2O_3 and goethite), mineral (illite) and humic substances isolated from Yangtze River sediments was investigated by batch and dialysis techniques under the laboratory conditions. In addition, three commercial multi-walled carbon nanotubes (MWCNTs) were applied as innovative adsorbents to remove NP111 and PFOA from aqueous solutions. The influence of solution chemical factors, such as pH, salinity and cation species, was investigated. Both radioactively labeled and non-labeled NP111 and PFOA were used as target solutes. ^{14}C -solute concentrations in the solution and the solid phase were detected by means of a liquid scintillation counter (LSC) and the oxidizer tandem LSC method, respectively. The sorption isotherms of NP111 and PFOA were simulated by different models. Humic substances were characterized by solid-state ^{13}C direct polarization/magic angle spinning (DP/MAS) nuclear magnetic resonance (NMR) spectroscopy. The relationship between the organic carbon-normalized sorption coefficients (K_{OC}) and the quantitative structural composition of humic substances was analyzed by statistical methods.

The adsorption isotherms of NP111 on geosorbents were significantly non-linear and were well described by the Freundlich model. At the given equilibrium concentration, illite and δ - Al_2O_3 had a lower sorption capacity of NP111 than the sediments. In contrast, goethite and Suwannee River natural organic matter (SR NOM) as the reference organic matter exhibited a sorption capacity of NP111 that was two orders of magnitude higher than the sediments. This result indicates that both OM and goethite play an important role in the sorption (sequestration) of NP111 on sediments. Indeed, the high K_{OC} on sediments verified the above result.

CHAPTER 5 CONCLUSIONS

The adsorption isotherms of NP111 on HAs with comparable origins (HAs isolated from Yangtze River sediments) were well described by a linear model (Henry's law). The K_{OC} varied slightly depending on the HAs of different locations. In general, the sorption affinity of NP111 on HA was higher than on fulvic acid (FA). The influence of pH on the sorption of NP111 was only significant under alkaline conditions. Interestingly, a clear correlation between the K_{OC} value of NP111 and the alkyl C content of humic acids was observed, indicating that the aliphaticity of HAs significantly dominates the sorption of NP111. These results show that the fate of nonylphenol in soil or sediment depends not only on the content of HA, but also on its structural composition. The relationship between the aliphaticity of HAs and the K_{OC} value of NP111, which was established for the first time, is helpful for understanding the sorption mechanism of NP111 on humic substances.

Adsorption isotherms of PFOA on Yangtze River sediments and their model components were well fitted by nonlinear models *i.e.* the Freundlich model. In the equilibrium concentration range studied, slight differences were observed for the adsorption capacity of PFOA on different sediments. Goethite exhibited a higher adsorption capacity of PFOA than δ - Al_2O_3 due to electrostatic interaction. Conversely, no pronounced sorption of PFOA on illite was observed. This result indicates that goethite in sediments contributes to the sorption of PFOA. In the case of PFOA sorption on SR NOM, no sorption was observed. The probable reason is electrostatic interaction. It must be noted that the K_{OC} determined on both the sorption coefficient (K_d) and organic carbon fraction (f_{OC}) was not appropriate for PFOA because of the amphiphilic characteristics of PFOA. The K_{OC} overestimates the sorption behavior of PFOA in the environment.

MWCNTs were suggested for removing PFOA from aqueous solutions. Sorption isotherms of PFOA on MWCNTs were well described by the Freundlich model.

SORPTION OF A NONYLPHENOL ISOMER AND PERFLUOROOCTANOIC ACID ON GEOSORBENTS AND CARBON NANOTUBES

The thermodynamic data demonstrated that the sorption of PFOA on MWCNTs was characterized by physisorption. The sorption affinity and capacity of MWCNTs with traces of catalyst on the outer surface were significantly higher than that of MWCNTs without such traces. The adsorption of PFOA on MWCNTs was reversible. HCl treatment for MWCNTs with traces of metal catalyst on the outer surface strongly decreased the adsorbed amount of PFOA. HCl treatment significantly decreased the sorption affinity (K_L), but affected the monolayer sorption capacity (b) to a lesser extent. It is assumed that the decrease in the metal catalyst concentration on the outer surface of MWCNTs diminished the adsorption affinity of the MWCNTs due to the absence of electrostatic interaction. In a general way, the PFOA adsorption was significantly reduced with increasing salinity and pH values. The divalent cation Ca^{2+} significantly enhanced the adsorption compared with the monovalent cation Na^+ . This result shows that the solution factors distinctly affect the sorption isotherm of PFOA.

Adsorption isotherms of NP111 on MWCNTs were linear. In comparison to the sorption of PFOA, the sorption affinity of NP111 on MWCNTs was much higher due to the hydrophobic interaction as well as the π - π interaction. No effect of the impurity of MWCNTs and pH in solution was observed. The results suggest a potential application of MWCNTs in waste water treatment plants to remove hydrophobic organic compounds once MWCNTs become cost-efficient products.

The sorption behavior of NP111 and PFOA on geosorbents such as Yangtze River sediments and their model components and MWCNTs provides fundamental information for further research. More humic acids of different origins should be used to verify the correlation observed between the K_{OC} value of NP111 and the quantitative structural composition of HAs. The high sorption capacity of NP111 on MWCNTs suggests that MWCNTs are ideal

CHAPTER 5 CONCLUSIONS

materials to effectively remove NP111 from aqueous phase. Nevertheless, at low equilibrium concentrations, the low sorption affinity of PFOA on MWCNTs indicates that MWCNTs are insufficiently sorbent to remove PFOA from aquatic phase. However, the presence of traces of metal catalyst on the outer CNT surface may lead to enhanced sorption through electrostatic interaction, suggesting that the surface modification of MWCNTs may be a promising way to improve the sorption capacity of MWCNTs for PFOA. The effective removal of PFOA from aqueous solutions is a relevant issue and needs to be investigated in the future.

References

- Ahel, M., Giger, W., 1993. Partitioning of alkylphenols and alkylphenol polyethoxylates between water and organic solvents. *Chemosphere* 26, 1471-1478.
- Antelo, J., Avena, M., Fiol, S., López, R., Arce, F., 2005. Effects of pH and ionic strength on the adsorption of phosphate and arsenate at the goethite-water interface. *Journal of Colloid and Interface Science* 285, 476-486.
- Armitage, J., Cousins, I.T., Buck, R.C., Prevedouros, K., Russell, M.H., Macleod, M., Korzeniowski, S.H., 2006. Modeling global-scale fate and transport of perfluorooctanoate emitted from direct sources. *Environmental Science and Technology* 40, 6969-6975.
- Armitage, J.M., MacLeod, M., Cousins, L.T., 2009. Modeling the global fate and transport of perfluorooctanoic acid (PFOA) and perfluorooctanoate (PFO) emitted from direct sources using a multispecies mass balance model. *Environmental Science and Technology* 43, 1134-1140.
- Bao, J., Liu, W., Liu, L., Jin, Y.H., Ran, X.R., Zhang, Z.X., 2010. Perfluorinated compounds in urban river sediments from Guangzhou and Shanghai of China. *Chemosphere* 80, 123-130.
- Bassmann-Schnitzler, F., Sequaris, J.M., 2005. Sorption properties of hydrophobically modified poly(acrylic acids) as natural organic matter model substances to pyrene. *Colloids and Surfaces A: Physicochemical and Engineering Aspects* 260, 119-128.
- Berns, A.E., Conte, P., 2010. Effect of field inhomogeneity and sample restriction on spectral resolution of CP/MAS-13C NMR spectra of natural organic matter. *The Open Magnetic Resonance Journal* 3, 75-83.
- Berryman, D., Houde, F., DeBlois, C., O'Shea, M., 2004. Nonylphenolic compounds in drinking and surface waters downstream of treated textile and pulp and paper effluents: a survey and preliminary assessment of their potential effects on public health and aquatic life. *Chemosphere* 56, 247-255.
- Braida, W.J., Pignatello, J.J., Lu, Y., Ravikovitch, P.I., Neimark, A.V., Xing, B., 2002. Sorption hysteresis of benzene in charcoal particles. *Environmental Science and Technology* 37, 409-417.

REFERENCES

- Bride, M.B.M., 1994. *Environmental Chemistry of Soils*. Oxford University Press, New York, Oxford.
- Brunner, P.H., Capri, S., Marcomini, A., Giger, W., 1988. Occurrence and behaviour of linear alkylbenzenesulfonates, nonylphenol, nonylphenol monophenol and nonylphenol diethoxylates in sewage and sewage-sludge treatment. *Water Research* 22, 1465-1472.
- Burgess, R.M., Pelletier, M.C., Gundersen, J.L., Perron, M.M., Ryba, S.A., 2005. Effects of different forms of organic carbon on the partitioning and bioavailability of nonylphenol. *Environmental Toxicology and Chemistry* 24, 1609-1617.
- Burns, D.C., Ellis, D.A., Li, H., McMurdo, C.J., Webster, E., 2008. Experimental pK_a determination for perfluorooctanoic acid (PFOA) and the potential impact of pK_a concentration dependence on laboratory-measured partitioning phenomena and environmental modeling. *Environmental Science and Technology* 42, 9283-9288.
- Cai, Y., Jiang, G., Liu, J., Zhou, Q., 2003. Multiwalled carbon nanotubes as a solid-phase extraction adsorbent for the determination of bisphenol A, 4-n-nonylphenol, and 4-tert-octylphenol. *Analytical Chemistry* 75, 2517-2521.
- Chefetz, B., Deshmukh, A.P., Hatcher, P.G., Guthrie, E.A., 2000. Pyrene sorption by natural organic matter. *Environmental Science and Technology* 34, 2925-2930.
- Chen, B., Duan, J.-C., Mai, B.-X., Luo, X.-J., Yang, Q.-S., Sheng, G.-Y., Fu, J.-M., 2006. Distribution of alkylphenols in the Pearl River Delta and adjacent northern South China Sea, China. *Chemosphere* 63, 652-661.
- Chen, G.-C., Shan, X.-Q., Wang, Y.-S., Wen, B., Pei, Z.-G., Xie, Y.-N., Liu, T., Pignatello, J.J., 2009. Adsorption of 2, 4, 6-trichlorophenol by multi-walled carbon nanotubes affected by Cu (II). *Water Research* 43, 2409-2418.
- Chen, G., Shan, X., Wang, Y., Pei, Z., Shen, X., Wen, B., Owens, G., 2008a. Effects of copper, lead, and cadmium on the sorption and desorption of atrazine onto and from carbon nanotubes. *Environmental Science and Technology* 42, 8297-8302.
- Chen, J., Chen, W., Zhu, D., 2008b. Adsorption of nonionic aromatic compounds to single-walled carbon nanotubes: Effects of aqueous solution chemistry. *Environmental Science and Technology* 42, 7225-7230.
- Chen, J., Hamon, M.A., Hu, H., Chen, Y., Rao, A.M., Eklund, P.C., Haddon, R.C., 1998.

SORPTION OF A NONYLPHENOL ISOMER AND PERFLUOROOCTANOIC ACID ON
GEOSORBENTS AND CARBON NANOTUBES

Solution properties of single-walled carbon nanotubes. *Science* 282, 95-98.

Chen, W., Duan, L., Zhu, D., 2007. Adsorption of polar and nonpolar organic chemicals to carbon nanotubes. *Environmental Science and Technology* 41, 8295-8300.

Chin, Y.-P., Aiken, G.R., Danielsén, K.M., 1997. Binding of pyrene to aquatic and commercial humic substances: The role of molecular weight and aromaticity. *Environmental Science and Technology* 31, 1630-1635.

Chiou, C.T., 2002. Partition and adsorption of organic contaminants in environmental systems. John Wiley & Sons, Inc., New Jersey.

Chiou, C.T., McGroddy, S.E., Kile, D.E., 1998. Partition characteristics of polycyclic aromatic hydrocarbons on soils and sediments. *Environmental Science and Technology* 32, 264-269.

Chiou, C.T., Peters, L.J., Freed, V.H., 1979. A physical concept of soil-water equilibria for nonionic organic compounds. *Science* 206, 831-832.

Chiou, C.T., Porter, P.E., Schmedding, D.W., 1983. Partition equilibria of nonionic organic compounds between soil organic matter and water. *Environmental Science and Technology* 17, 227-231.

Cirja, M., Zuehlke, S., Ivashechkin, P., Schaeffer, A., Corvini, P.F.X., 2006. Fate of a ¹⁴C-labeled nonylphenol isomer in a laboratory-scale membrane bioreactor. *Environmental Science and Technology* 40, 6131-6136.

Dörfler, H.-D., 2002. Grenzflächen und Kolloid-disperse Systeme: Physik und Chemie. Springer-Verlag Berlin Heidelberg.

Düring, R.-A., Krahe, S., Gäth, S., 2002. Sorption behavior of nonylphenol in terrestrial soils. *Environmental Science and Technology* 36, 4052-4057.

Dai, J., Li, M., Jin, Y., Saito, N., Xu, M., Wei, F., 2006. Perfluorooctanesulfonate and perfluorooctanoate in red panda and giant panda from China. *Environmental Science and Technology* 40, 5647-5652.

Das, K.C., Xia, K., 2008. Transformation of 4-nonylphenol isomers during biosolids composting. *Chemosphere* 70, 761-768.

Datsyuk, V., Kalyva, M., Papagelis, K., Parthenios, J., Tasis, D., Siokou, A., Kallitsis, I., Galiotis, C., 2008. Chemical oxidation of multi-walled carbon nanotubes. *Carbon* 46,

REFERENCES

833-840.

Davis, K.L., Aucoin, M.D., Larsen, B.S., Kaiser, M.A., Hartten, A.S., 2007. Transport of ammonium perfluorooctanoate in environmental media near a fluoropolymer manufacturing facility. *Chemosphere* 67, 2011-2019.

De Paolis, F., Kukkonen, J., 1997. Binding of organic pollutants to humic and fulvic acids: Influence of pH and the structure of humic material. *Chemosphere* 34, 1693-1704.

Deon, J.C., Hurley, M.D., Wallington, T.J., Mabury, S.A., 2006. Atmospheric chemistry of N-methyl perfluorobutane sulfonamidoethanol, $C_4F_9SO_2N(CH_3)CH_2CH_2OH$: Kinetics and mechanism of reaction with OH. *Environmental Science and Technology* 40, 1862-1868.

Division, U.S.E.P.A.O.o.P.P.a.T.R.A., 2002. Draft hazard assessment of perfluorooctanoic acid and its salts.

Ekelund, R., Bergman, A., Granmo, A., Berggren, M., 1990. Bioaccumulation of 4-nonylphenol in marine animals - A reevaluation. *Environmental Pollution* 64, 107-120.

Ekelund, R., Granmo, A., Magnusson, K., Berggren, M., 1993. Biodegradation of 4-nonylphenol in seawater and sediment. *Environmental Pollution* 79, 59-61.

Ellefson, M., 2001. Soil adsorption/desorption study of potassium perfluorooctane sulfonate(PFOS). In: AR226-1030a030, E.D. (Ed.), 3M Company: Maplewood, MN.

Ellis, D.A., Martin, J.W., Silva, A.O.D., Mabury, S.A., Hurley, M.D., Andersen, M.P.S., Wallington, T.J., 2004. Degradation of fluorotelomer alcohols: A likely atmospheric source for perfluorinated carboxylic acids. *Environmental Science and Technology* 38, 3361-3371.

Engelbreton, R.R., von Wandruszka, R., 1999. Effects of humic acid purification on interactions with hydrophobic organic matter: Evidence from fluorescence behavior. *Environmental Science and Technology* 33, 4299-4303.

Ericson, I., Marti-Cid, R., Nadal, M., Bavel, B.V., Lindstroem, G., Domingo, J.L., 2008. Human exposure to perfluorinated chemicals through the diet: Intake of perfluorinated compounds in foods from the Catalan (Spain) Market. *Journal of Agricultural and Food Chemistry* 56, 1787-1794.

Ferguson, P.L., Iden, C.R., Brownawell, B.J., 2001. Distribution and fate of neutral alkylphenol ethoxylate metabolites in a sewage-impacted urban estuary. *Environmental Science and Technology* 35, 2428-2435.

SOPRTION OF A NONYLPHENOL ISOMER AND PERFLUOROOCTANOIC ACID ON
GEOSORBENTS AND CARBON NANOTUBES

- Fontecha-Cámara, M.A., López-Ramón, A.V., Álvarez-Merino, M.A., Moreno-Catilla, C., 2007. Effects of surface chemistry, solution pH, and ionic strength on the removal of herbicides diuron and amitrole from water by an activated carbon fiber. *Langmuir* 23, 1242-1247.
- Fuentes, S., Colomina, M.T., Vicens, P., Franco-Pons, N., Domingo, J.L., 2007. Concurrent exposure to perfluorooctane sulfonate and restraint stress during pregnancy in mice: Effects on postnatal development and behavior of the offspring. *Toxicological Sciences* 98, 589-598.
- George, J., Sudheesh, P., Reddy, P., Sreejith, L., 2009. Influence of salt on cationic surfactant-biopolymer interactions in aqueous media. *Journal of Solution Chemistry* 38, 373-381.
- Giger, W., Brunner, P.H., Schaffner, C., 1984. 4-nonylphenol in sewage sludge: Accumulation of toxic metabolites from non-ionic surfactants. *Science* 225, 623-625.
- Goss, K.U., 2008. The pK_a values of PFOA and other highly fluorinated carboxylic acids. *Environmental Science and Technology* 42, 456-458.
- Goss, K.U., Schwarzenbach, R.P., 2001. Linear free energy relationships used to evaluate equilibrium partitioning of organic compounds. *Environmental Science and Technology* 35, 1-9.
- Granmo, A., Ekelund, R., Magnusson, K., Berggren, M., 1989. Lethal and sublethal toxicity of 4-nonylphenol to the common mussel (*Mytilus edulis* L.). *Environmental Pollution* 59, 115-127.
- Gunasekara, A.S., Simpson, M.J., Xing, B., 2003. Identification and characterization of sorption domains in soil organic matter using structurally modified humic acids. *Environmental Science and Technology* 37, 852-858.
- Höllrigl-Rosta, A., Vinken, R., Schäffer, A., 2005. Binding of endocrine disrupters and herbicide metabolites to soil humic substances. In: Lichtfouse, E., Schwarzbauer, J., Robert, D. (Eds.). *Environmental Chemistry: Green Chemistry and Pollutants in Ecosystems*. Springer Heidelberg, pp. 517-528.
- Hamwi, A., Alvergnat, H., Bonnamy, S., Béguin, F., 1997. Fluorination of carbon nanotubes. *Carbon* 35, 723-728.
- Hansen, K.J., Johnson, H.O., Eldridge, J.S., Butenhoff, J.L., Dick, L.A., 2002. Quantitative

REFERENCES

- characterization of trace levels of PFOS and PFOA in the Tennessee River. *Environmental Science and Technology* 36, 1681-1685.
- Hatcher, P.G., 1987. Chemical structural studies of natural lignin by dipolar dephasing solid-state ^{13}C nuclear magnetic resonance. *Organic Geochemistry* 11, 31-39.
- He, M.C., Shi, Y.H., Lin, C.Y., 2008. Characterization of humic acids extracted from the sediments of the various rivers and lakes in China. *Journal of Environmental Sciences* 20, 1294-1299.
- Hedges, J.I., Cowie, G.L., Richey, J.E., Quay, P.D., 1994. Origins and processing of organic matter in the Amazon River as indicated by carbohydrates and amino acids. *Limnology and Oceanography* 39, 743-753.
- Heemken, O.P., Reincke, H., Stachel, B., Theobald, N., 2001. The occurrence of xenoestrogens in the Elbe river and the North Sea. *Chemosphere* 45, 245-259.
- Higgins, C.P., Field, J.A., Criddle, C.S., Luthy, R.G., 2005. Quantitative determination of perfluorochemicals in sediments and domestic sludge. *Environmental Science and Technology* 39, 3946-3956.
- Higgins, C.P., Luthy, R.G., 2006. Sorption of perfluorinated surfactants on sediments. *Environmental Science and Technology* 40, 7251-7256.
- Higgins, C.P., Luthy, R.G., 2007. Modeling sorption of anionic surfactants onto sediment materials: An a priori approach for perfluoroalkyl surfactants and linear alkylbenzene sulfonates. *Environmental Science and Technology* 41, 3254-3261.
- Hites, R.A., 2006. *Persistent organic pollutants in the great lakes*. Springer-Verlag Berlin Heidelberg.
- Hoellrigl-Rosta, A., Vinken, R., Lenz, M., Schaeffer, A., 2003. Sorption and dialysis experiments to assess the binding of phenolic xenobiotics to dissolved organic matter in soil. *Environmental Toxicology and Chemistry* 22, 746-752.
- Hoellrigl-Rosta, A., Vinken, R., Schäffer, A., 2005. Binding of endocrine disrupters and herbicide metabolites to soil humic substances. In: Lichtfouse, E., Schwarzbauer, J., Robert, D. (Eds.). *Environmental Chemistry: Green Chemistry and Pollutants in Ecosystems*. Springer Heidelberg, pp. 517-528.
- Hu, H., Bhowmik, P., Zhao, B., Hamon, M.A., Itkis, M.E., Haddon, R.C., 2001.

SORPTION OF A NONYLPHENOL ISOMER AND PERFLUOROOCTANOIC ACID ON
GEOSORBENTS AND CARBON NANOTUBES

Determination of the acidic sites of purified single-walled carbon nanotubes by acid-base titration. *Chemical Physics Letters* 345, 25-28.

Hu, J.Y., Wan, Y., Shao, B., Jin, X.H., An, W., Jin, F., Yang, M., Wang, X.J., Sugisaki, M., 2005. Occurrence of trace organic contaminants in Bohai Bay and its adjacent Nanpaiwu River, North China. *Marine Chemistry* 95, 1-13.

Hu, W.-G., Mao, J., Xing, B., Schmidt-Rohr, K., 1999. Poly(methylene) crystallites in humic substances detected by nuclear magnetic resonance. *Environmental Science and Technology* 34, 530-534.

Huang, W., Weber, W.J., 1997. A distributed reactivity model for sorption by soils and sediments. 10. Relationships between desorption, hysteresis, and the chemical characteristics of organic domains. *Environmental Science and Technology* 31, 2562-2569.

Huang, W., Yu, H., Weber, W.J., 1998. Hysteresis in the sorption and desorption of hydrophobic organic contaminants by soils and sediments: 1. A comparative analysis of experimental protocols. *Journal of Contaminant Hydrology* 31, 129-148.

Iijima, S., 1991. Helical microtubules of graphitic carbon. *Nature* 354, 56-58.

Ji, L.L., Shao, Y., Xu, Z.Y., Zheng, S.R., Zhu, D.Q., 2010. Adsorption of monoaromatic compounds and pharmaceutical antibiotics on carbon nanotubes activated by KOH etching. *Environmental Science and Technology* 44, 6429-6436.

Jin, F., Hu, J., Liu, J., Yang, M., Wang, F., Wang, H., 2008. Sequestration of nonylphenol in sediment from Bohai Bay, North China. *Environmental Science and Technology* 42, 746-751.

Jonkers, N., Laane, R.W.P.M., Voogt, P.D., 2003. Fate of nonylphenol ethoxylates and their metabolites in two Dutch estuaries: Evidence of biodegradation in the field. *Environmental Science and Technology* 37, 321-327.

Kan, A.T., Fu, G., Tomson, M.B., 1994. Adsorption/desorption hysteresis in organic pollutant and soil/sediment interaction. *Environmental Science and Technology* 28, 859-867.

Kan, A.T., Tomson, M.B., 1990. Ground water transport of hydrophobic organic compounds in the presence of dissolved organic matter. *Environmental Toxicology and Chemistry* 9, 253-263.

Kang, S., Xing, B., 2005. Phenanthrene sorption to sequentially extracted soil humic acids and humins. *Environmental Science and Technology* 39, 134-140.

REFERENCES

- Kile, D.E., Wershaw, R.L., Chiou, C.T., 1999. Correlation of soil and sediment organic matter polarity to aqueous sorption of nonionic compounds. *Environmental Science and Technology* 33, 2053-2056.
- Klaine, S.J., Alvarez, P.J.J., Batley, G.E., Fernandes, T.F., Handy, R.D., Lyon, D.Y., Mahendra, S., McLaughlin, M.J., Lead, J.R., 2008. Nanomaterials in the environment: Behavior, fate, bioavailability, and effects. *Environmental Toxicology and Chemistry* 27, 1825-1851.
- Kleineidam, S., Rügner, H., Ligouis, B., Grathwohl, P., 1999. Organic matter facies and equilibrium sorption of phenanthrene. *Environmental Science and Technology* 33, 1637-1644.
- Ko, E.-J., Kim, K.-W., Kang, S.-Y., Kim, S.-D., Bang, S.-B., Hamm, S.-Y., Kim, D.-W., 2007. Monitoring of environmental phenolic endocrine disrupting compounds in treatment effluents and river waters, Korea. *Talanta* 73, 674-683.
- Koglin, E., Witte, E.G., Meier, R.J., 2003. The vibrational spectra of metabolites of methabenzthiazuron: 2-amino-benzothiazole and 2-(methylamino)benzothiazole. *Vibrational Spectroscopy* 33, 49-61.
- Koopal, L.K., Goloub, T.P., Davis, T.A., 2004. Binding of ionic surfactants to purified humic acid. *Journal of Colloid and Interface Science* 275, 360-367.
- Krahe, S., During, R.A., Huisman, J.A., Horn, A.L., Gath, S., 2006. Statistical modeling of the partitioning of nonylphenol in soil. *Water Air and Soil Pollution* 172, 221-237.
- Kudo, N., Kawashima, Y., 2003. Toxicity and toxicokinetics of perfluorooctanoic acid in humans and animals. *The Journal of Toxicological Sciences* 28, 49-57.
- Lan, Y., Deng, B., Kim, C., Thornton, E.C., 2007. Influence of soil minerals on chromium(VI) reduction by sulfide under anoxic conditions. *Geochemical Transactions* 8, 1-10.
- Langmuir, I., 1918. The adsorption of gases on plane surfaces of glass, mica, and platinum. *Journal of American Chemistry Society* 40, 1361-1403.
- Li, C., Ji, R., Vinken, R., Hommes, G., Bertmer, M., Schäffer, A., Corvini, P.F.X., 2007. Role of dissolved humic acids in the biodegradation of a single isomer of nonylphenol by *Sphingomonas* sp. *Chemosphere* 68, 2172-2180.
- Li, X., Zhao, H., Quan, X., Chen, S., Zhang, Y., Yu, H., 2010. Adsorption of ionizable organic contaminants on multi-walled carbon nanotubes with different oxygen contents. *Journal of*

SORPTION OF A NONYLPHENOL ISOMER AND PERFLUOROOCTANOIC ACID ON
GEOSORBENTS AND CARBON NANOTUBES

Hazardous Materials, (in press).

Lin, D., Xing, B., 2008. Adsorption of phenolic compounds by carbon nanotubes: Role of aromaticity and substitution of hydroxyl groups. *Environmental Science and Technology* 42, 7254-7259.

Liou, J.S.C., Szostek, B., DeRito, C.M., Madsen, E.L., 2010. Investigating the biodegradability of perfluorooctanoic acid. *Chemosphere* 80, 176-183.

Liu, W.X., Xu, S.S., Xing, B.S., Pan, B., Tao, S., 2010. Nonlinear binding of phenanthrene to the extracted fulvic acid fraction in soil in comparison with other organic matter fractions and to the whole soil sample. *Environmental Pollution* 158, 566-575.

Loos, R., Locoro, G., Huber, T., Wollgast, J., Christoph, E.H., Jager, A.d., Gawlik, B.M., Hanke, G., Umlauf, G., Zaldivar, J.-M., 2007. Analysis of perfluorooctanoate (PFOA) and other perfluorinated compounds (PFCs) in the River Po watershed in N-Italy. *Chemosphere*.

Lu, C., Chiu, H., 2006. Adsorption of zinc(II) from water with purified carbon nanotubes. *Chemical Engineering Science* 61, 1138-1145.

Lu, C., Chung, Y., Chang, K., 2005. Adsorption of trihalomethanes from water with carbon nanotubes. *Water Research* 39, 1183-1189.

Lu, J., He, Y.L., Wu, J., Jin, Q., 2009. Aerobic and anaerobic biodegradation of nonylphenol ethoxylates in estuary sediment of Yangtze River, China. *Environmental Geology* 57, 1-8.

Maguire, R.J., 1999. Review of the persistence of nonylphenol and nonylphenol ethoxylates in aquatic environments. *Water Quality Research Journal of Canada* 34, 37-38.

Mak, Y.L., Taniyasu, S., Yeung, L.W.Y., Lu, G., Jin, L., Yang, Y., Lam, P.K.S., Kannan, K., Yamashita, N., 2009. Perfluorinated Compounds in Tap Water from China and Several Other Countries. *Environmental Science and Technology* 43, 4824-4829.

Manes, M., 1998. Activated carbon adsorption fundamentals. Wiley, New York.

Martin-Mousset, B., Croue, J.P., Lefebvre, E., Legube, B., 1997. Distribution and characterization of dissolved organic matter of surface waters. *Water Research* 31, 541-553.

Mathias, P.M., Kumar, R., Moyer, J.D., Schork, J.M., Srinivasan, S.R., Auvil, S.R., Talu, O., 1996. Correlation of multicomponent gas adsorption by the dual-site langmuir model. Application to nitrogen/oxygen adsorption on 5A-zeolite. *Industrial and Engineering Chemistry Research* 35, 2477-2483.

REFERENCES

- McGinley, P.M., Katz, L.E., Weber, W.J., 1993. A distributed reactivity model for sorption by soils and sediments. 2. Multicomponent systems and competitive effects. *Environmental Science and Technology* 27, 1524-1531.
- McIachlan, M.S., Holmstrom, K.E., Reth, M., Berger, U., 2007. Riverine discharge of perfluorinated carboxylates from the European Continent. *Environmental Science and Technology* 41, 7260-7265.
- McMurdo, C.J., Ellis, D.A., Webster, E., Christensen, R.D., Reid, L.K., 2008. Aerosol enrichment of the surfactant PFO and mediation of the water-air transport of gaseous PFOA. *Environmental Science and Technology* 42, 3969-3974.
- Nagasaki, S., Nakagawa, Y., Tanaka, S., 2004. Sorption of nonylphenol on Na-Montmorillonite. *Colloids and Surfaces A: Physicochemical and Engineering Aspects* 230, 131-139.
- Nanny, M.A., Maza, J.P., 2000. Noncovalent interactions between monoaromatic compounds and dissolved humic acids: A deuterium NMR T_1 relaxation study. *Environmental Science and Technology* 35, 379-384.
- Navarro, A., Endo, S., Gocht, T., Barth, J.A.C., Lacorte, S., Barcelo, D., Grathwohl, P., 2009. Sorption of alkylphenols on Ebro River sediments: Comparing isotherms with field observations in river water and sediments. *Environmental Pollution* 157, 698-703.
- Nowack, B., Bucheli, T.D., 2007. Occurrence, behavior and effects of nanoparticles in the environment. *Environmental Pollution* 150, 5-22.
- Ochoa-Herrera, V., Sierra-Alvarez, R., 2008. Removal of perfluorinated surfactants by sorption onto granular activated carbon, zeolite and sludge. *Chemosphere* 72, 1588-1593.
- Ohshima, H., 1994. A Simple expression for henry's function for the retardation effect in electrophoresis of spherical colloidal particles. *Journal of Colloid and Interface Science* 168, 269-271.
- Oren, A., Chefetz, B., 2005. Sorption-desorption behavior of polycyclic aromatic hydrocarbons in upstream and downstream river sediments. *Chemosphere* 61, 19-29.
- Pan, B., Ghosh, S., Xing, B.S., 2008a. Dissolved organic matter conformation and its interaction with pyrene as affected by water chemistry and concentration. *Environmental Science and Technology* 42, 1594-1599.

SORPTION OF A NONYLPHENOL ISOMER AND PERFLUOROOCTANOIC ACID ON
GEOSORBENTS AND CARBON NANOTUBES

- Pan, B., Lin, D., Mashayekhi, H., Xing, B., 2008b. Adsorption and hysteresis of bisphenol A and 17 α -ethinyl estradiol on carbon nanomaterials. *Environmental Science and Technology* 42, 5480-5485.
- Pan, B., Xing, B., 2008. Adsorption mechanisms of organic chemicals on carbon nanotubes. *Environmental Science and Technology* 42, 9005-9013.
- Parroleggio, L., Capri, S., Angelis, S.D., Pagnotta, R., Polesello, S., Valsecchi, S., 2006. Partition of nonylphenol and related compounds among different aquatic compartments in Tiber River (Central Italy). *Water, Air, and Soil Pollution* 172, 151-166.
- Pettersson, T., Feldoto, Z., Claesson, P.M., Dedinaite, A., 2008. The effect of salt concentration and cation valency on interactions between mucin-coated hydrophobic surfaces. In: Auernhammer, G.K., Auernhammer, G.K., Butt, H.J., Vollmer, D. (Eds.). *Surface and Interfacial Forces - from Fundamentals to Applications*. Springer-Verlag Berlin, Berlin, pp. 1-10.
- Pichon, V., Bouzige, M., Hennion, M.-C., 1998. New trends in environmental trace-analysis of organic pollutants: class-selective immunoextraction and clean-up in one step using immunosorbents. *Analytica Chimica Acta* 376, 21-35.
- Pignatello, J.J., Xing, B., 1995. Mechanisms of slow sorption of organic chemicals to natural particles. *Environmental Science and Technology* 30, 1-11.
- Pistocchi, A., Loos, R., 2009. A map of European emissions and concentration of PFOS and PFOA. *Environmental Science and Technology* 43, 9237-9244.
- Preuss, T.G., Gehrhardt, J., Schirmer, K., Coors, A., Rubach, M., Russ, A., Jones, P.D., Giesy, J.P., Ratte, H.T., 2006. Nonylphenol isomers differ in estrogenic activity. *Environmental Science and Technology* 40, 5147-5153.
- Prevedouros, K., Cousins, I.T., Buck, R.C., Koryniowski, S.H., 2006. Sources, fate and transport of perfluorocarboxylates. *Environmental Science and Technology* 40, 32-44.
- Qu, Y., Zhang, C., Li, F., Bo, X., Liu, G., Zhou, Q., 2009. Equilibrium and kinetics study on the adsorption of perfluorooctanoic acid from aqueous solution onto powdered activated carbon. *Journal of Hazardous Materials* 169, 146-152.
- Rees, J.F., 1980. The fate of carbon compounds in the landfill disposal of organic matter. *Journal of Chemical Technology and Biotechnology* 30, 161-175.

REFERENCES

- Renner, R., 2008. Do perfluoropolymers biodegrade into PFOA? *Environ. Sci. Technol.*, 648-650.
- Saleh, N.B., Pfefferle, L.D., Elimelech, M., 2008a. Aggregation kinetics of multi-walled carbon nanotubes in aquatic systems: Measurements and environmental implication. *Environmental Science and Technology* 42, 7963-7969.
- Saleh, N.B., Pfefferle, L.D., Elimelech, M., 2008b. Aggregation kinetics of multiwalled carbon nanotubes in aquatic systems: Measurements and environmental implication. *Environmental Science and Technology* 42, 7963-7969.
- Salloum, M.J., Chefetz, B., Hatcher, P.G., 2002. Phenanthrene sorption by aliphatic-rich natural organic matter. *Environmental Science and Technology* 36, 1953-1958.
- Salloum, M.J., Dudas, M.J., McGill, W.B., 2001. Variation of 1-naphthol sorption with organic matter fractionation: the role of physical conformation. *Organic Geochemistry* 32, 709-719.
- Sano, M., Okamura, J., Shinkai, S., 2001. Colloidal nature of single-walled carbon nanotubes in electrolyte solution: The Schulze-Hardy rule. *Langmuir* 17, 7172-7173.
- Schaftenaar, G., Noordik, J.H., 2000. Molden: a pre- and post-processing program for molecular and electronic structures. *Journal of Computer-Aided Molecular Design* 14, 123-134.
- Schierz, A., Zaenker, H., 2009. Aqueous suspension of carbon nanotubes: Surface oxidation, colloidal stability and uranium sorption. *Environmental Pollution* 157, 1088-1094.
- Schultz, M.M., Barofsky, D.F., Field, J.A., 2005. Quantitative determination of fluorinated alkyl substances by large-volume-injection liquid chromatography tandem mass spectrometry characterization of municipal wastewaters. *Environmental Science and Technology* 40, 289-295.
- Sekar, M., Sakthi, V., Rengaraj, S., 2004. Kinetics and equilibrium adsorption study of lead(II) onto activated carbon prepared from coconut shell. *Journal of Colloid and Interface Science* 279, 307-313.
- Senesi, N., 1992. Binding mechanisms of pesticides to soil humic substances. *Science of The Total Environment* 123-124, 63-76.
- Shao, B., Hu, J.Y., Yang, M., An, W., Tao, S., 2005. Nonylphenol and nonylphenol ethoxylates

SORPTION OF A NONYLPHENOL ISOMER AND PERFLUOROOCTANOIC ACID ON
GEOSORBENTS AND CARBON NANOTUBES

in river water, drinking water, and fish tissues in the area of Chongqing, China. *Archives of Environmental Contamination and Toxicology* 48, 467-473.

Shen, X., Shan, X., Dong, D., Hua, X., Owens, G., 2009. Kinetics and thermodynamics of sorption of nitroaromatic compounds to as-grown and oxidized multiwalled carbon nanotubes. *Journal of Colloid and Interface Science* 330, 1-8.

Shoeib, M., Harner, T., Vlahos, P., 2006. Perfluorinated chemicals in the arctic atmosphere. *Environmental Science and Technology* 40, 7577-7583.

Sinclair, E., Kannan, K., 2006. Mass loading and fate of perfluoroalkyl surfactants in wastewater treatment plants. *Environmental Science and Technology* 40, 1408-1414.

Singh, N., Berns, A.E., Hennecke, D., Hoerner, J., Koerdel, W., Schaeffer, A., 2010. Effect of soil organic matter chemistry on sorption of trinitrotoluene and 2, 4-dinitrotoluene. *Journal of Hazardous Materials* 173, 343-348.

So, M.K., Miyake, Y., Yeung, W.Y., Ho, Y.M., Taniyasu, S., Rostkowski, P., Yamashita, N., Zhou, B.S., Shi, X.J., Wang, J.X., Giesy, J.P., Yu, H., Lam, P.K.S., 2007. Perfluorinated compounds in the Pearl River and Yangtze River of China. *Chemosphere* 68, 2085-2095.

So, M.K., Taniyasu, S., Yamashita, N., Giesy, J.P., Zheng, J., Fang, Z., Im, S.H., Lam, P.K.S., 2004. Perfluorinated compounds in coastal waters of Hong Kong, South China, and Korea. *Environmental Science and Technology* 38, 4056-4063.

Stemmer, M., Gerzabek, M.H., Kandeler, E., 1998. Organic matter and enzyme activity in particle-size fractions of soils obtained after low-energy sonication. *Soil Biology & Biochemistry* 30, 9-17.

Stone, A.T., Torrents, A., Smolen, J., Vasudevan, D., Hadley, J., 1993. Adsorption of organic compounds possessing ligand donor groups at the oxide/water interface. *Environmental Science and Technology* 27, 895-909.

Su, F., Lu, C., Hu, S., 2010. Adsorption of benzene, toluene, ethylbenzene and p-xylene by NaOCl-oxidized carbon nanotubes. *Colloids and Surfaces A: Physicochemical and Engineering Aspects* 353, 83-91.

Taniyasu, S., Kannan, K., Horii, Y., Hanari, N., Yamashita, N., 2003. A survey of perfluorooctane sulfonate and related perfluorinated organic compounds in water, fish, birds, and humans from Japan. *Environmental Science and Technology* 37, 2634-2639.

REFERENCES

- Tessonnier, J.-P., Rosenthal, D., Hansen, T.W., Hess, C., Schuster, M.E., Blume, R., Girgsdies, F., Pfaender, N., Timpe, O., Su, D.S., Schloegl, R., 2009. Analysis of the structure and chemical properties of some commercial carbon nanostructures. *Carbon* 47, 1779-1798.
- Thiele, B., Heinke, V., Kleist, E., Guenther, K., 2004. Contribution to the structural elucidation of 10 isomers of technical *p*-nonylphenol. *Environmental Science and Technology* 38, 3405-3411.
- Thiele, S., 2000. Adsorption of the antibiotic pharmaceutical compound sulfapyridine by a long-term differently fertilized loess Chernozem. *Journal of Plant Nutrition and Soil Science* 163, 589-594.
- Tipping, E., 2002. Cation binding by humic substances. Cambridge University Press, Cambridge.
- Tombácz, E., Szekeres, M., 2001. Effects of impurity and solid-phase dissolution on surface charge titration of aluminium oxide. *Progress in Colloid & Polymer Science* 117, 18-26.
- Tombacz, E., Szekeres, M., 2006. Surface charge heterogeneity of kaolinite in aqueous suspension in comparison with montmorillonite. *Applied Clay Science* 34, 105-124.
- Tombacz, E., Szekeres, N., 2002. Effects of impurity and solid-phase dissolution on surface charge titration of aluminium oxide. *Adsorption and Nanostructures* 117, 18-26.
- Traina, S.J., McAvoy, D.C., Versteeg, D.J., 1996. Association of linear alkylbenzenesulfonates with dissolved humic substances and its effect on bioavailability. *Environmental Science and Technology* 30, 1300-1309.
- Vinken, R., Schaeffer, A., Ji, R., 2005. Abiotic association of soil-borne monomeric phenols with humic acids. *Organic Geochemistry* 36, 583-593.
- Vinken, R., Schmidt, B., Schaeffer, A., 2002. Synthesis of tertiary ¹⁴C-labelled nonylphenol isomers. *Journal of Labelled Compd. Radiopharm* 45, 1253-1263.
- von Oepen, B., Kördel, W., Klein, W., 1991. Sorption of nonpolar and polar compounds to soils: Processes, measurements and experience with the applicability of the modified OECD-Guideline 106. *Chemosphere* 22, 285-304.
- Wang, X., Chen, C., Hu, W., Ding, A., Xu, D., Zhou, X., 2005. Sorption of ²⁴³Am(III) to multiwall carbon nanotubes. *Environmental Science and Technology* 39, 2856-2860.
- Wania, F., 2007. A global mass balance analysis of the source of perfluorocarboxylic acids in

SOPRTION OF A NONYLPHENOL ISOMER AND PERFLUOROOCTANOIC ACID ON GEOSORBENTS AND CARBON NANOTUBES

the Arctic ocean. *Environmental Science and Technology* 41, 4529-4535.

Weber, W.J., Kim, S.H., Johnson, M.D., 2002. Distributed reactivity model for sorption by soils and sediments. 15. High-concentration Co-contaminant effects on phenanthrene sorption and desorption. *Environmental Science and Technology* 36, 3625-3634.

Weber, W.J., McGinley, P.M., Katz, L.E., 1992. A distributed reactivity model for sorption by soils and sediments. 1. Conceptual basis and equilibrium assessments. *Environmental Science and Technology* 26, 1955-1962.

Wilson, M.A., 1987. NMR techniques and applications in geochemistry and soil chemistry. Pergamon Press, London, UK.

Xing, B., 1997. The effect of the quality of soil organic matter on sorption of naphthalene. *Chemosphere* 35, 633-642.

Xing, B., Pignatello, J.J., 1997. Dual-mode sorption of low-polarity compounds in glassy poly(vinyl chloride) and soil organic matter. *Environmental Science and Technology* 31, 792-799.

Yamamoto, H., Liljestrand, H.M., Shimizu, Y., 2004. Effects of dissolved organic matter surrogates on the partitioning of 17-Estradiol and *p*-Nonylphenol between synthetic membrane vesicles and water. *Environmental Science and Technology* 38, 2351-2358.

Yamamoto, H., Liljestrand, H.M., Shimizu, Y., Morita, M., 2003. Effects of physical-chemical characteristics on the sorption of selected endocrine disruptors by dissolved organic matter surrogates. *Environmental Science and Technology* 37, 2646-2657.

Yamashita, N., Taniyasu, S., Petrick, G., Wei, S., Gamo, T., Lam, P.K.S., Kannan, K., 2008. Perfluorinated acids as novel chemical tracers of global circulation of ocean waters. *Chemosphere* 70, 1247-1255.

Yang, K., Zhu, L., Xing, B., 2006. Adsorption of polycyclic aromatic hydrocarbons by carbon nanomaterials. *Environmental Science and Technology* 40, 1855-1861.

Young, C.J., Furdui, V.I., Franklin, J., Koerner, R.M., Muir, D.C.G., Marbury, S.A., 2007. Perfluorinated acids in arctic snow: new evidence for atmospheric formation. *Environmental Science and Technology* 41, 3455-3461.

Zech, W., Senesi, N., Guggenberger, G., Kaiser, K., Lehmann, J., Miano, T.M., Miltner, A., Schroth, G., 1997. Factors controlling humification and mineralization of soil organic matter

REFERENCES

in the tropics. *Geoderma* 79, 117-161.

Zhang, J., Séquaris, J.-M., Narres, H.-D., Vereecken, H., Klumpp, E., 2010a. Effect of organic carbon and mineral surface on the pyrene sorption and distribution in Yangtze River sediments. *Chemosphere* 80, 1321-1327.

Zhang, J., Séquaris, J.-M., Narres, H.-D., Vereecken, H., Klumpp, E., 2010b. Pyrene and phenanthrene sorption to model and natural geosorbents in single- and binary-solute Systems. *Environmental Science and Technology* 44, 8102-8107.

Zhang, S., Shao, T., Bekaroglu, S.S.K., Karanfil, T., 2009. The impacts of aggregation and surface chemistry of carbon nanotubes on the adsorption of synthetic organic compounds. *Environmental Science and Technology* 43, 5719-5725.

Acknowledgements

I thank the Deutscher Akademischer Austausch Dienst (DAAD) for providing a scholarship and the Agrosphere Institute (IBG-3) for generously supporting my research in Forschungszentrum Jülich, Germany.

I wish to express my sincere gratitude to my supervisor, PD Dr. Erwin Klumpp (IBG-3: Agrosphere). He helped me to get over the handicaps on the way of my PhD program. I learned a lot of knowledge from him, for instance, how to design the topic and solve questions and how to write the scientific paper under his guidance, which would be invaluable to my career in the future.

My deeply appreciation is given to Prof. Dr. Andreas Schäffer in Bio5-Environmental Biology and Chemodynamics, RWTH Aachen University, for his insightful comments and constructive advices at our regular meeting in the past three years. I sincerely acknowledge for Prof. Dr. Rong Ji in School of the Environment, Nanjing University, China, for his sincere assistance on sampling from Yangtze River and constructive criticisms in paper writing and my thesis.

I am thankful to Prof. Dr. Harry Vereecken, Director of the Agrosphere Institute (IBG-3), for reading my reports and commenting on my views at different stages of this work. I would also like to give my sincere thanks to Dr. Hans-Dieter Narres, Dr. Jean-Marie Séquaris, Dr. Hans Lewandowski and Dr. Anne E. Berns for sharing their experiences and always being supportive.

I am grateful to Prof. Dr. Krisztina László for the introduction of surface characterization. I also thank Prof. Dr. Etelka Tombácz for her involvement of my work.

ACKNOWLEDGEMENTS

Special thanks are due to people worked in ZCH Forschungszentrum Jülich for the determination of various samples for me. Thanks to those who have aided me in the laboratory. Specially, I want to express my deep appreciation to Mr. Peter Klahre for his general help in the laboratory. I also appreciate the helps of Dr. Björn Thiele for the LC-MS/MS measurements, of Mrs. Claudia Walraf for the SSA measurement, of Mrs. Ursula Paffen for the TOC measurements, and of Dr. Marc Heggen for the TEM images of MWCNTs.

Not only is the professional help mentioned, I very appreciate all my colleagues and friends for their supporting, helping and sharing my failure and success experienced in the past 3 years. I am also grateful to Dr. Nan Meng, Dr. Jing Zhang and Miss Jing Ning for their warmhearted encouragement and professional involvement of my PhD work, and to Mr. Bastain Niedrée and Miss Juliana Araújo for the joy of sharing an office. Genuine gratitude is given to Dr. Yuhong Xu, Dr. Xiaoyi Xu, Dr. Fangli Luo, Miss Canlan Jiang, Miss Yan Liang, Mr. Xi Yang and etc. for sharing the funny time together.

I seriously want to thank my dear parents. I could not fluently complete my Ph. D work without their cares, love and encouragement. Last but not least, no words can be sufficient to express my thanks to my beautiful wife Dr. Yanli Liu. The patience, love, sacrifice, encouragement, care and support freely offered by her are invaluable during my study.

08.02.2011

Chengliang Li

Appendix

Thermogravimetry (TG) of MWCNTs

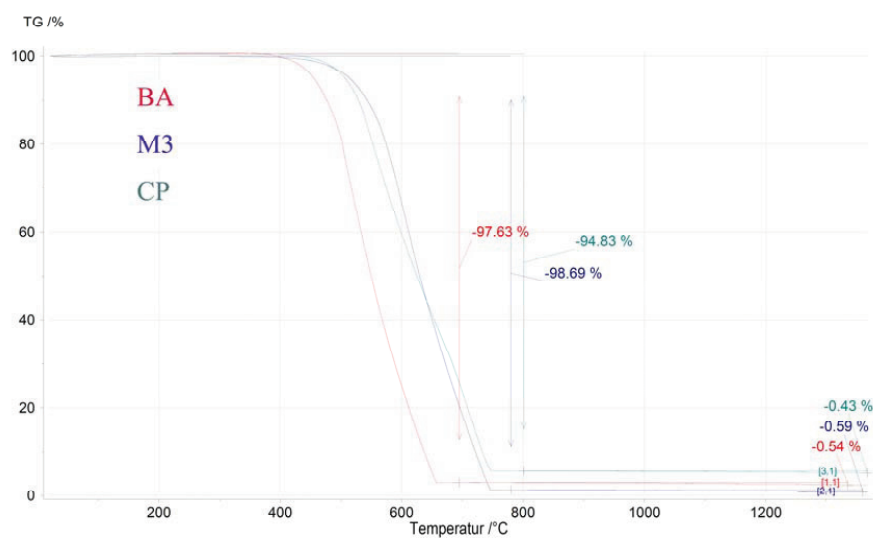


Fig. A1 Thermogravimetry of pristine MWCNTs

Table A1 pH in the supernatant during NP111 adsorption on pristine MWCNTs

(adsorption isotherm)

	250*	500*	1000*	2000*	3000*	4000*	5000*
CP	6.60	6.80	6.73	6.72	6.72	6.79	6.72
BA	6.70	6.80	6.80	6.80	6.80	6.80	6.80
M3	6.78	6.94	6.89	6.86	6.85	6.81	6.85

Note * initial concentration of NP111

CURRICUIUM VITAE

Curriculum vitae

Personal data

Surname: Li
First name: Chengliang
Sex: Male
Date of birth: 3rd of April, 1976
Place of birth: Weifang, China
Nationality: Chinese
Marital status: Married
Tel: +49-2461 61 8663
E-mail: ch.li@fz-juelich.de
Present address: Düsseldorf Str. 16, D-52428 Jülich, Germany

Education

Since 09.2007 Ph. D in Environmental Chemistry & Science, Forschungszentrum Jülich GmbH, Germany, Scholarship by Deutscher Akademischer Austausch Dienst (DAAD)
09.1999-08.2002 M.Sc. in Ecology, Institute of Soil Science, Nanjing, China
09.1995-07.1999 B.Sc. in Soil Science, Shandong Agricultural University, China

Vocational Activity

03.2006-08.2007 Research associate in the Institute of Soil Science, Nanjing, China
04.2005-02.2006 Research scientist in the Institute of Biology 5, RWTH Aachen, Germany (Financed by Sino-German cooperation research centre, German DFG and Marie Cuie fellowship)
08.2002-03.2005 Research associate in the Institute of Soil Science, Nanjing, China
My research focuses on the effect of long term fertilization on nutrient cycle, soil fertility and plant production.

SORPTION OF A NONYLPHENOL ISOMER AND PERFLUOROOCTANOIC ACID ON
GEOSORBENTS AND CARBON NANOTUBES

Publications

- 1 **Chengliang Li**, Andreas Schäffer, Jean-Marie Séquaris, Kristina László, Ajna Toth, Etelka Tombácz, Harry Vereecken, Rong Ji, Erwin Klumpp. Surface-associated metal catalyst enhances the sorption of perfluorooctanoic acid to multi-walled carbon nanotubes. *Water Research* (Submitted).
- 2 **Chengliang Li**, Rong Ji, Andreas Schäffer, Harry Vereecken, Erwin Klumpp. Sorption of a branched nonylphenol and perfluorooctanoic acid on model and natural geochemical sorbents. *Journal of Soils and Sediments* (Submitted).
- 3 Ajna Tóth, Andrea Töröcsik, Etelka Tombácz, Erzsébet Oláh, Marc Heggen, **Chengliang Li**, Erwin Klumpp, Erik Geissler, Krisztina László. pH dependence of phenol dopamine adsorption on commercial MWCNTs. *Journal of Hazardous Materials* (Submitted).
- 4 **Chengliang Li**, Anne E. Berns, Andreas Schäffer, Jean-Marie Séquaris, Rong Ji, Harry Vereecken and Erwin Klumpp. Effect of structural composition of humic acids on the sorption of a branched nonylphenol isomer. *Chemosphere* (doi:10.1016/j.chemosphere.2011.03.057).
- 5 Jun Shan, Bingqi Jiang, Bin Yu, **Chengliang Li**, Andreas Schäffer, Erwin Klumpp, Rong Ji. Isomer-specific degradation of branched and linear 4-nonylphenol isomers in an oxic soil. *Environmental Science and Technology* (Submitted).
- 6 Jun Shan, Ting Wang, **Chengliang Li**, Erwin Klumpp, Rong Ji. Bioaccumulation and bound residues formation of one ¹⁴C-labeled branched 4-nonylphenol isomer in the geophagous earthworm *Metaphire guillelmi* in paddy rice soil. *Environmental Science and Technology*. 2010, 44: 4558-4563

1. **Einsatz von multispektralen Satellitenbilddaten in der Wasserhaushalts- und Stoffstrommodellierung – dargestellt am Beispiel des Rureinzugsgebietes**
von C. Montzka (2008), XX, 238 Seiten
ISBN: 978-3-89336-508-1
2. **Ozone Production in the Atmosphere Simulation Chamber SAPHIR**
by C. A. Richter (2008), XIV, 147 pages
ISBN: 978-3-89336-513-5
3. **Entwicklung neuer Schutz- und Kontaktierungsschichten für Hochtemperatur-Brennstoffzellen**
von T. Kiefer (2008), 138 Seiten
ISBN: 978-3-89336-514-2
4. **Optimierung der Reflektivität keramischer Wärmedämmschichten aus Yttrium-teilstabilisiertem Zirkoniumdioxid für den Einsatz auf metallischen Komponenten in Gasturbinen**
von A. Stuke (2008), X, 201 Seiten
ISBN: 978-3-89336-515-9
5. **Lichtstreuende Oberflächen, Schichten und Schichtsysteme zur Verbesserung der Lichteinkopplung in Silizium-Dünnschichtsolarzellen**
von M. Berginski (2008), XV, 171 Seiten
ISBN: 978-3-89336-516-6
6. **Politiksznarien für den Klimaschutz IV – Szenarien bis 2030**
hrsg.von P. Markewitz, F. Chr. Matthes (2008), 376 Seiten
ISBN 978-3-89336-518-0
7. **Untersuchungen zum Verschmutzungsverhalten rheinischer Braunkohlen in Kohledampferzeugern**
von A. Schlüter (2008), 164 Seiten
ISBN 978-3-89336-524-1
8. **Inorganic Microporous Membranes for Gas Separation in Fossil Fuel Power Plants**
by G. van der Donk (2008), VI, 120 pages
ISBN: 978-3-89336-525-8
9. **Sinterung von Zirkoniumdioxid-Elektrolyten im Mehrlagenverbund der oxidkeramischen Brennstoffzelle (SOFC)**
von R. Mücke (2008), VI, 165 Seiten
ISBN: 978-3-89336-529-6
10. **Safety Considerations on Liquid Hydrogen**
by K. Verfondern (2008), VIII, 167 pages
ISBN: 978-3-89336-530-2

11. **Kerosinreformierung für Luftfahrtanwendungen**
von R. C. Samsun (2008), VII, 218 Seiten
ISBN: 978-3-89336-531-9
12. **Der 4. Deutsche Wasserstoff Congress 2008 – Tagungsband**
hrsg. von D. Stolten, B. Emonts, Th. Grube (2008), 269 Seiten
ISBN: 978-3-89336-533-3
13. **Organic matter in Late Devonian sediments as an indicator for environmental changes**
by M. Klopisch (2008), XII, 188 pages
ISBN: 978-3-89336-534-0
14. **Entschwefelung von Mitteldestillaten für die Anwendung in mobilen Brennstoffzellen-Systemen**
von J. Latz (2008), XII, 215 Seiten
ISBN: 978-3-89336-535-7
15. **RED-IMPACT**
Impact of Partitioning, Transmutation and Waste Reduction Technologies on the Final Nuclear Waste Disposal
SYNTHESIS REPORT
ed. by W. von Lensa, R. Nabbi, M. Rossbach (2008), 178 pages
ISBN 978-3-89336-538-8
16. **Ferritic Steel Interconnectors and their Interactions with Ni Base Anodes in Solid Oxide Fuel Cells (SOFC)**
by J. H. Froitzheim (2008), 169 pages
ISBN: 978-3-89336-540-1
17. **Integrated Modelling of Nutrients in Selected River Basins of Turkey**
Results of a bilateral German-Turkish Research Project
project coord. M. Karpuzcu, F. Wendland (2008), XVI, 183 pages
ISBN: 978-3-89336-541-8
18. **Isotopengeochemische Studien zur klimatischen Ausprägung der Jünger Dryas in terrestrischen Archiven Eurasiens**
von J. Parplies (2008), XI, 155 Seiten, Anh.
ISBN: 978-3-89336-542-5
19. **Untersuchungen zur Klimavariabilität auf dem Tibetischen Plateau - Ein Beitrag auf der Basis stabiler Kohlenstoff- und Sauerstoffisotope in Jahrringen von Bäumen waldgrenznaher Standorte**
von J. Griessinger (2008), XIII, 172 Seiten
ISBN: 978-3-89336-544-9

20. **Neutron-Irradiation + Helium Hardening & Embrittlement Modeling of 9%Cr-Steels in an Engineering Perspective (HELENA)**
by R. Chaouadi (2008), VIII, 139 pages
ISBN: 978-3-89336-545-6
21. **in Bearbeitung**
22. **Verbundvorhaben APAWAGS (AOEV und Wassergenerierung) – Teilprojekt: Brennstoffreformierung – Schlussbericht**
von R. Peters, R. C. Samsun, J. Pasel, Z. Porš, D. Stoltz (2008), VI, 106 Seiten
ISBN: 978-3-89336-547-0
23. **FREEVAL**
Evaluation of a Fire Radiative Power Product derived from Meteosat 8/9 and Identification of Operational User Needs
Final Report
project coord. M. Schultz, M. Wooster (2008), 139 pages
ISBN: 978-3-89336-549-4
24. **Untersuchungen zum Alkaliverhalten unter Oxycoal-Bedingungen**
von C. Weber (2008), VII, 143, XII Seiten
ISBN: 978-3-89336-551-7
25. **Grundlegende Untersuchungen zur Freisetzung von Spurstoffen, Heißgaschemie, Korrosionsbeständigkeit keramischer Werkstoffe und Alkalirückhaltung in der Druckkohlenstaubfeuerung**
von M. Müller (2008), 207 Seiten
ISBN: 978-3-89336-552-4
26. **Analytik von ozoninduzierten phenolischen Sekundärmetaboliten in *Nicotiana tabacum* L. cv Bel W3 mittels LC-MS**
von I. Koch (2008), III, V, 153 Seiten
ISBN 978-3-89336-553-1
27. **IEF-3 Report 2009. Grundlagenforschung für die Anwendung**
(2009), ca. 230 Seiten
ISBN: 978-3-89336-554-8
28. **Influence of Composition and Processing in the Oxidation Behavior of MCrAlY-Coatings for TBC Applications**
by J. Toscano (2009), 168 pages
ISBN: 978-3-89336-556-2
29. **Modellgestützte Analyse signifikanter Phosphorbelastungen in hessischen Oberflächengewässern aus diffusen und punktuellen Quellen**
von B. Tetzlaff (2009), 149 Seiten
ISBN: 978-3-89336-557-9

30. **Nickelreaktivlot / Oxidkeramik – Fügungen als elektrisch isolierende Dichtungskonzepte für Hochtemperatur-Brennstoffzellen-Stacks**
von S. Zügner (2009), 136 Seiten
ISBN: 978-3-89336-558-6
31. **Langzeitbeobachtung der Dosisbelastung der Bevölkerung in radioaktiv kontaminierten Gebieten Weißrusslands – Korma-Studie**
von H. Dederichs, J. Pillath, B. Heuel-Fabianek, P. Hill, R. Lennartz (2009),
Getr. Pag.
ISBN: 978-3-89336-532-3
32. **Herstellung von Hochtemperatur-Brennstoffzellen über physikalische Gasphasenabscheidung**
von N. Jordán Escalona (2009), 148 Seiten
ISBN: 978-3-89336-532-3
33. **Real-time Digital Control of Plasma Position and Shape on the TEXTOR Tokamak**
by M. Mitri (2009), IV, 128 pages
ISBN: 978-3-89336-567-8
34. **Freisetzung und Einbindung von Alkalimetallverbindungen in kohlebefeuchten Kombikraftwerken**
von M. Müller (2009), 155 Seiten
ISBN: 978-3-89336-568-5
35. **Kosten von Brennstoffzellensystemen auf Massenbasis in Abhängigkeit von der Absatzmenge**
von J. Werhahn (2009), 242 Seiten
ISBN: 978-3-89336-569-2
36. **Einfluss von Reoxidationszyklen auf die Betriebsfestigkeit von anodengestützten Festoxid-Brennstoffzellen**
von M. Ettler (2009), 138 Seiten
ISBN: 978-3-89336-570-8
37. **Großflächige Plasmaabscheidung von mikrokristallinem Silizium für mikromorphe Dünnschichtsolarmodule**
von T. Kilper (2009), XVII, 154 Seiten
ISBN: 978-3-89336-572-2
38. **Generalized detailed balance theory of solar cells**
by T. Kirchartz (2009), IV, 198 pages
ISBN: 978-3-89336-573-9
39. **The Influence of the Dynamic Ergodic Divertor on the Radial Electric Field at the Tokamak TEXTOR**
von J. W. Coenen (2009), xii, 122, XXVI pages
ISBN: 978-3-89336-574-6

40. **Sicherheitstechnik im Wandel Nuklearer Systeme**
von K. Nünighoff (2009), viii, 215 Seiten
ISBN: 978-3-89336-578-4
41. **Pulvermetallurgie hochporöser NiTi-Legierungen für Implantat- und Dämpfungsanwendungen**
von M. Köhl (2009), XVII, 199 Seiten
ISBN: 978-3-89336-580-7
42. **Einfluss der Bondcoatzusammensetzung und Herstellungsparameter auf die Lebensdauer von Wärmedämmschichten bei zyklischer Temperaturbelastung**
von M. Subanovic (2009), 188, VI Seiten
ISBN: 978-3-89336-582-1
43. **Oxygen Permeation and Thermo-Chemical Stability of Oxygen Permeation Membrane Materials for the Oxyfuel Process**
by A. J. Ellett (2009), 176 pages
ISBN: 978-3-89336-581-4
44. **Korrosion von polykristallinem Aluminiumoxid (PCA) durch Metalljodidschmelzen sowie deren Benetzungseigenschaften**
von S. C. Fischer (2009), 148 Seiten
ISBN: 978-3-89336-584-5
45. **IEF-3 Report 2009. Basic Research for Applications**
(2009), 217 Seiten
ISBN: 978-3-89336-585-2
46. **Verbundvorhaben ELBASYS (Elektrische Basissysteme in einem CFK-Rumpf) - Teilprojekt: Brennstoffzellenabgase zur Tankinertisierung - Schlussbericht**
von R. Peters, J. Latz, J. Pasel, R. C. Samsun, D. Stolten
(2009), xi, 202 Seiten
ISBN: 978-3-89336-587-6
47. **Aging of ¹⁴C-labeled Atrazine Residues in Soil: Location, Characterization and Biological Accessibility**
by N. D. Jablonowski (2009), IX, 104 pages
ISBN: 978-3-89336-588-3
48. **Entwicklung eines energetischen Sanierungsmodells für den europäischen Wohngebäudesektor unter dem Aspekt der Erstellung von Szenarien für Energie- und CO₂ - Einsparpotenziale bis 2030**
von P. Hansen (2009), XXII, 281 Seiten
ISBN: 978-3-89336-590-6

49. **Reduktion der Chromfreisetzung aus metallischen Interkonnektoren für Hochtemperaturbrennstoffzellen durch Schutzschichtsysteme**
von R. Trebbels (2009), iii, 135 Seiten
ISBN: 978-3-89336-591-3
50. **Bruchmechanische Untersuchung von Metall / Keramik-Verbundsystemen für die Anwendung in der Hochtemperaturbrennstoffzelle**
von B. Kuhn (2009), 118 Seiten
ISBN: 978-3-89336-592-0
51. **Wasserstoff-Emissionen und ihre Auswirkungen auf den arktischen Ozonverlust**
Risikoanalyse einer globalen Wasserstoffwirtschaft
von T. Feck (2009), 180 Seiten
ISBN: 978-3-89336-593-7
52. **Development of a new Online Method for Compound Specific Measurements of Organic Aerosols**
by T. Hohaus (2009), 156 pages
ISBN: 978-3-89336-596-8
53. **Entwicklung einer FPGA basierten Ansteuerungselektronik für Justageeinheiten im Michelson Interferometer**
von H. Nöldgen (2009), 121 Seiten
ISBN: 978-3-89336-599-9
54. **Observation – and model – based study of the extratropical UT/LS**
by A. Kunz (2010), xii, 120, xii pages
ISBN: 978-3-89336-603-3
55. **Herstellung polykristalliner Szintillatoren für die Positronen-Emissions-Tomographie (PET)**
von S. K. Karim (2010), VIII, 154 Seiten
ISBN: 978-3-89336-610-1
56. **Kombination eines Gebäudekondensators mit H₂-Rekombinatorelementen in Leichtwasserreaktoren**
von S. Kelm (2010), vii, 119 Seiten
ISBN: 978-3-89336-611-8
57. **Plant Leaf Motion Estimation Using A 5D Affine Optical Flow Model**
by T. Schuchert (2010), X, 143 pages
ISBN: 978-3-89336-613-2
58. **Tracer-tracer relations as a tool for research on polar ozone loss**
by R. Müller (2010), 116 pages
ISBN: 978-3-89336-614-9

59. **Sorption of polycyclic aromatic hydrocarbon (PAH) to Yangtze River sediments and their components**
by J. Zhang (2010), X, 109 pages
ISBN: 978-3-89336-616-3
60. **Weltweite Innovationen bei der Entwicklung von CCS-Technologien und Möglichkeiten der Nutzung und des Recyclings von CO₂**
Studie im Auftrag des BMWi
von W. Kuckshinrichs et al. (2010), X, 139 Seiten
ISBN: 978-3-89336-617-0
61. **Herstellung und Charakterisierung von sauerstoffionenleitenden Dünnschichtmembranstrukturen**
von M. Betz (2010), XII, 112 Seiten
ISBN: 978-3-89336-618-7
62. **Politiksznarien für den Klimaschutz V – auf dem Weg zum Strukturwandel, Treibhausgas-Emissionsszenarien bis zum Jahr 2030**
hrsg. von P. Hansen, F. Chr. Matthes (2010), 276 Seiten
ISBN: 978-3-89336-619-4
63. **Charakterisierung Biogener Sekundärer Organischer Aerosole mit Statistischen Methoden**
von C. Spindler (2010), iv, 163 Seiten
ISBN: 978-3-89336-622-4
64. **Stabile Algorithmen für die Magnetotomographie an Brennstoffzellen**
von M. Wannert (2010), ix, 119 Seiten
ISBN: 978-3-89336-623-1
65. **Sauerstofftransport und Degradationsverhalten von Hochtemperaturmembranen für CO₂-freie Kraftwerke**
von D. Schlehüser (2010), VII, 139 Seiten
ISBN: 978-3-89336-630-9
66. **Entwicklung und Herstellung von foliengegossenen, anodengestützten Festoxidbrennstoffzellen**
von W. Schafbauer (2010), VI, 164 Seiten
ISBN: 978-3-89336-631-6
67. **Disposal strategy of proton irradiated mercury from high power spallation sources**
by S. Chiriki (2010), xiv, 124 pages
ISBN: 978-3-89336-632-3
68. **Oxides with polyatomic anions considered as new electrolyte materials for solid oxide fuel cells (SOFCs)**
by O. H. Bin Hassan (2010), vii, 121 pages
ISBN: 978-3-89336-633-0

69. **Von der Komponente zum Stack: Entwicklung und Auslegung von HT-PEFC-Stacks der 5 kW-Klasse**
von A. Bendzulla (2010), IX, 203 Seiten
ISBN: 978-3-89336-634-7
70. **Satellitengestützte Schwerewellenmessungen in der Atmosphäre und Perspektiven einer zukünftigen ESA Mission (PREMIER)**
von S. Höfer (2010), 81 Seiten
ISBN: 978-3-89336-637-8
71. **Untersuchungen der Verhältnisse stabiler Kohlenstoffisotope in atmosphärisch relevanten VOC in Simulations- und Feldexperimenten**
von H. Spahn (2010), IV, 210 Seiten
ISBN: 978-3-89336-638-5
72. **Entwicklung und Charakterisierung eines metallischen Substrats für nanostrukturierte keramische Gastrennmembranen**
von K. Brands (2010), vii, 137 Seiten
ISBN: 978-3-89336-640-8
73. **Hybridisierung und Regelung eines mobilen Direktmethanol-Brennstoffzellen-Systems**
von J. Chr. Wilhelm (2010), 220 Seiten
ISBN: 978-3-89336-642-2
74. **Charakterisierung perowskitischer Hochtemperaturmembranen zur Sauerstoffbereitstellung für fossil gefeuerte Kraftwerksprozesse**
von S.A. Möbius (2010) III, 208 Seiten
ISBN: 978-3-89336-643-9
75. **Characterization of natural porous media by NMR and MRI techniques: High and low magnetic field studies for estimation of hydraulic properties**
by L.-R. Stingaciu (2010), 96 pages
ISBN: 978-3-89336-645-3
76. **Hydrological Characterization of a Forest Soil Using Electrical Resistivity Tomography**
by Chr. Oberdörster (2010), XXI, 151 pages
ISBN: 978-3-89336-647-7
77. **Ableitung von atomarem Sauerstoff und Wasserstoff aus Satellitendaten und deren Abhängigkeit vom solaren Zyklus**
von C. Lehmann (2010), 127 Seiten
ISBN: 978-3-89336-649-1

78. **18th World Hydrogen Energy Conference 2010 – WHEC2010**
Proceedings
Speeches and Plenary Talks
ed. by D. Stolten, B. Emonts (2010)
ISBN: 978-3-89336-658-3
- 78-1. **18th World Hydrogen Energy Conference 2010 – WHEC2010**
Proceedings
Parallel Sessions Book 1:
Fuel Cell Basics / Fuel Infrastructures
ed. by D. Stolten, T. Grube (2010), ca. 460 pages
ISBN: 978-3-89336-651-4
- 78-2. **18th World Hydrogen Energy Conference 2010 – WHEC2010**
Proceedings
Parallel Sessions Book 2:
Hydrogen Production Technologies – Part 1
ed. by D. Stolten, T. Grube (2010), ca. 400 pages
ISBN: 978-3-89336-652-1
- 78-3. **18th World Hydrogen Energy Conference 2010 – WHEC2010**
Proceedings
Parallel Sessions Book 3:
Hydrogen Production Technologies – Part 2
ed. by D. Stolten, T. Grube (2010), ca. 640 pages
ISBN: 978-3-89336-653-8
- 78-4. **18th World Hydrogen Energy Conference 2010 – WHEC2010**
Proceedings
Parallel Sessions Book 4:
Storage Systems / Policy Perspectives, Initiatives and Cooperations
ed. by D. Stolten, T. Grube (2010), ca. 500 pages
ISBN: 978-3-89336-654-5
- 78-5. **18th World Hydrogen Energy Conference 2010 – WHEC2010**
Proceedings
Parallel Sessions Book 5:
Strategic Analysis / Safety Issues / Existing and Emerging Markets
ed. by D. Stolten, T. Grube (2010), ca. 530 pages
ISBN: 978-3-89336-655-2
- 78-6. **18th World Hydrogen Energy Conference 2010 – WHEC2010**
Proceedings
Parallel Sessions Book 6:
Stationary Applications / Transportation Applications
ed. by D. Stolten, T. Grube (2010), ca. 330 pages
ISBN: 978-3-89336-656-9

78 Set (complete book series)

18th World Hydrogen Energy Conference 2010 – WHEC2010

Proceedings

ed. by D. Stolten, T. Grube, B. Emonts (2010)

ISBN: 978-3-89336-657-6

79. Ultrafast voltex core dynamics investigated by finite-element micromagnetic simulations

by S. Gliga (2010), vi, 144 pages

ISBN: 978-3-89336-660-6

80. Herstellung und Charakterisierung von keramik- und metallgestützten Membranschichten für die CO₂-Abtrennung in fossilen Kraftwerken

von F. Hauler (2010), XVIII, 178 Seiten

ISBN: 978-3-89336-662-0

81. Experiments and numerical studies on transport of sulfadiazine in soil columns

by M. Unold (2010), xvi, 115 pages

ISBN: 978-3-89336-663-7

82. Prompt-Gamma-Neutronen-Aktivierungs-Analyse zur zerstörungsfreien Charakterisierung radioaktiver Abfälle

von J.P.H. Kettler (2010), iv, 205 Seiten

ISBN: 978-3-89336-665-1

83. Transportparameter dünner geträgerter Kathodenschichten der oxidkeramischen Brennstoffzelle

von C. Wedershoven (2010), vi, 137 Seiten

ISBN: 978-3-89336-666-8

84. Charakterisierung der Quellverteilung von Feinstaub und Stickoxiden in ländlichem und städtischem Gebiet

von S. Urban (2010), vi, 211 Seiten

ISBN: 978-3-89336-669-9

85. Optics of Nanostructured Thin-Film Silicon Solar Cells

by C. Haase (2010), 150 pages

ISBN: 978-3-89336-671-2

86. Entwicklung einer Isolationsschicht für einen Leichtbau-SOFC-Stack

von R. Berhane (2010), X, 162 Seiten

ISBN: 978-3-89336-672-9

87. Hydrogen recycling and transport in the helical divertor of TEXTOR

by M. Clever (2010), x, 172 pages

ISBN: 978-3-89336-673-6

88. **Räumlich differenzierte Quantifizierung der N- und P-Einträge in Grundwasser und Oberflächengewässer in Nordrhein-Westfalen unter besonderer Berücksichtigung diffuser landwirtschaftlicher Quellen**
von F. Wendland et. al. (2010), xii, 216 Seiten
ISBN: 978-3-89336-674-3
89. **Oxidationskinetik innovativer Kohlenstoffmaterialien hinsichtlich schwerer Luftfeinbruchstörfälle in HTR's und Graphitentsorgung oder Aufarbeitung**
von B. Schlögl (2010), ix, 117 Seiten
ISBN: 978-3-89336-676-7
90. **Chemische Heißgasreinigung bei Biomassenvergasungsprozessen**
von M. Stemmler (2010), xv, 196 Seiten
ISBN: 978-3-89336-678-1
91. **Untersuchung und Optimierung der Serienverschaltung von Silizium-Dünnschicht-Solarmodulen**
von S. Haas (2010), ii, 202 Seiten
ISBN: 978-3-89336-680-4
92. **Non-invasive monitoring of water and solute fluxes in a cropped soil**
by S. Garré (2010), xxiv, 133 pages
ISBN: 978-3-89336-681-1
93. **Improved hydrogen sorption kinetics in wet ball milled Mg hydrides**
by L. Meng (2011), II, 119 pages
ISBN: 978-3-89336-687-3
94. **Materials for Advanced Power Engineering 2010**
ed. by J. Lecomte-Beckers, Q. Contrepolis, T. Beck and B. Kuhn
(2010), 1327 pages
ISBN: 978-3-89336-685-9
95. **2D cross-hole MMR – Survey design and sensitivity analysis for cross-hole applications of the magnetometric resistivity**
by D. Fielitz (2011), xvi, 123 pages
ISBN: 978-3-89336-689-7
96. **Untersuchungen zur Oberflächenspannung von Kohleschlacken unter Vergasungsbedingungen**
von T. Melchior (2011), xvii, 270 Seiten
ISBN: 978-3-89336-690-3
97. **Secondary Organic Aerosols: Chemical Aging, Hygroscopicity, and Cloud Droplet Activation**
by A. Buchholz (2011), xiv, 134 pages
ISBN: 978-3-89336-691-0

98. **Chrom-bezogene Degradation von Festoxid-Brennstoffzellen**
von A. Neumann (2011), xvi, 218 Seiten
ISBN: 978-3-89336-692-7
99. **Amorphous and microcrystalline silicon applied in very thin tandem solar cells**
by S. Schicho (2011), XII, 190 pages
ISBN: 978-3-89336-693-4
100. **Sol-gel and nano-suspension electrolyte layers for high performance solid oxide fuel cells**
by F. Han (2011), iv, 131 pages
ISBN: 978-3-89336-694-1
101. **Impact of different vertical transport representations on simulating processes in the tropical tropopause layer (TTL)**
by F. Plöger (2011), vi, 104 pages
ISBN: 978-3-89336-695-8
102. **Untersuchung optischer Nanostrukturen für die Photovoltaik mit Nahfeldmikroskopie**
von T. Beckers (2011), xiii, 128 Seiten
ISBN: 978-3-89336-696-5
103. **Impact of contamination on hydrogenated amorphous silicon thin films & solar cells**
by J. Wördenweber (2011), XIV, 138 pages
ISBN: 978-3-89336-697-2
104. **Water and Organic Nitrate Detection in an AMS: Laboratory Characterization and Application to Ambient Measurements**
by A. Mensah (2011), XI, 111 pages
ISBN: 978-3-89336-698-9
105. **Entwicklung eines neuen Konzepts zur Steuerung der thermischen Ausdehnung von glaskeramischen Verbundwerkstoffen mit angepasster Fließfähigkeit am Beispiel der Hochtemperatur-Brennstoffzelle**
von E. Wanko (2011), xi, 134 Seiten
ISBN: 978-3-89336-705-4
106. **Tomographic reconstruction of atmospheric volumes from infrared limb-imager measurements**
by J. Ungermann (2011), xiv, 153 pages
ISBN: 978-3-89336-708-5
107. **Synthese und Identifizierung von substituierten Mg-Al-Cl Doppelhydroxidverbindungen mit Schwerpunkt IR-Spektroskopie**
von B. Hansen (2011), XII, 121 Seiten
ISBN: 978-3-89336-709-2

108. **Analysis of spatial soil moisture dynamics using wireless sensor networks**
by U. Rosenbaum (2011), xxii, 120 pages
ISBN: 978-3-89336-710-8
109. **Optimierung von APS-ZrO₂-Wärmedämmschichten durch Variation der Kriechfestigkeit und der Grenzflächenrauigkeit**
von M. E. Schweda (2011), 168 Seiten
ISBN: 978-3-89336-711-5
110. **Sorption of a branched nonylphenol isomer and perfluorooctanoic acid on geosorbents and carbon nanotubes**
by C. Li (2011), X, 102 pages
ISBN: 978-3-89336-716-0

